Meal Timing & Its Effects on the Pathogenesis of Metabolic Syndrome

by

Michael Jeffrey Wayne

A thesis submitted to the Graduate Faculty of
Auburn University
in partial fulfillment of the
requirements for the Degree of
Master of Science

Auburn, Alabama
August 1, 2015

Keywords: meal timing, metabolic syndrome, metabolic cage

Approved by

Michael Greene, Chair, Assistant Professor, Nutrition and Dietetics
Ramesh Jeganathan, Assistant Professor, Nutrition and Dietetics
Douglas White, Associate Professor, Nutrition and Dietetics

Abstract

Metabolic syndrome is an assortment of biochemical abnormalities associated with cardiovascular diseases and type 2 diabetes. Characterized by obesity, insulin resistance, and hepatic steatosis, it affects approximately 47 million Americans. This disease condition is promoted through impaired lipid metabolism and inflammation caused by a high fat diet and sugary drinks. Meal timing, or restricting food access to a specific time, inhibits disease progression. However, the potential of sugary water to negate these effects are unknown. Metabolic cage measurements indicated meal timed mice had decreased daily energy expenditure, increased nightly activity, and elevated respiratory quotient versus animals on high fat plus sugar diet. Physiological assessments also identified significantly decreased normalized inguinal adipose tissue and liver weights, decreased body mass, and improved glucose tolerance in meal timed animals. Taken together, this data illustrates that meal timing can make animals fed a high fat Western diet plus sugary water more metabolically fit.

Acknowledgments

I would like to thank my advisor, Dr. Michael Greene, for his support and guidance during my time here at Auburn University. I would also like to thank the members of my committee, Dr. Remesh Jeganathan and Dr. Douglas White. Throughout the course of my studies, numerous individuals made significant contributions to the initiation and completion of the experiments. I would like to thank the members of the Greene laboratory, Dr. Ann Marie O'Neill and Yuwen Luo. Additionally, I am grateful to the students of the HONR 3789 course and the Honors College for their funding support.

Table of Contents

List of Tables

List of Figures

I. Introduction

Nonalcoholic fatty liver disease (NAFLD) consists of a variety of hepatic conditions. These range from the benign condition of excessive retention of lipid within the liver known as simple steatosis (will be referred to as NAFLD throughout), to nonalcoholic steatohepatitis (NASH) lesions of moderate severity, to the far end of the spectrum with cirrhosis where most liver-related morbidity occurs. NAFLD is characterized by its hallmark symptom of triglyceride accumulation within hepatocytes. Progression from NAFLD to NASH is accompanied by hepatic inflammation, hepatocyte injury and fibrosis, ultimately increasing the rate of cirrhosis development and subsequent liver-related mortality as seen in Figure 1 (1).

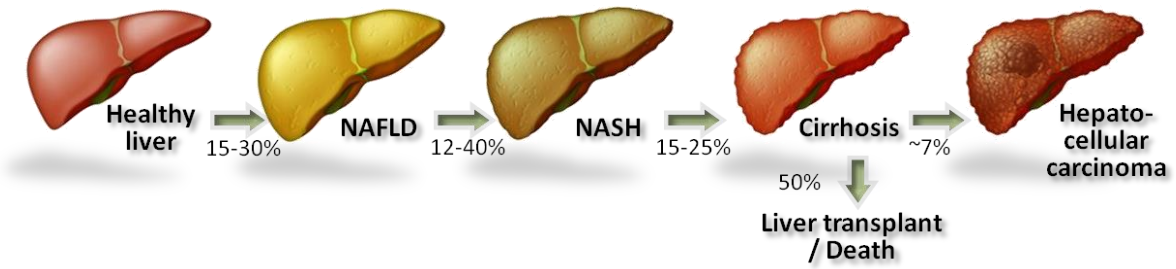

***Figure 1**: Progression of liver disease* *Journal of Gastroenterology and Hepatology, 2013*

NAFLD is the most common cause of liver disease in the Western world (2) and is widely accepted as the hepatic manifestation of metabolic syndrome which includes hypertension, obesity, dyslipidemia, and insulin resistance (3). The complete pathogenesis and progression of NAFLD is not entirely understood, but the "two-hit hypothesis" is commonly recognized (4). This idea proposes the initiator, or "first hit", involves impaired fatty acid metabolism and results in hepatic triglyceride accumulation (steatosis). This is followed by the "second hit" of oxidative and metabolic stress and overproduction of cytokines as a compensatory response for

the increased hepatic lipid concentration (4). Ultimately, these stresses increase hepatocyte death rates and facilitate the progression from NASH to cirrhosis (1).

Lipid metabolism within the liver is regulated and balanced through the processes of hepatic uptake of free fatty acids (FFAs) from de novo synthesis, disposal of these FFAs via oxidation or de novo triglyceride synthesis, and export of triglycerides as very low density lipoproteins (VLDL) (5). FFAs are generated through lipolysis within peripheral adipose tissues and consumption of lipid. They are eventually taken up by hepatocytes where they are metabolized through oxidation or form triglycerides via esterification and are either stored within the hepatocytes or exported as VLDL (1). This process of normal lipid metabolism within hepatocytes is depicted in Figure 2.

.

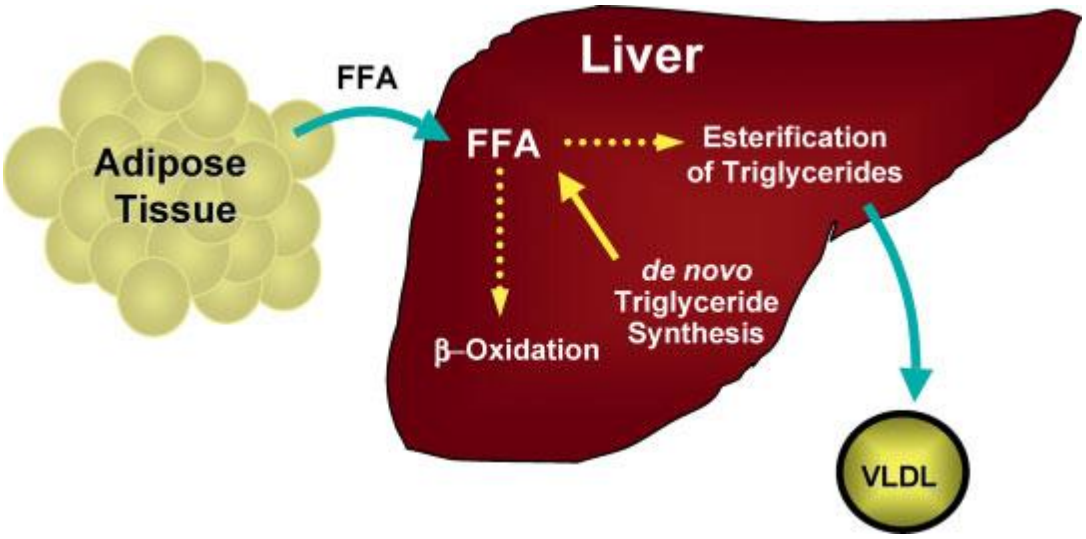

Figure 2*: Normal lipid metabolism. Adipose tissue undergoes lipolysis releasing free fatty acids (FFA) into the circulation. FFA are taken up in the liver where they either are oxidized in mitochondria or are esterified to triglycerides that can then be packaged and exported as very low-density lipoproteins (VLDL). De novo FFA synthesis within the liver also contributes to the pool of FFA.*
Diehl et al. Mechanisms of disease progression in nonalcoholic fatty liver disease. Seminars in Liver Disease. 2008

In NAFLD this hepatic lipid metabolism balance is disturbed as the uptake and de novo synthesis of fatty acids are increased and exceeds the capacity for fatty acid oxidation (6). In an attempt to dispose of the excess FFAs triglyceride synthesis is increased (7). However, this upregulation in triglyceride synthesis is not matched by VLDL synthesis, preventing the newly formed triglycerides from being exported and instead accumulating within hepatocytes, thus leading to steatosis (8). This process is considered the "first hit" in the pathogenesis of NAFLD (4).

It should be noted that triglycerides themselves are not harmful to the liver and rather act as biomarkers of increased hepatic interaction with potentially toxic FFAs (1). However, knockdown of diacylglycerol acyltransferase (DGAT), the enzyme responsible for the final step of FFA esterification into triglyceride by catalyzing the linkage of sn-1, 2-diacylglycerol with long chain acyl-CoA (both isoforms, DGAT1 & DGAT2) (9), does not lead to abnormal hepatic triglyceride content (10). This suggests that DGAT1 does not have a rate-limiting role in hepatic triglyceride production, despite the common assertion to the contrary (11). Despite catalyzing the same reaction, DGAT2 does play a role in hepatic triglyceride synthesis as evidenced by the ability to reduce hepatic triglyceride content, reverse steatosis, and improve insulin sensitivity in a small animal model of NAFLD (12). However, in an animal model of NAFLD in which NASH and fibrosis typically develop, blockage of triglyceride synthesis through downregulation of DGAT2 expectedly led to reduced hepatic steatosis, while also exacerbating liver injury and fibrosis via increased hepatic FFA content, oxidative stress and lipid peroxidation (13). This reinforces that triglycerides themselves are not harmful to hepatocytes, but rather protect

against FFA lipotoxicity (13). This incriminates FFAs in the progression from NAFLD to NASH as they can be directly cytotoxic (14) and stimulate synthesis of pro-inflammatory cytokines, such as tumor necrosis factor-α (TNF-α) (15).

Furthermore, this FFA accumulation and subsequent production of TNF-α inhibits production of the adipokine adiponectin, a potent factor produced from adipocytes that functions as an insulin sensitizer and enhances storage of FFA in triglyceride depots, while reducing the release of FFA into the circulation (16). In addition to its ability to decrease lipolysis and prevent lipid accumulation in tissues (17) animal models of NAFLD have revealed adiponectin can increase fatty acid oxidation and decrease fatty acid synthesis, resulting in reduced steatosis (18). Adiponectin and TNF-α are mutually antagonistic and concentrations are inversely related (19). Studies of NASH patients confirmed increased circulating TNF-α plasma levels and subsequent increases in inflammatory cytokines IL-6 and IL-8 parallel reductions in adiponectin (20) and ultimately exacerbate hepatic lipotoxicity and NAFLD pathogenesis (21).

Oxidation of FFA generates reactive oxygen species (ROS) in addition to reducing equivalents, such as nicotinamide adenine dinucleotide (NADH) and nicotinamide adenine dinucleotide phosphate (NADPH) (1). Similar to the attempt to export newly esterfied triglycerides in VLDL, the disproportionately high amount of FFA leads to excessive ROS production that exceeds the capacity of antioxidants and forms hepatoxic lipid peroxides (22). Cytochrome P450 2E1 (CYP2E1), the primary enzyme in fatty acid oxidation, has been shown to

be consistently elevated in NASH patients compared to those with simple steatosis, reaffirming the detrimental effects of excess ROS production from an abundance of FFA (23).

The more advanced condition of steatohepatitis (NASH) is distinguished from steatosis by the buildup of injured and dead hepatocytes within the liver (1). Due to the chronic inflammatory, redox, and apoptotic stresses undergone by hepatocytes in NASH, hepatocyte replication is blocked and replacement of cells requires expansion and differentiation of hepatic progenitors (24). This regenerative response determines the progression from NASH to fibrosis and cirrhosis, thereby considering hepatocyte death as a potential “third hit” in NAFLD progression (1).

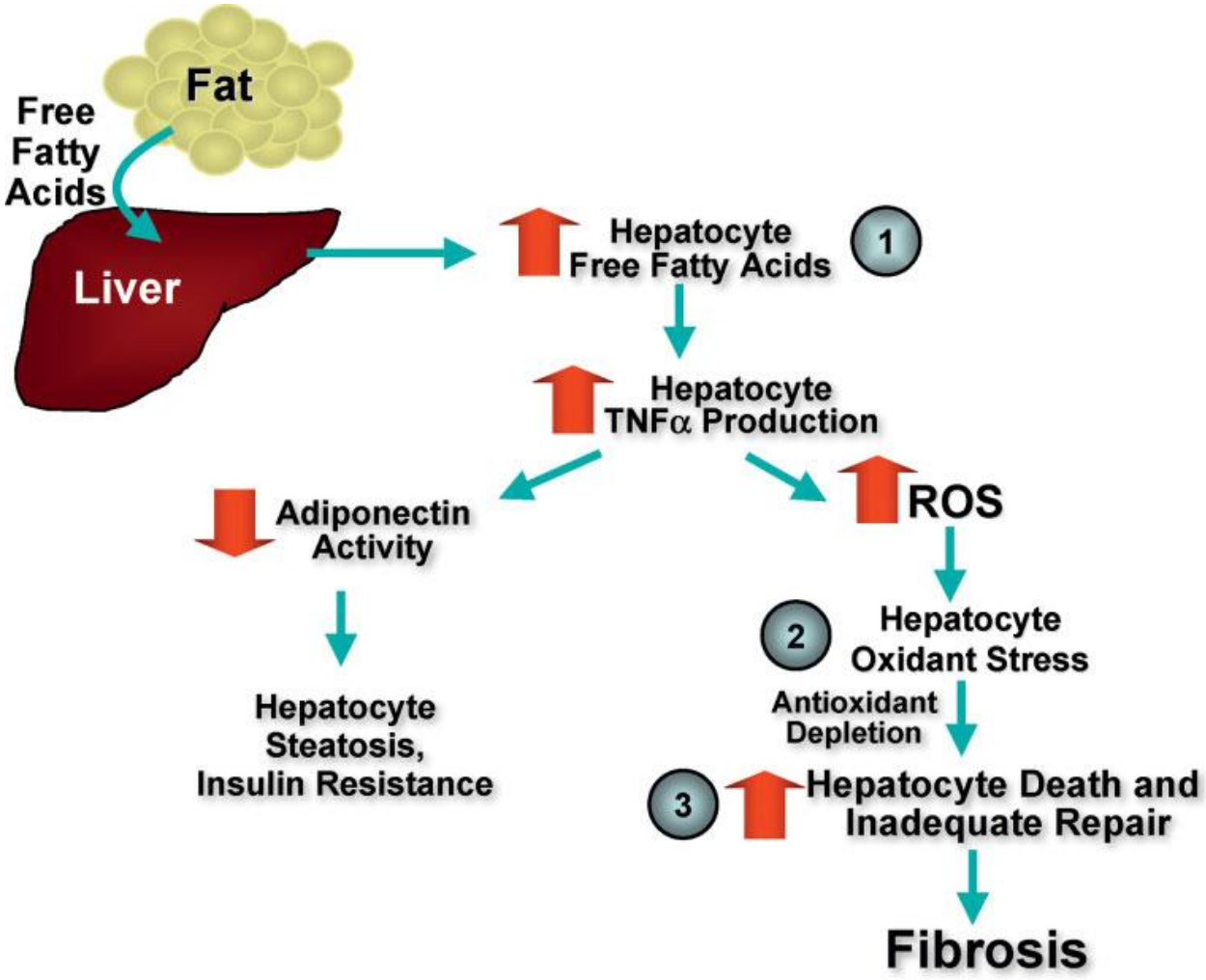

Figure 3*: Progression to fibrosis in nonalcoholic fatty liver disease (NAFLD). The first hit in NAFLD is increased accumulation of free fatty acid (FFA) and triglyceride in the liver resulting in steatosis (1). Increased hepatocyte oxidant stress can ensue to promote inflammation and hepatocyte death. This is typically considered to be the second hit (2). A suggested third hit in this sequence results from the inability to properly repair the hepatocyte cell death that ultimately results in fibrosis in the liver and progression of disease (3).*
Diehl et al. Mechanisms of disease progression in nonalcoholic fatty liver disease. Seminars in Liver Disease

Obesity is a complex condition largely defined by the accumulation of excess adipose tissue within the body that affects over one-third of the world's population (25). The most common measure or definition of obesity is the body mass index (BMI) (26). This utilizes the weight to height ratio and is calculated by the equation BMI = body weight (kg) / height^2 (m) or BMI = body weight (lbs) x 703 / height^2 (in) as a corollary to percent body fat in a population.

An index score between 18.5 and 24.9 is considered healthy while overweight is defined as a BMI between 25.0 and 29.9 (27). A BMI exceeding 30.0 indicates obesity. Although several classes of obesity exist, a BMI surpassing 40.0 is categorized as Class 3 or morbid obesity (26). Measurement of abdominal adiposity via waist circumference is also utilized in determination of obesity (28). Abdominal adipose tissue is thought to be primarily visceral fat that surrounds the organs and increases health risks (29). Abdominal adiposity is considered a waist circumference >94 cm in men or >80 cm in women and adults with excessive abdominal fat stores are said be "apple shaped" (27).

Obesity is the result of a positive energy balance. In short, energy balance is the equilibrium, or lack thereof, of calories metabolized (energy in) versus energy expended through activity and resting metabolism (energy out) to determine body energy content stored as fat mass (27). Whereas a negative energy balance indicates energy output exceeds energy input, resulting in weight loss, a positive energy balance demonstrates a greater energy input than energy output, leading to weight gain. However, these fluctuations in weight don't occur linearly due to powerful effects of energy expenditure (EE) on obesity pathogenesis.

This simplistic explanation understates the far more complex pathophysiology in obesity manifestation and places a disproportionate emphasis on energy intake without properly evaluating the energy expenditure components of the energy balance equation. However, measuring energy expenditure can be difficult because, unlike food intake studies, EE measures are typically made over a short period of time, such as a matter of hours up to a couple of days,

offering only a glimpse of the full picture (30). Body size also plays a fundamental role in EE determination. Due to an increase in overall metabolically active mass, larger animals typically have greater EE than smaller animals, who often exhibit greater per-kg rates of EE (31). This is due in large part to the larger surface area of their body relative to volume which increases heat loss and requires greater basal metabolic energy output for heat production to maintain body temperature homeostasis (27). Therefore, to assess if a change in EE invoked a change in weight for an experimental model, EE data must be adjusted to account for variations in body size.

A common practice to remedy this problem and allow for comparisons between groups without size disparities influencing results is to divide individual EE by either total body mass (TBM) or lean body mass (LBM) (32). Unfortunately, these formulas can offer different results and lead to conflicting conclusions. Specifically, the use of TBM in EE normalization can conclude that obese animals have a lower EE than lean animals because the total EE is divided by a denominator that is increased disproportionately to the relatively small increase in LBM (33). Additionally, normalization through the division of EE by LBM has also been shown to be confounded by both physiological and mathematical factors (34). It was determined that even if the effect of fat mass on EE were only a fraction of that in an equal amount of LBM, the inclusion of fat mass in comparisons of lean and obese animals was essential (35). Further analysis revealed the effect of fat mass on mouse energy expenditure was approximately 50% of the per-gram influence measured in LBM, illustrating the necessity of including fat mass in any EE normalization strategy (30). Isolating energy expenditure data during periods of

inactivity or rest eliminates variables such as activity and provides a clearer insight into the metabolic outputs when animals are sedentary.

This invokes the question of how adipose tissue can play such an influential role in EE determination despite itself having low EE. It is hypothesized that EE is indirectly coupled with fat mass through the negative feedback generated by hormones such as leptin and insulin proportionate to the level of fat mass that induce compensatory adjustments to affect energy balance and attempt to maintain the current amount of energy stored as fat (36). This proposes that a significant change in the amount of adipose tissue causes negative feedback signaling to alter energy input and energy output mechanisms to restore fat mass to its previous value.

However, this hormonal and biochemical feedback loop is not the exclusive control system for food intake and energy homeostasis as multiple other factors, such as composition of diet, environmental influences, and behavioral responses all play key roles. As such, experimental design dictates these conditions be strictly controlled for proper data collection. For example, the lower critical temperature of a mouse is approximately 30°C, but mice are typically housed in environments ranging from 20-23°C, indicating that more often animals are housed under mild thermoregulatory stress (37). Similarly, diet inconsistencies must be considered. A common oversight in diet compositions involves soy-isoflavone content within the control chow diet and its partial removal in protein extraction (37). This bioactive component has well-established involvement in estrogen receptor activation and AMPK,

therefore seasonal differences in soy-isoflavone content can considerably impact baseline measurements and affect interpretation of dietary effects. Experimental procedures and other stress-inducing events can also alter energy expenditure and necessitate a proper acclimation and recovery period (37). Animals housed in groups are susceptible to spilling of food in addition to aggressive behavior or social dominance from other animals within the cage, introducing considerable bias and variability in EE metrics (38). Group-housed animals also huddle together, reducing thermoregulatory requirements.

Another vital aspect in analysis of energy metabolism is consistent and accurate measurement techniques of food intake. A precise and repeatable process for EE determination is also needed. Indirect calorimetry calculates EE based on oxygen consumption and the amount of carbon dioxide produced (30). This utilizes a gas-tight metabolic cage through which fresh air is flowed, then the system measures the flow rate of the expired air and analyzes the concentration of the incoming and outgoing air for both CO_2 and O_2 (39). These methods of assessing energy expenditure inform on the pathogenesis of and contributors to obesity and shed a light on the manifestation and progression of other conditions associated with the disease.

A classical condition linked with both obesity and NAFLD in addition to type 2 diabetes, hypertension, and dyslipidemia is insulin resistance (40) (Fig 4). Just as overnutrition contributes to impaired lipid metabolism in NAFLD development, excess caloric consumption leading to weight gain and excessive growth of adipose tissue has a causal relationship with

decreased insulin sensitivity (41). However, expansion of visceral adipose depots significantly increases the risk of insulin resistance relative to other fat stores (42). Visceral adipose tissue is associated with increased waist and belly size given its location surrounding organs within body cavities, and is typically drained by the portal vein, exposing the liver to the plethora of adipokines and inflammatory cytokines released by the adipose tissue (43). This makes visceral adipose stores such as the mesenteric and epididymal fat pads key contributors to the development of obesity, NAFLD, and insulin resistance.

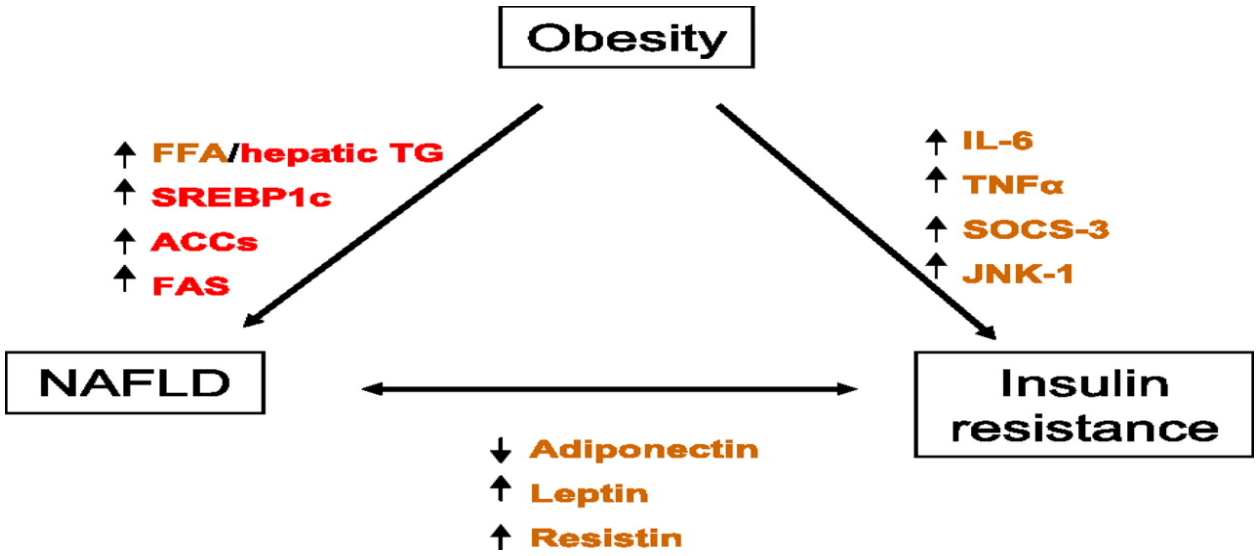

Figure 4: *The link between obesity, NAFLD, and insulin resistance*

Insulin resistance is considered a decreased disposal rate of glucose in response to a defined concentration of insulin (40), and can result from impaired insulin signaling and action within the liver, skeletal muscle, and adipose tissue (43). Within muscle insulin sensitivity is reduced, leading to decreases in glucose transport and glycogen synthesis (44). Treatment or culturing of myocytes with adipocyte-derived lipids decreases insulin sensitivity, reinforcing the concept that excess lipids and their metabolic derivatives impair insulin signaling within skeletal

muscle (45, 46). Hepatic insulin resistance causes uncoupling of glucose and lipid metabolism in the insulin signaling pathway, resulting in failed suppression gluconeogenesis without interrupting fatty acid synthesis, ultimately manifesting as hypertriglyceridemia and hyperglycemia (47). Insulin resistance within adipose tissue exhibits impaired inhibition of lipogenesis and impaired insulin-stimulated glucose transport via inhibition of the effects of glucose transporter 4 (GLUT-4) (48).

Consistent with observations in the pathogenesis of NAFLD and NASH, increased inflammatory cytokine secretions of TNF-α and IL-6 from visceral adipocytes draining into the portal vein contribute to insulin resistance (49). It was discovered using mice with fat transplanted into either the parietal peritoneum or the mesenterium, that only mice receiving the portal drained lipid transplant developed impaired glucose tolerance and hepatic insulin resistance. This supports the concept that excess visceral adipose tissue drainage into the liver causes insulin resistance (49). Similarly, increased visceral adipose depot and adipocyte size in humans has been shown to be directly related to systemic insulin resistance and immune cell expression of cytokines, reaffirming the link between inflammation and insulin resistance (50). A correlation between increased visceral fat quantities, adipocyte hypertrophy, insulin resistance, and increased expression of autophagy genes within the omental depot that begins near the stomach and spleen and extends to the ventral abdomen has also been discovered (51). The omental adipose depot has been well-linked to risk of developing obesity-related conditions, such as insulin resistance and fatty liver disease (52). Together, these results suggest that the increased inflammation and subsequent secretion of cytokines associated with

large quantities of visceral adipose tissue impair insulin signaling and contribute to systemic insulin resistance.

Inflammatory signals responsible for adipose inflammation are mediated by interleukin-1 receptor 1 (IL-1R1) as evidenced by IL-1R1 deficient mice fed a high fat diet exhibiting increased insulin sensitivity and decreased cytokine production relative to wild type animals (53). Similarly, reduction in adipose tissue expression of nucleotide binding domain, leucine-rich containing family, pyrin domain containing-3 (Nlrp3) inflammasome, an immune cell sensor that responds to metabolic danger signals such as lipids, is associated with improved insulin sensitivity as mice lacking Nlrp3 exhibit improved insulin sensitivity and reduced inflammation, even in a diet-induced obesity model (54). Specifically, it was shown that weight loss in obese individuals with type 2 diabetes was associated with reduced expression of Nlrp3 in adipose tissue and that Nlrp3 ablation in mice improved insulin signaling. Treatment of obese mice with resolvins, endogenous lipid mediators that promote inflammatory resolution, enhance insulin signaling in adipose tissue, improve glucose tolerance, and decrease fasting blood glucose levels (55). Anti-inflammatory agents have also illustrated improved glucose level control in human diabetics (56). Together, these results clearly illustrate the causal role of inflammation on insulin resistance.

Although inflammation is undeniably involved in the development of insulin resistance, enlarged adipocytes exhibit insulin resistance after short-term high fat diet without macrophage infiltration or eliciting an inflammatory response (57). After only three days mice on a high fat diet displayed insulin resistance in both wild-type and inflammation-resistant

animals, indicating that at least the initial stage of obesity-induced insulin resistance does not require inflammation. It is believed that excess lipid accumulation within adipocytes and ectopic lipid accumulation in liver and skeletal muscle promote insulin resistance through the formation of metabolically toxic products, such as increased ceramide production from saturated fatty acids (58). Similarly, adipose triglyceride lipase (ATGL) and hormone sensitive lipase (HSL) convert triacylglycerol to diacylglycerol. Elevated expression of ATGL and HSL in skeletal muscle increases diacylglycerol accumulation, impairing insulin signaling (59). Increased hepatic diacylglycerol content is also strongly correlated with insulin resistance (60). Liver examination from obese, non-diabetic individuals found hepatic diacylglycerol content to be the best predictor of insulin resistance, and to also be strongly correlated with activation of hepatic PKCε (60). Therefore, it is proposed that the products of incomplete fatty acid oxidation may impair one or more steps in the insulin signaling cascade and that lipids may activate signaling pathways, such as one or more of the protein kinase C (PKC) proteins that negatively impact insulin signal transduction (43).

A critical factor in protecting against insulin resistance is the ability of adipose tissue to expand and form new adipocytes. This adipose tissue expandability allows for the accumulation of excess energy stores and protects against adipocyte hypertrophy and ectopic lipid accumulation in the visceral adipose tissue, liver, and muscle (61). Although the precise mechanisms that underline adipose tissue expandability are unclear, the capacity to remodel the extracellular matrix and increase capillary vascularization for nutrient and oxygen supply, as seen in any growing tissue, are involved (43). Hypoxia within adipose tissue of obese individuals has also been illustrated (62). Insulin sensitivity was positively correlated with tissue

oxygen partial pressure and capillary density, suggesting that low capillary density contributes to adipose tissue dysfunction (63). Hypoxia within adipose tissue is also believed to initiate abnormal remodeling of the extracellular matrix, leading to inflammation and fibrosis (64). This suggests that the expansion of capillary networks within expanding adipose tissue plays a crucial role in the prevention of inflammation, hypoxia, and fibrosis. This assertion is supported by the discovery of a positive correlation between the angiogenic capacity of subcutaneous tissue and insulin sensitivity in morbidly obese individuals, suggesting the pathogenesis of metabolic disease is due in part to insufficient angiogenic growth within adipose tissue (65). These findings underscore the importance of clarifying the factors that determine the ability of the individual to expand adipose tissue. The identification of adipocyte progenitors within the stromo-vascular fraction of macrophages harvested from mice suggests natural variation in the number of progenitor cells, as well as the ability of adipocytes to differentiate from these progenitors as key determinants (66, 67).

Investigation into therapeutic strategies for improving insulin sensitivity can heighten understanding of the mechanisms linking insulin resistance, obesity, and NAFLD. The commonly performed Roux-en-Y gastric bypass procedure has been shown to resolve type 2 diabetes in patients (68) and use of hyperinsulinemic-euglycemic clamps illustrated improved adipose tissue insulin sensitivity and reduced lipolysis (69). Although the procedure results in altered gut anatomy leading to caloric restriction and significantly reduced absorption, this bypass of the upper intestinal tract does not explain the immediate improvement observed in glycemic control, leaving the mechanisms that lead to this dramatic improvement in glucose homeostasis unclear (43). However, other bariatric procedures that do not include

gastrointestinal bypass in addition to the partial removal of subcutaneous (liposuction) or visceral (omentectomy) adipose depots do not improve insulin sensitivity (69-71). Although caloric restriction has demonstrated the ability to reduced adipose cell quantities in both skeletal muscle and adipose tissue itself, weight loss due to exercise in previously sedentary individuals illustrated almost double the effect (72). MRI analysis of intermuscular and visceral adipose tissues in sedentary patients subjected to caloric restriction or exercise-induced weight loss revealed comparable degrees of weight loss in both groups and greater loss of intermuscular and visceral adipose tissue in addition to enhanced insulin sensitivity in the exercise-induced group (72). Similarly, acute and chronic exercise in a diet-induced obesity rat model resulted in improved insulin signaling via suppression of inflammatory signaling in the liver, muscle, and adipose tissue (73). These findings indicate increased activity can modulate some of the negative conditions associated with diet-induced obesity.

The association between obesity and fatty liver disease highlights the importance of nutrition in disease pathogenesis. Feeding studies provide insight into the development of these conditions; however, assessment of feeding behaviors in laboratory animals can be complex. Studies of energy homeostasis and food intake in mouse models are widely accepted as obesity often arises from environmental variables such as diet composition, ambient temperature, and time of feeding (74). One of the many considerations when determining adiposity in both human and mouse models is that body adiposity is determined by the active and upward regulation of the defended level of body fat stores, not simply by passive accumulation of excess calories as fat (74). For example, if an animal experiences weight maintenance or weight loss during hyperphagia, the increased food intake is probably

secondary to increased energy expenditure, reflecting a properly functioning regulatory system that differs significantly from the underlying mechanisms driving hyperphagia in conditions associated with obesity. Similarly, hyperphagia associated with uncontrolled diabetes is a secondary manifestation of a metabolic disease as it arises in conjunction with decreased adipose mass and can be improved through restoration of regulatory hormone concentrations such as insulin and leptin (75).

Conversely, when hyperphagia is observed in conjunction with obesity, conventional wisdom says that the latter is due, at least in part, to the former. A less intuitive and often debated topic in obesity models is the merit to the normalization of food intake to body weight in the same manner that is often seen in energy expenditure measures. An argument in opposition of this practice is that differences in body weight can reflect differences in both lean body mass and fat mass, requiring normalized values be interpreted differently when comparing lean and obese animals (74). Additionally, normalizing food intake by simple division presumes that intake is regulated as a function of change in body weight, which is often not the case (74). For example, food intake normalized to body weight in leptin-deficient mice can lead to the conclusion that the mice are either hypophagic or hyperphagic relative to controls depending on the age at which measurements are taken, even if absolute intake does not change. At a young age the relative increase of food intake exceeds the weight increase, but as weight continues to rise with age body weight exceeds the increase in food intake, despite nonnormalized food intakes revealing mice to be hyperphagic at any age (74). Given these considerations the normalization of food intake to body weight is not recommended, especially in models of obesity.

Another consideration for obesity studies is the strain of mouse used as subtle genetic, dietary, and pharmacological manipulations can widely impact phenotype depending on the animals' background. The C57BL/6 mouse was the first strain to have its genome completely sequenced and is susceptible to diet-induced obesity (DIO), making it the most commonly used model in energy homeostasis studies (76). Models of obesity that are diet-induced are preferable to genetically-induced obese mice as DIO animals have greater relevance to common forms of obesity seen in humans as the DIO phenotype arises from both genetic susceptibility and exposure to calorically dense diets that are high in fat and refined carbohydrates (74). The DIO mouse model also eliminates a major source of experimental variability as it allows for comparisons between lean and obese animals that are genetically identical.

Due to the effects of the estrous cycle on many key determinants of energy expenditure and balance, male mice are preferred in studies relating to obesity (77). Body composition and fat distribution also differs among the sexes as female mice and humans have a greater percentage of body fat relative to males, but a lesser amount of fat deposition within the abdomen (74).

Inadvertent and designed experimental stressors such as routine handling, noise, or placement in a different cage can also have profound impacts on study results as stresses influence all aspects of energy homeostasis, such as locomotor activity, energy expenditure, and food intake (78). Many study endpoints and physiological markers such as circulating glucose and insulin levels are also sensitive to stress (74). To minimize stress, animal handling should be limited to a few experienced individuals (79).

A significant difference between mice and humans to consider in these studies is the meal patterns in animals. Under a typical 12 hour light/ 12 hour dark cycle mice consume the vast majority of their food in the dark with only short bouts of feeding during the light according to the averages across 13 different strains from the Jackson Laboratory Mouse Phenome Database (74). Obese hyperphagic mice can exceed expected food intakes and demonstrate increased feeding during the light cycle (74). Water consumption is also strongly linked with food intake and dramatically decreases in food-restricted or fasted animals (74). To eliminate extraneous variables that influence food intake, feeding behavior studies are typically conducted in singly-housed animals. A simple test to ensure the feeding behavior is normal and homeostatic regulation of food intake is intact is to measure refeeding after fasting the animal until body mass returns to the prefasted level. Another option is to assess the response to a high fat diet (HFD) as lean mice typically become hyperphagic within 48 hours and begin to gain body weight beyond that of control mice on a standard chow diet (80).

It has also been demonstrated that *ad libiutm* access to a HFD causes obesity, insulin resistance, hypercholesterolemia, dyslipidemia, and hepatic steatosis (81). Similar access to a high-fructose diet without elevated fat content does not cause increased adiposity, but does lead to glucose intolerance and hepatic steatosis (82). Unfortunately, pharmacological agents designed to offset many of the detrimental effects associated with nutrient imbalance and excess typically only treat one aspect of the underlying metabolic condition and are often short lived (83). Lifestyle interventions such as changes in diet composition, reduced caloric intake, and increased exercise are common, but remarkably ineffective with success limited to a small percentage of individuals (84).

Interventions involving recent discoveries that many metabolic pathways have diurnal rhythms offer an innovative strategy for prevention and treatment of obesity and associated metabolic diseases (85, 86). The cyclical expression of metabolic regulators coordinates a wide range cellular process to improve metabolic efficiency under healthy conditions, but in DIO models this regulation is blunted (87). Therefore, restoration of this diurnal regulation is believed to be an effective treatment to counter the negative effects seen in nutrient imbalance.

Extensive assessment and profiling of metabolic regulators revealed that a defined period of feeding and fasting throughout the day is a prominent determinant of diurnal rhythms in metabolic pathways (88). Accordingly, intervention consisting of restricted feeding to an 8 hour period when mice are most active (night) demonstrated the ability to prevent the adverse effects of DIO with a HF diet without altering caloric intake or nutrient content in the food (89). A much larger and more extensive study evaluated the effectiveness of restricted feeding, or meal timing (MT), against multiple diet types and eating patterns in more than 300 C57BL/6 mice (90). Given that increased fructose consumption is implicated with the increasing obesity rates (91), mice were subjected to *ad libitum* or MT feeding of a high fat plus high sucrose diet (32% energy from fat, 25% energy from sucrose) (90). Despite the access to food only during a nine hour period during the dark phase for MT animals, both groups consumed the same amount of calories yet MT animals gained significantly less weight (90). This demonstrates that MT effectively attenuates body weight gain in 12 week old mice fed diets rich in fat and sucrose. Investigation of the efficacy of MT over extended durations of time

restricted feeding discovered that longer daily HFD feeding times resulted in larger increases in body weight, effectively minimizing the beneficial effects seen in meal timing.

The ability of MT to offset interruptions in the restricted feeding schedule was also assessed (90). Mice on MT diet for five days and allowed *ad lib* access the following two days still showed incredible reductions in weight gain relative to controls (29% weight gain in MT animals and 61% weight gain in controls constantly with *ad lib* access). However, over a larger period of time (13 weeks MT followed by 12 weeks *ad lib*) there was no reduction in weight compared to animals without restricted access over the 25 week period. Meal timing also showed the ability to reverse weight gain in preexisting DIO by imposing restricted access to food after mice had become obese (90). Body composition assessment via MRI revealed significantly reduced levels of fat mass in MT animals and increased duration of access to food resulted in a linear increase in percentage of fat mass. Similar to body weight, animals on MT for five days followed by a two day break had less percentage of fat mass than chronic *ad lib* access. This decrease in fat mass was also observed in preexisting DIO animals. These reductions were confirmed via histological examination. H&E staining of the liver in DIO animals on constant *ad lib* HF diet showed increased inflammation and mRNA levels of proinflammatory cytokines, while mice with restricted access did not exhibit these markers of inflammation (90). Meal timed animals all showed reduced total triglyceride and lipid accumulation in the liver compared to *ad lib* mice. Animals with restricted access to food also demonstrated improved glucose homeostasis and the ability to reverse previously established glucose intolerance induced by DIO. It has been proposed that meal timing can protect mice

on a HFD from obesity and its associated conditions by reducing insulin signaling during fasting and switching energy usage from glucose to fat stores (90).

Previous studies have clearly demonstrated a strong link between the manifestation and pathogenesis of obesity, insulin resistance, and NAFLD. Increased adiposity from high fat and high sucrose in the diet is associated with chronic inflammation and impaired lipid metabolism, contributing to hepatic steatosis, steatohepatitis, and insulin resistance. The presence of sucrose-rich drinking water in conjunction with a HFD has also illustrated the ability to exacerbate and accelerate the progression of NAFLD in DIO mice beyond that seen in only HFD models, implicating sugary drinking water as a key contributor to disease pathogenesis. Timed restricted feeding of a high fat diet has illustrated the capacity to reduce weight gain, attenuate metabolic disease development, and reverse the progression of metabolic diseases in mice with preexisting obesity.

It is our goal to determine the effect of meal timing on feeding and drinking behavior, activity, substrate utilization, and energy expenditure as it relates to the accelerated development and progression of non-alcoholic fatty liver disease observed in a high fat diet with sugary drinks. The rationale for adding carbohydrates to the drinking water is to replicate a high fructose corn syrup drink which has been found in combination with a high fat diet to induce steatohepatitis in mice. The limited success of weight loss therapies and the lack of approved therapeutic treatments for steatohepatitis make time-restricted feeding an innovative strategy for prevention and treatment of obesity and obesity-related metabolic diseases, including non-alcoholic fatty liver disease.

II. Materials and Methods

Animals and Diets

For the purposes of this study, C57Bl/6 mice were singly housed in standard microisolator cages within the Greene Hall Annex of the Veterinary Research Building (VRB), College of Veterinary Medicine, Auburn University (AU-CVM) upon arrival from the Harlan distributor. Animals were fed standard facility chow for one week during acclimation to the facility. After the one week acclimation period, the mice remained on the standard chow diet or received a High Fat Western Diet (HFWD) with sugar-containing drinking water (HF+S) for 12 weeks. The chow diet (Teklad Global Rodent Diet 2018) contained 24% of calories from protein, 18% from fat, and 58% from carbohydrate. The HF+S diet was based on the AIN-93G diet and consisted of 44% carbohydrate, 16% protein, and 40% fat, 30% of which was provided from lard, 30% from butterfat, 30% from Crisco, 7% from soybean oil and 3% from corn oil. Calculations based on diet compositions reveal that the chow diet equals 4.9 kcal/g while the HF+S diet contains 6.0 kcal/g, indicating that the chow diet contains just under 82% of the calories compared to the high fat diet. The HF+S diet also included 42g/L fructose/sucrose (55%/45%) in the drinking water. All diets provide water (regular and sugar-containing) ad libitum.

A total of 22 animals completed the study. Due to a limited number of metabolic cages, only 19 of the mice were transferred to the metabolic cages for data collection while the remaining four animals were only subjected to physiological assessments. Specifically, 4 chow-

fed animals, 7 HF+S animals, and 8 MT animals were in metabolic cages while an additional mouse in each diet group underwent evaluation for the physiological parameters. An eighth mouse in the HF+S group was originally included but died during the insulin tolerance test. Additionally, another four mice from the chow group were expected to be included in the study. However, this litter of animals exhibited abnormal behavior, including extreme food intake, constant activity, and aggression during the one week acclimation period and were subsequently removed from the study

At seven weeks, half of the animals on HF+S diet were selected for meal timing (MT), meaning that access to their HF+S diet would be regulated and limited to certain times. After eight weeks, animals in the MT group began meal timing. A two-day period between return to the microisolator cages from the metabolic cages and the start of meal timing was given in order for the animals to acclimate to the change in environment. Food was completely removed from the cages of MT animals at 5:15 am and returned at 8:15 pm every day. This ensured animals only had access to food at night, forcing the animals to practice traditional feeding habits of eating during the night. When MT animals were in the metabolic cages the food hopper was completely removed and returned at the appropriate times. Food was removed by hand and placed in individual zip lock bags when animals were in their microisolator cages. Animals in the chow and HF+S groups had continuous access to food throughout the study. Although access to food was limited in MT animals, access to the sugary drinking water was not restricted and was constantly available.

Metabolic Cages

Eight of the Promethion 3721 Mouse Cages (Fig 5) were utilized to house animals for the purpose of metabolic screening and phenotyping. Animals were transferred from their microisolator cages and singly housed in the metabolic cages at multiple time points. At seven weeks animals were put in metabolic cages (Monday) and given one day to acclimate to the environmental change. The following day (Tuesday) data collection within the cages began and ran for three days (Friday) at which point animals were returned to their previous microisolator cages. This process was repeated at 12 weeks.

The cages themselves monitor activity, food and water intake, body mass, and gas exchanges to determine energy expenditure and substrate utilization as depicted in Figure 5. The BXYZ Beambreak Activity Monitor enables real time analysis of total activity with a 0.25cm calculated centroid. Promethion Metabolic Screening features high precision MM-1 Load Cell sensors for measuring real time food intake, monitoring both individual feeding bouts and total food intake. Water uptake also utilizes MM-1 Load Cell sensors and provides time monitoring, allowing for drip mitigation that differentiates between drinking bouts and dripping events. Promethion body mass monitors are in-cage enrichment devices attached to a universal MM-1 load cell. The body mass monitor allows the real time recording of body mass when the animal interacts with the device and can be synchronized with metabolic movement to provide energy expenditure information. The Promethian GA-3 gas analyzer includes water vapor, CO_2, and O_2 analysis to provide detailed respirometry information.

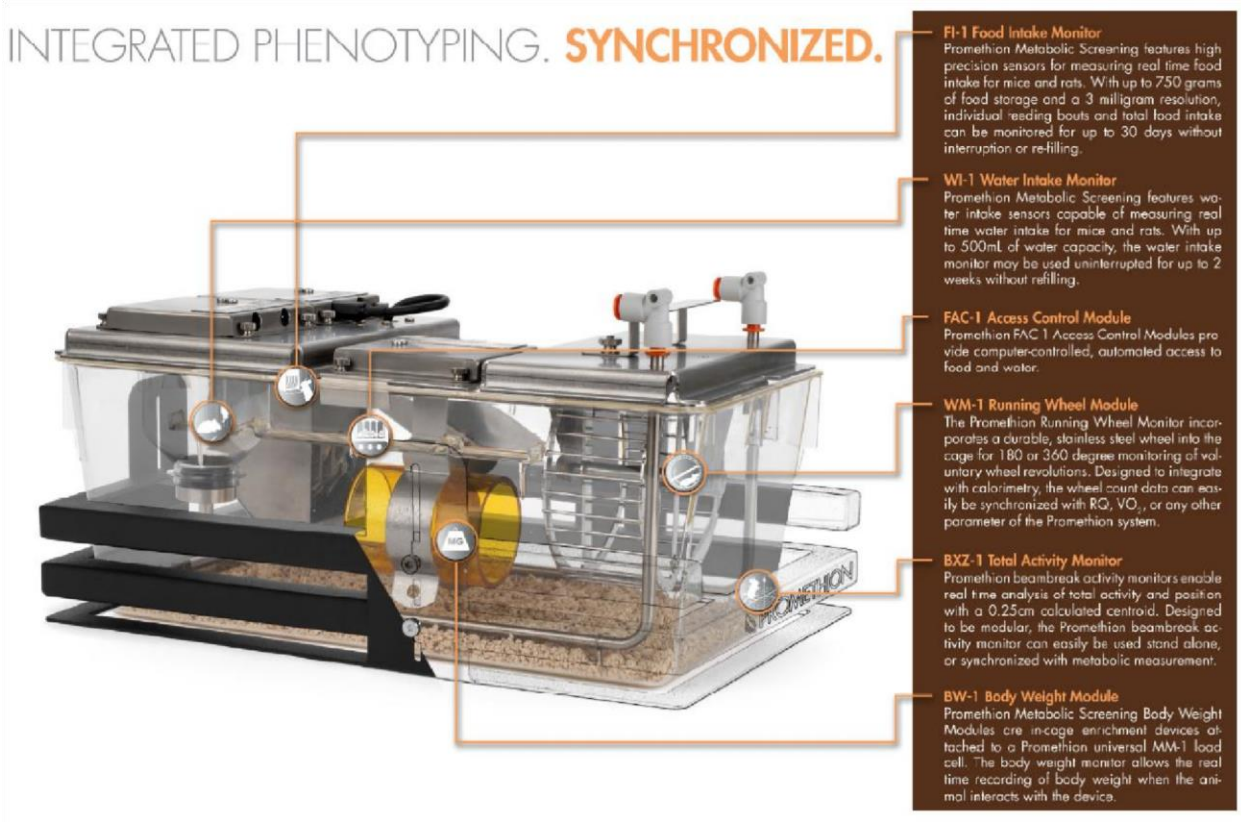

***Figure 5**: Overview of Promethion 3721 mouse metabolic cage*

Food Uptake

Within the metabolic cages, the amount, frequency, duration, and rate at which food was withdrawn from the food hopper was measured and analyzed. The composition of the food within the food hoppers did not impact the process by which the data was collected.

Specifically, food amount, labeled UptakeA_Sum within the Expedata-provided macros, was the summation of all food removed from an individual food hopper. Measured in grams, this value was calculated by multiplying the food uptake rate with the total number of feeding bouts for a food hopper (UptakeA_Sum = UptakeA_g * UptakeA_N). UptakeA_g, the food uptake rate, is defined as the mean rate of food uptake in g, while UptakeA_N, feeding frequency, is defined as the total number of feeding bouts. A feeding bout is considered an interaction with the food hopper in which food is withdrawn and does not include brief interactions by the animal. These feeding bouts consist of an event with the food hopper lasting a minimum of 30 seconds and a maximum pause of 150 seconds. Uptake exceeding 1 g in a single interaction with the food hopper is not considered a feeding bout and therefore not included in UptakeA_N data and subsequently excluded from UptakeA_Sum calculations, as removal of such a large quantity of food exceeds daily consumption and does not indicate feeding, but rather suggest stockpiling or hoarding of food. Food intake duration, labeled UptakeA_Min, represents the average food intake duration in minutes for each individual food hopper. During meal timing, the entire food hopper was removed while its accompanying sensor was detached from the food hopper and returned to the metabolic cage. This process

ensured a level of consistency with the cages and allowed the cages to continue to make readings despite the removal of the food hoppers rather than change the settings during a run or potentially have to start a new run once the food hoppers were removed. By briefly suspending the readings from the food uptake modules while the food hoppers were removed then resuming their activity, the food uptake modules provided a continuous stream of data for a single run. This ability for the food hoppers to continually make their readings' on schedule allowed for the collection of data over three consecutive days with very mild interruption. Animals that were not meal timed did not have their food uptake readings suspended at any time. As previously described, animals that were meal timed had their food removed at 5:15 am CST and had it provided at 8:15 pm CST.

Manual Food Uptake

Prior to putting animals in the metabolic cages their food intake measured manually. For animals entering the metabolic cages at seven weeks, food intake was manually measured the morning of in addition to the morning and evening prior to animals being put into the metabolic cages. Animals entered the metabolic cages for analysis at 7 weeks at 3:00 pm CST on Monday February 16, February 23, and March 2. Therefore, food uptake for these animals were determined at 7:00 pm CST Sunday February 15, February 22, and March 1 in addition to 7:15 am CST both February 15 and 16, February 22 and 23, and March 1 and 2. Measurement of food was determined by placing the food from each animals' microisolator cage on a balance and recording its mass in grams.

Water Uptake

Water uptake determinations utilized the same calculations and criteria as food uptake. The amount, frequency, duration, and rate at which water was withdrawn from the water hopper was assessed. The absence or presence of sugar within the drinking water did not alter the mechanisms in which values were obtained. Similar to food uptake amount,

UptakeW_Sum, indicating the total amount of water withdrawn from each individual water hopper, measured in g and was calculated by multiplying the water uptake rate with the total number of drinking bouts (UptakeW_Sum = UptakeW_g * UptakeW_N). UptakeW_g, water uptake rate, represents the mean water intake in g and is calculated similarly to food uptake. Water uptake frequency, UptakeW_N, represents the number of drinking bouts or significant interactions with the water hopper. The criteria for an interaction to be considered a drinking bout includes an interaction with the water hopper a minimum of 10 seconds with a maximum pause of 30 seconds. Uptake exceeding 1 g in a single bout was excluded from the UptakeW_N and UptakeW_Sum data sets. Water intake duration, UptakeW_Min, is defined as the mean water intake duration in minutes.

Behavior

The behaviors of the animals immediately following interaction with the food hopper and water hopper were observed and analyzed to determine the most likely activity or behavior following an eating or drinking event. When in the Promethion system metabolic cages,

animals are constantly interacting with the various sensors in their cages - the mass sensors attached to their food and water dispensers, their body mass sensor, and the X-Y-Z open-field position sensors. This abundance of analytics allows for the construction of detailed analytics of the animal's behavior. With each interaction precisely recorded every second, the mouse's transitions between different behaviors are very obvious, the times at which they occur are precisely known, and they are quantifiable. Utilizing ExpeData's EthoScan automated behavior analysis software, outputs of behaviors are generated. Each behavior has a five letter code (Table 1):

EFODA	Interaction with food hopper A (significant uptake found)
TFODA	Interaction with food hopper A (no significant uptake)
DWATR	Interaction with water dispenser (significant uptake found)
TWATR	Interaction with water dispenser (no significant uptake)
IHOME	Entered habitat (stable mass reading)
THOME	Interaction with habitat (no stable mass reading)
LLNGE	Long lounge (> 60 sec
SLNGE	Short lounge (5 - 60 sec

***Table 1**: Behavioral codes*

Each behavior has a start and end time and date, a duration in seconds, and an "amount", a quantification based on the behavior - body mass for IHOME, mL of water consumed for DWATR, grams of food eaten for EFODA, and centimeters locomoted for SLNGE.

Time budgets including total minutes and percent of a 24 hour day spent on each individual behavior are provided in addition to a "transition matrix" that illustrates the behavior that occurs next. Specifically, after a certain event or activity takes place, the probabilities of every other behavioral event occurring are provided. Based on the quantification of every interaction and beam break, the frequency at which an animal engages in any other activity after a feeding or drinking event is provided. This data was collected and averaged over a 24 hour period. Animals on MT diet only had access to their food hoppers from 8:15 pm CST to 5:15 am CST, only 9 of the possible 24 hours (37.5%).

Activity

The Promethion beam break activity monitors provide real time analysis of total activity and position with a 0.25cm calculated centroid. This system allows for the quantification and analysis of total distance traveled, pedestrian locomotion distance and mean speed, number of beam breaks along the X, Y, and Z axis, percentage of time spent "quiet" or stationary, and the percentage of time spent sleeping. Measured in cm, ped meters is the summation of all X and Y beam breaks that are a minimum of 1.0 cm. Units are then converted to meters. Ped speed uses a 1cm/sec cutoff and linearly transforms all samples to a slope of 0.1 and intercept of 0, ultimately providing the mean rate of pedestrian locomotion in m/s. All meters is the summation of all X, Y, and Z beam breaks without a minimum distance. Also utilizing the XY array data, still percentage is calculated from the differentiated all meters data, so that any moment of coarse of fine movement is recorded. This differentiated all meters data is

transformed to have an intercept of 1 and slope of 0. Sleep percentage is calculated the same way, however, a stationary or quiet period must exceed 40 seconds to count as sleep.

Energy Expenditure

Energy expenditure was calculated in kcal by utilizing the Weir equation: 60*(0.003941*VO2_{n}+0.001106*VCO2_{n}) in which VO_2 is the oxygen uptake and VCO_2 is the carbon dioxide output, both of which are measured in ml/min. Total energy expenditure is the summed amount for an entire day or night cycle, while average energy expenditure is the mean value per hour (Avg_EE = Tot_EE / 12). Resting energy expenditure (QR_EE_30) is the mean value from the isolated 30 minute period in which the activity score was lowest.

Substrate Utilization

Respiratory quotient was determined by measuring gas exchange within the metabolic cages to identify the substrate being primarily utilized for energy within the body. Specifically, RQ is the ratio of CO_2 produced to the volume of O_2 consumed (RQ = VCO2 / VO2). Given the molecular formula for glucose ($C_6H_{12}O_6$) specifies there are equal quantities of carbon and oxygen, an RQ of 1.0 indicates carbohydrate utilization. Although the molecular formula varies among different lipid types, fats contain considerably fewer oxygen atoms in proportion to atoms of carbon and hydrogen, thus require more oxygen to oxidize fat to carbon dioxide and water. For example, palmitic acid has a formula of $C_{16}H_{32}O_2 + 23\ O_2 \rightarrow 16\ CO_2 + 16\ H_2O$,

equaling a value of 0.696. Therefore, an RQ of 0.7 is indicative of the utilization of lipid for energy.

Physiological

Animals were weighed every Monday afternoon at 3:00 pm to collect body mass and weight gain information.

Glucose tolerance tests (GTT) were conducted three days prior (Tuesday) to animals entering the metabolic cages (Friday) at the 12 week mark, beginning at 8:00 am and concluding by 11:00 am. Animals were fasted at 5-6 pm the day prior (Monday) to the test. The animals were each weighed to determine the proper dosage of glucose to inject for each animal (0.04 X mouse weight (g)/5 = ml 25% glucose to inject). Prior to glucose administration a blood sample was taken to assess baseline serum glucose concentrations. Collection of venous blood was achieved by nicking the tail with a small razor blade. Glucose was administered to the animals via intraperitoneal injection and blood samples were collected 15, 30, 60, and 120 minutes after injection to assess the ability of each animal to clear glucose from the blood.

Insulin tolerance tests (ITT) were conducted one day prior (Thursday) to animals entering the metabolic cages (Friday) at the 12 week mark, beginning at 1:00 pm and concluding by 4:00 pm. Animals were fasted at 8:00 am the day of the test. The animals were each weighed to determine the proper dosage of insulin to inject for each animal (0.0085 X mouse weight (g) = ml insulin to inject). Prior to insulin administration a blood sample was taken to assess baseline serum glucose concentrations. Collection of venous blood was achieved by nicking the tail with a small razor blade. Insulin was administered to the animals

via intraperitoneal injection and blood samples were collected 30, 60, 90, and 120 minutes after injection to assess the sensitivity to insulin in each animal.

Tissues

Collection and harvesting of tissues requires euthanasia of the animal. Animals were sacrificed by decapitation via guillotine. All mice were fasted at 5:15 am on the day of the procedure. All mice were removed to VRB 203. Mice were placed in an atmosphere of high CO_2 in a specifically-constructed sterile container. Thirty to forty seconds of exposure was sufficient to give an anesthetic response deep enough to properly position the animal for decapitation in the guillotine.

After euthanasia, the epididymal, retroperitoneal, and inguinal fat pads were all manually removed from the animals' body cavity and weighed. As shown in Figure 6, the epididymal fat pad is located next to the testes, retroperitoneal is behind the kidneys, and inguinal fat pad is subcutaneously located under the skin of the lower abdomen, extending to the groin. The liver was also harvested and weighed.

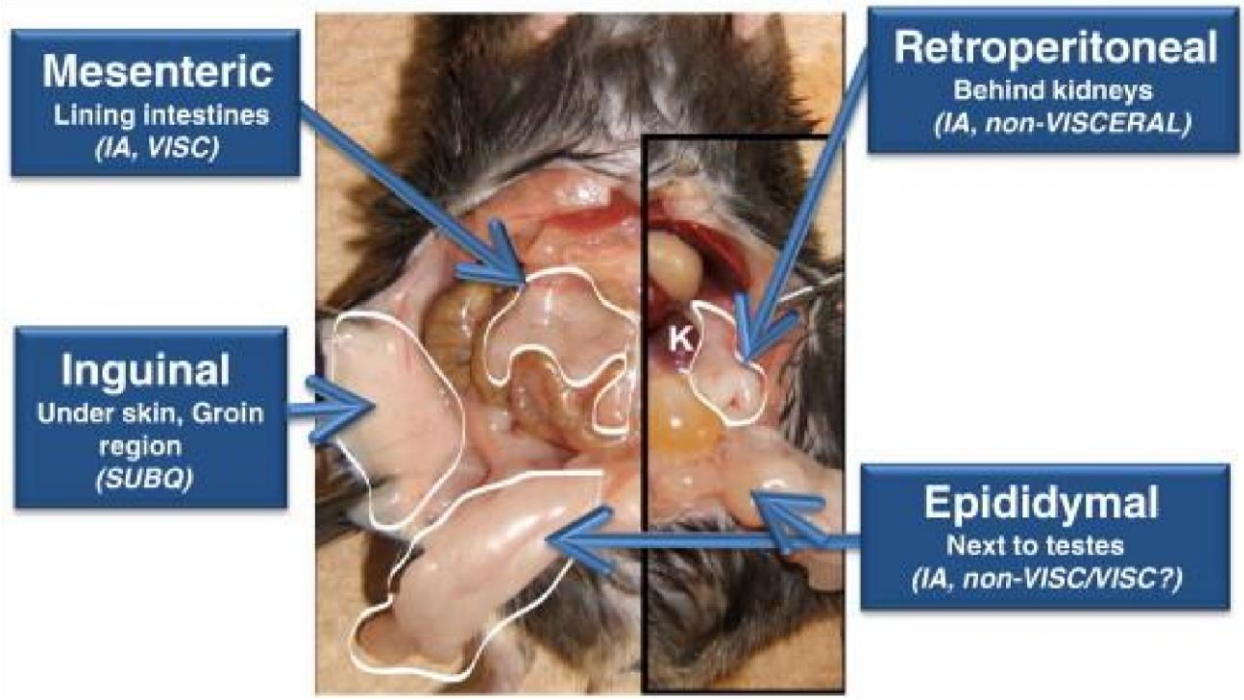

***Figure 6**: Overview fat pads in C57Bl/6 mice*

Following decapitation, blood was collected from the head of the animal to characterize the metabolic phenotype. Plasma glucose, triglyceride, and cholesterol were measured with a Lipid Panel test strip using a Cardio check PA analyzer.

Statistics

ANCOVA

Multiple linear regression analysis was employed to assess the impact of body mass on diet and metabolic cage parameters. Utilization of the National Mouse Metabolic Phenotyping Centers (MMPC) Energy Expenditure analysis page

(https://www.mmpc.org/shared/regression.aspx) allowed for the assessment of covariates, such as mass, on energy expenditures, food and water uptake, and diet. A p value greater than 0.05 indicates a significant difference exists between the specific parameter and diet after body mass is removed from consideration. Conversely, $p < 0.05$ illustrates that body mass is driving the differences for each parameter across dietary groups. This analysis investigated the relationships at 7 and 12 weeks for the average, resting, and total energy expenditures, food intake amounts from the metabolic cages and manual measurement, and total water intake against body mass and diet.

ANOVA

To test for statistical significance of multiple groups and determine if the means of several groups are equal, multiple analysis of variance, or ANOVA, tests were performed. These ANOVA results inform if differences exist, but are nonspecific as to which groups are different from which other groups. As such, the Newman-Keuls (SNK) Post-hoc test was performed to analyze the differences between categories with 95% confidence intervals ($p < 0.05$). Analysis

of the 24 hour cycle data required the use of a repeated measures ANOVA. This allowed for animals in one diet group to be compared with animals in another diet group at corresponding time points within the 24 hour cycle.

III. Results

All 22 animals were weighed weekly to collect body mass and weight gain information (Fig 7). Unsurprisingly, chow-fed animals had significantly lower body mass (29.7 g) than HF+S (42.5g) and MT (39.6 g) groups ($p < 0.05$). Animals on MT diet also had significantly lower body mass than HF+S animals. Weekly weight gain by HF+S and MT groups were nearly identical until week 8 when weight gain decreased in the MT group relative to HF+S animals. Chow-fed animals illustrated significantly less weekly weight gain than HF+S and MT animals at a relatively consistent rate for all 12 weeks.

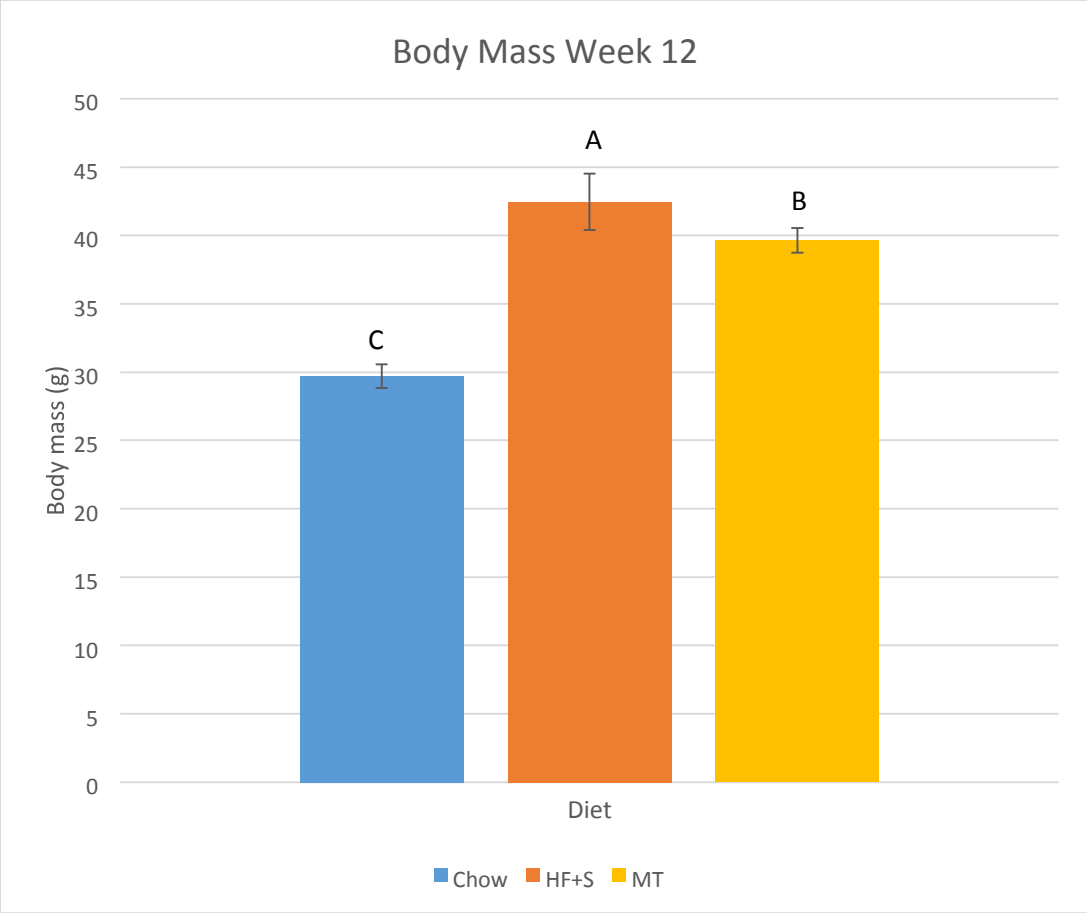

***Figure 7**: Body mass of animals at 12 weeks*

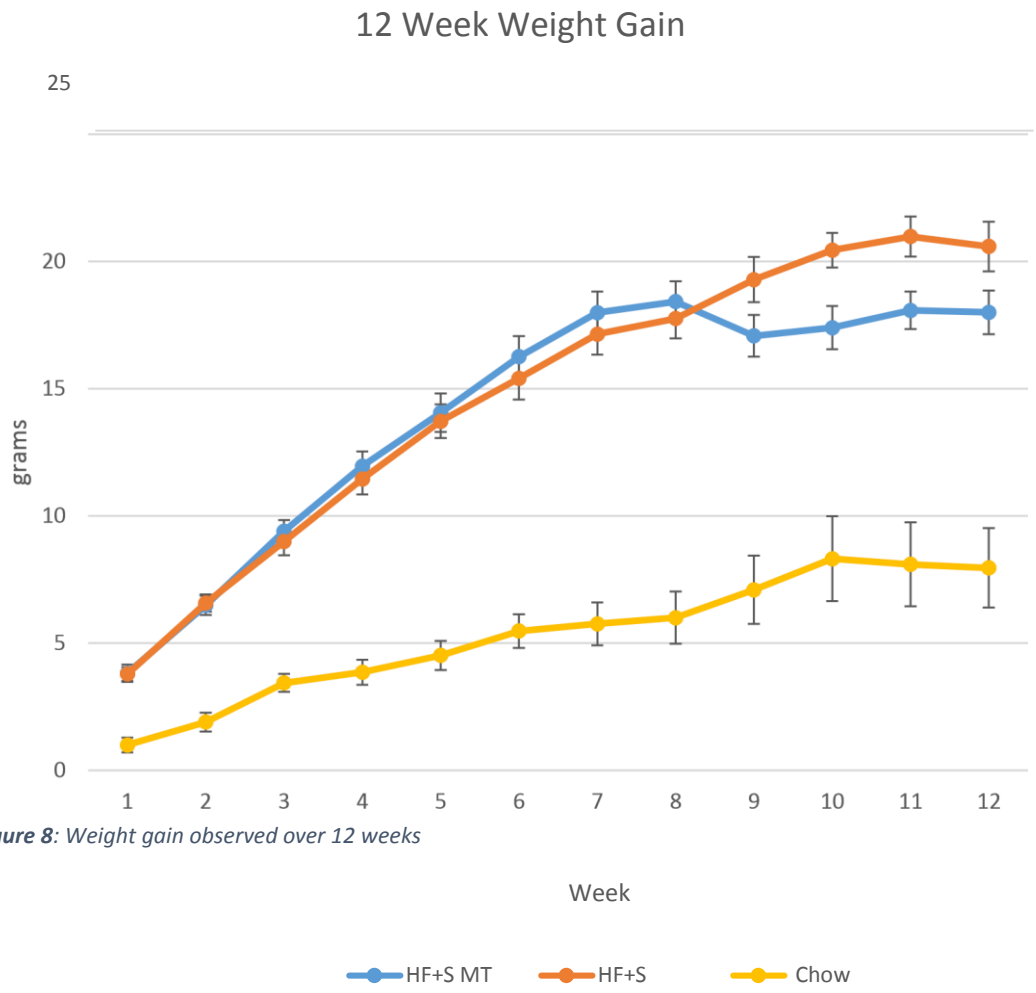

***Figure 8**: Weight gain observed over 12 weeks*

As expected the high fat diet in both HF+S and MT animals led to significantly greater body mass compared to chow-fed animals (Fig 8). The significant reduction in body mass observed in MT animals compared to the HF+S group clearly indicates meal timing leads to decreased body mass. This is confirmed by the weekly weight gain data. Weight gain is nearly identical between the MT and HF+S groups until meal timing is introduced at seven weeks. After meal timing begins weight gain begins to plateau then decreases, leading to considerably reduced weight gain over the final four weeks. Therefore, although a high fat diet with sugar added to the drinking water leads to significantly greater body mass and weekly weight gain

compared to a chow diet, meal timing of this HF+S diet significantly reduces both body mass and weekly weight gain.

Food Intake

As previously described, the amount, frequency, duration, and rate at which food was withdrawn from the food hopper within the metabolic cages was analyzed. Data for each of these parameters were collected at 7 and 12 weeks of age and organized based on diet type and time of day.

Regarding food uptake amount, the most obvious observation from this data is that the vast majority of food was consumed at night, regardless of age or diet (Fig 9). Concerning data collected at seven weeks, animals on chow diet consumed an average of 3.6 g at night and the significantly less amount of 0.3 g during the day ($p < 0.05$). This equates to 92% of food uptake occurring at night for animals on a chow diet. Conversely, animals on the HF+S diet at seven weeks had an intake of 1.3 g at night and the significantly less amount of 0.6 g during the day ($p < 0.05$), indicating only 68% of food intake occurred at night. Although daytime consumptions for both diets were not significantly different, a stark difference existed between nighttime food intakes as animals on chow diet (17.6 kcal) consumed a significantly greater amount than the HF+S group (7.8 kcal) ($p < 0.05$). Total intake for chow-fed animals also greatly exceeded that of HF+S groups (3.9 g and 1.9 g, respectively). Analysis of covariance determined that the relationship between body mass and diet regarding food intake amount was not significant when comparing the chow and HF+S diet during the day ($p = 0.33$) and at night ($p = 0.20$). This indicates that body mass is driving the differences in overall food consumption.

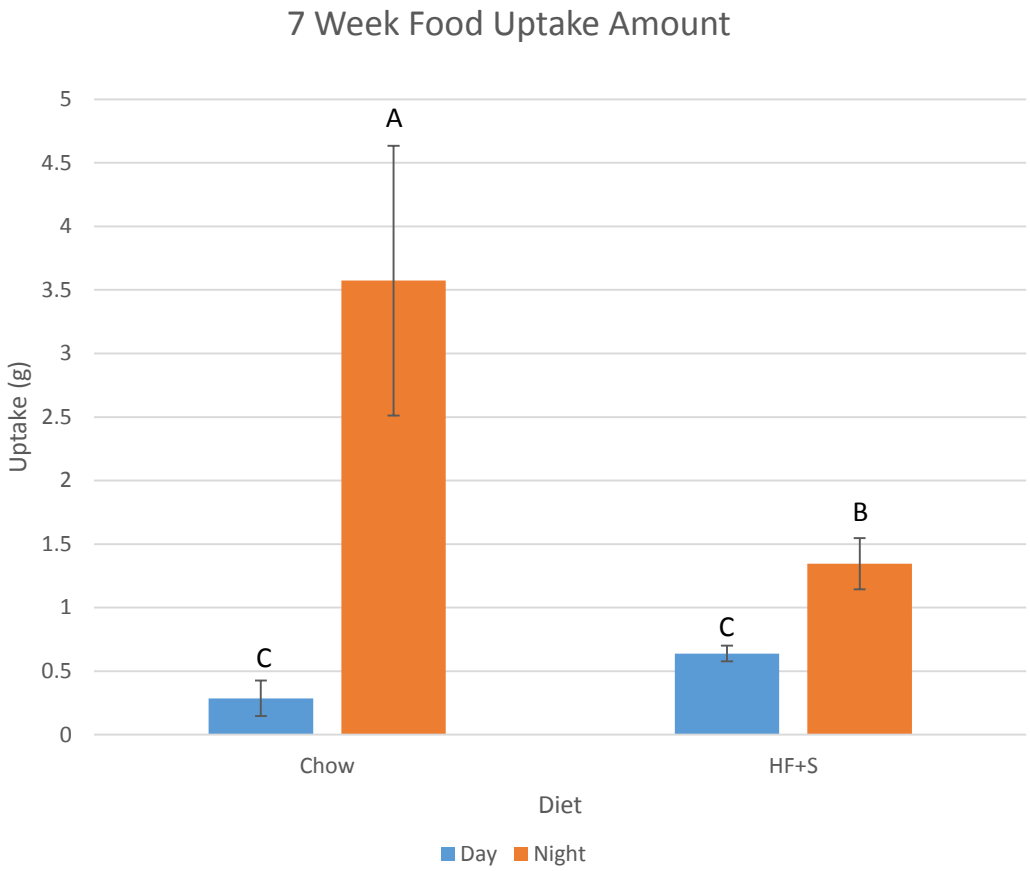

Figure 9: *Total amount of food eaten by animals at 7 weeks*

Furthermore, the results at 12 weeks were remarkably similar to the findings at 7 weeks (Fig 10). Daytime consumption among the chow, HF+S, and MT groups were not statistically different. Given that MT animals did not have access to their food hoppers during the day and had an intake of 0 g, the quantity of food consumed at this time by the other groups is negligible. At night the intake from the HF+S and MT groups were not statistically different, with the HF+S group reaching 1.8 g and MT animals ingesting 2.1 g of food. Animals of the chow diet had significantly greater nighttime consumption (14.7 kcal) compared to the HF+S (10.8 kcal) and MT diets (12.6 kcal) ($p < 0.05$), averaging 2.9 g. There are no apparent differences in the food intake amounts within dietary groups when comparing the seven week

data with the data collected at 12 weeks. Similarly, the ANCOVA revealed no significant differences between any of the diet groups during the day (chow vs HF+S p = 0.73, chow vs MT p = 0.42, HF+S vs MT p = 0.88) or at night (chow vs HF+S p = 0.92, chow vs MT p = 0.60, HF+S vs MT p = 0.53).

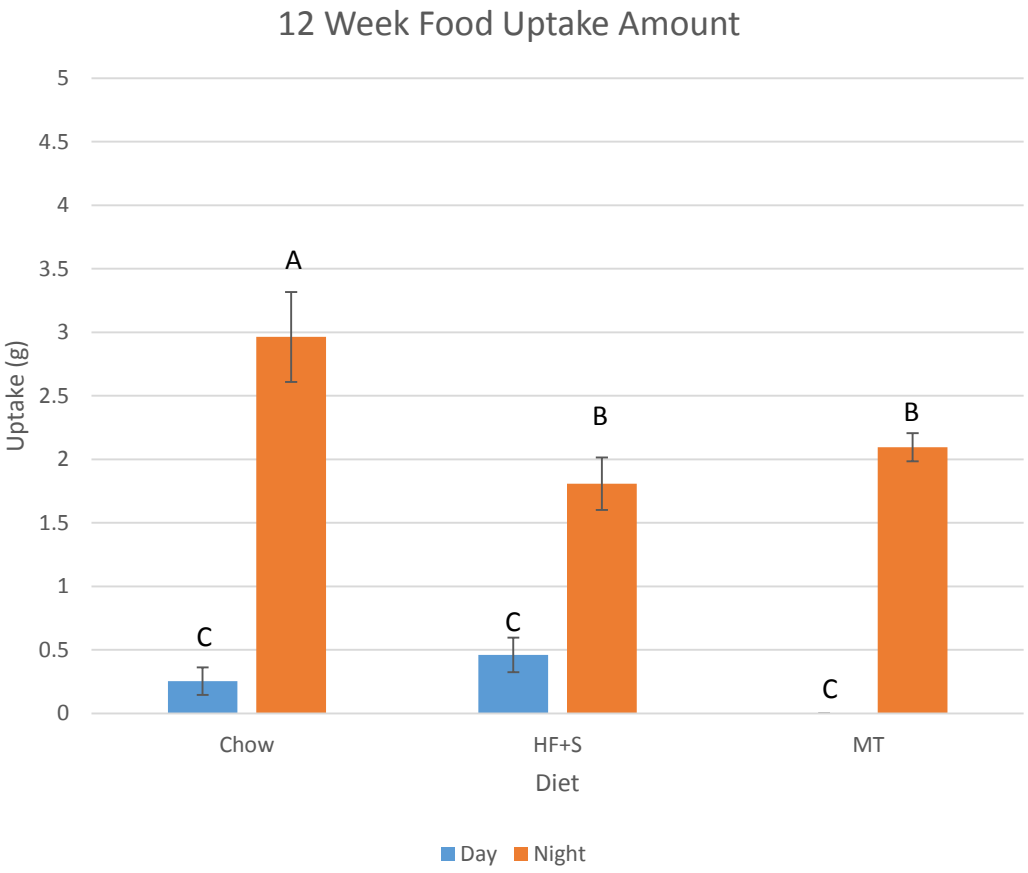

Figure 10: *Total amount of food eaten by animals at 12 weeks*

The majority of food consumption occurring at night is not surprising given that the animals are nocturnal. A review of the literature (90) indicated the ability of meal timing to negate the development and progression of adverse side effects associated with HF diet. The literature, as well as previous findings and observations by the Greene laboratory (data not

shown), revealed that animals on HF diets have an increased occurrence of daytime feeding while chow-fed animals exhibit more traditional eating habits in that food consumption takes place almost exclusively in the nighttime. In light of this, it was expected HF+S fed animals would not only have greater total food intake, but also significantly greater daytime food intake than animals on the chow diet, whose intake was expected to occur nearly entirely at night. Additionally, it was proposed the meal timed animals on the HF+S diet would more strongly resemble the eating habits of those on the chow diet compared to HF+S diet fed animals.

Although the vast majority of intake of the chow diet taking place at night was expected, the profound disparity in total intake was a surprise. It is important to note that several animals on the HF+S diet displayed an inclination for removing a large portion of their food from the hopper and leaving it scattered about their cage. Although withdrawals greater than or equal to 1 g were not treated as feeding events by the food hopper modules, the removed food was still present within the cage and available for consumption by the animals. This is believed to account for the dramatic difference in total food consumption between the two diets. This substantial removal and hoarding of food was only seen in the brief time the animals spent in the metabolic cages and did not occur when the animals were in their typical microisolator cages.

Given the proximity in nighttime intake amounts between MT and non-MT animals on HF+S diets, it is evident that meal timing did not significantly affect food consumption. The presence of HF food during the day also did not significantly increase the amount of daytime

consumption as food intake during the day between MT and non-MT animals were both in essence zero.

The analysis of the number of feeding events revealed results essentially identical to the food uptake amount findings. At seven weeks the frequency at which animals interacted with the food hopper was significantly greater at night than during the day in both diet groups (Fig 11) ($p < 0.05$). Similarly, the number of feeding events during the day was not significantly different between diet groups as chow-fed animals interacted with the food hopper an average of 5.2 times, while HF+S fed animals visited the food hopper 7.9 times on average. Also in agreement with the food intake amount results, the chow diet group averaged significantly more (29.2) feeding bouts compared to the chow group (14.0) at night.

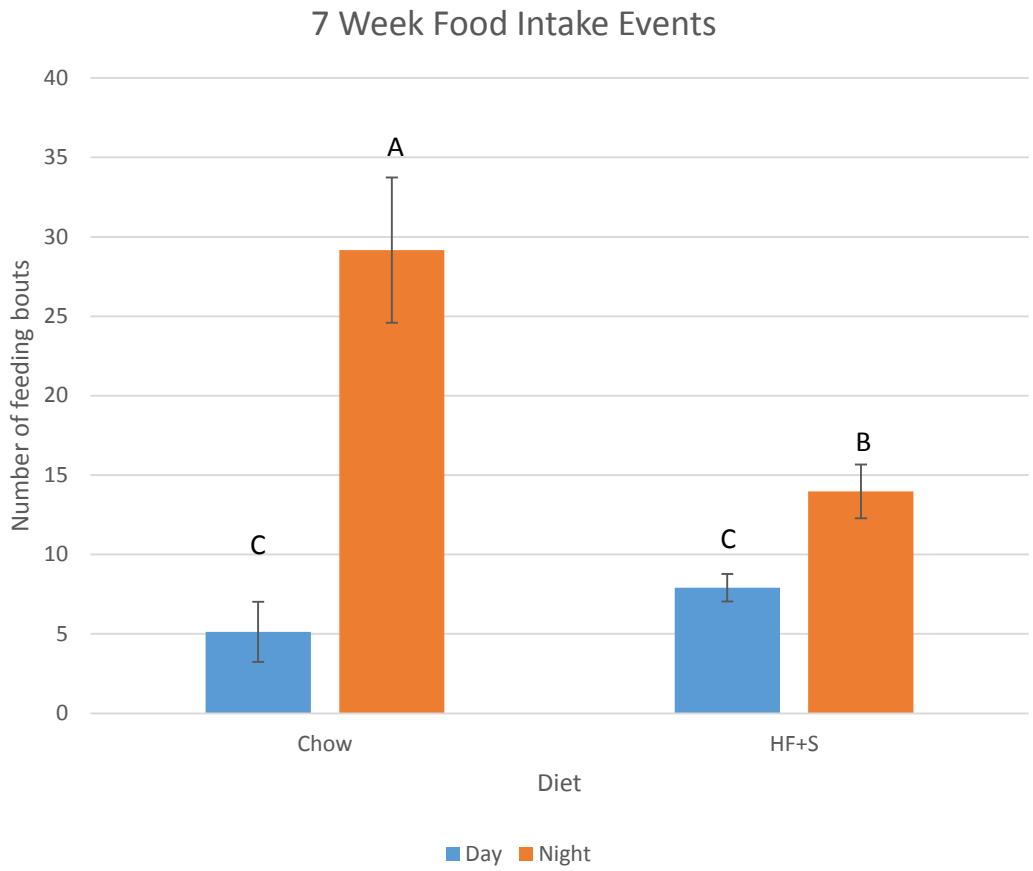

Figure 11: *Total number of feeding events at 7 weeks*

The food intake frequency results at 12 weeks are also strikingly similar to the food intake amount findings (Fig 12). The only difference between groups not seen in the food intake amount analysis was that the number of feeding bouts during the day was significantly greater in both the chow and HF+S diet groups compared to the MT group. In accordance with the food intake amount results, the 16.0 feeding bouts seen at night on average in MT animals was not significantly different from the 15.4 feeding bouts displayed in the HF+S group. However, although MT animals did display a similar number of feeding bouts at night compared to HF+S animals, the absence of a food hopper during the day allowed for more total feeding bouts in the HF+S group ($p < 0.05$). Interestingly enough, the food uptake amounts between

the two groups were not significantly different from one another during the day or at night. The food intake frequencies for both the HF+S and MT animals at night were significantly less than the 25.583 feeding bouts seen with chow-fed animals ($p < 0.05$). With the exception of the food hopper being removed, the number of feeding bouts for each dietary group does not appear to change from 7 to 12 weeks.

Figure 12: *Total number of feeding events at 12 weeks*

The results of the food intake frequency and food intake amount assessments were fundamentally the same. The fluctuations in the number of feeding bouts between time of day and dietary groups are in complete agreement with the total amount of food consumed. This

indicates that the number of feeding bouts for an animal is directly proportionate to their food intake at that particular time. The fact that the number of feeding bouts during the day for both the chow and HF+S groups at 12 weeks were significantly greater than the zero feeding bouts seen in MT animals that had their food hoppers removed suggests that although the animals did occasionally interact with the food hoppers, the amount of food withdrawn was minimal. Meal timing does not appear to impact the number of feeding bouts and food intake frequency is consistent at both 7 and 12 weeks for all of the diet groups.

The rate at which food was taken in at seven weeks did deviate from the pattern seen with the previous two parameters (Fig 13). The intake rates per interaction with the food hopper during the day for chow and HF+S fed animals (0.05 g and 0.09 g, respectively) were not significantly different than each other or the nighttime intake rate of 0.1 g for HF+S fed animals. The food intake rate of 0.12 g for the chow group at night was significantly greater than all other groups ($p < 0.05$).

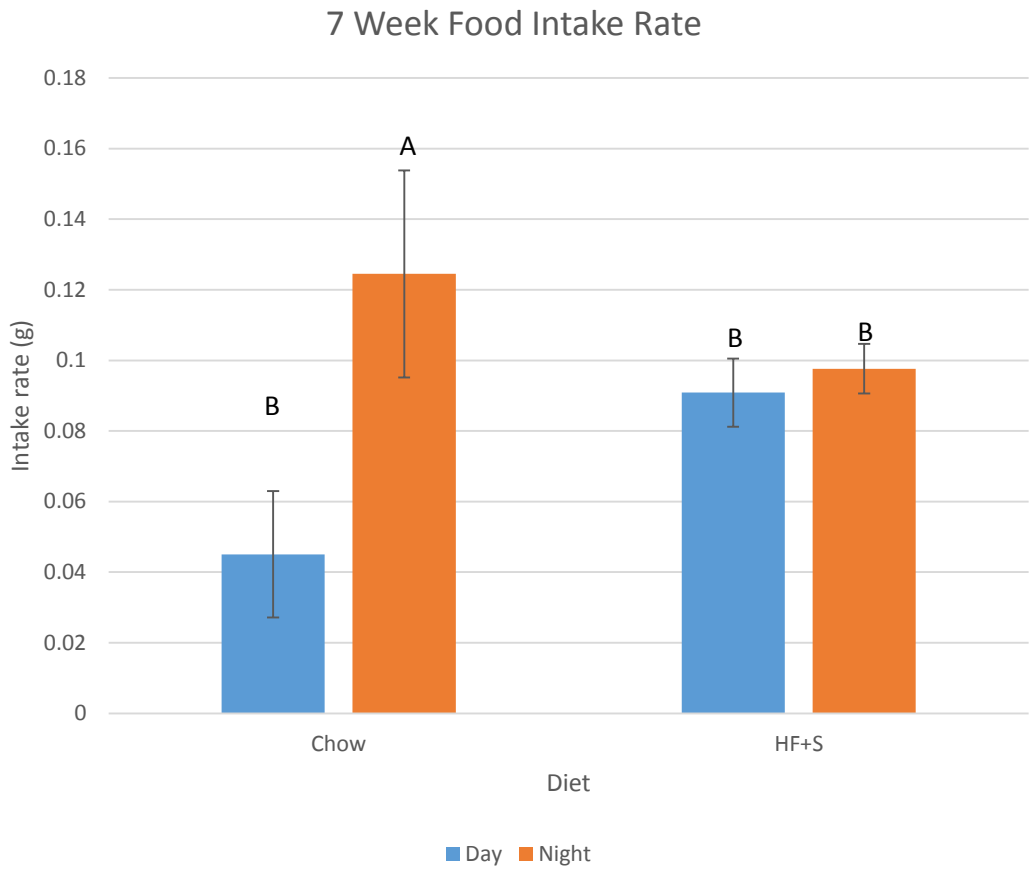

Figure 13: *Rate at which food was consumed at 7 weeks*

At 12 weeks there was no significant differences in food uptake rate between the three dietary groups at night, indicating that MT did not affect the food intake rate (Fig 14) ($p > 0.05$). The rates of 0.11 g for chow, 0.13 g for HF+S, and 0.14 g for MT were also not significantly different from the 0.10 g food intake rate exhibited during the day for animals on the HF+S diet. Furthermore, this HF+S daytime intake rate was not significantly different than the chow daytime intake rate of 0.05 g, although this daytime chow intake rate did differ significantly from the nighttime feeding rates ($p < 0.05$). The food intake rate of 0 g for MT animals was also significantly different than all other data.

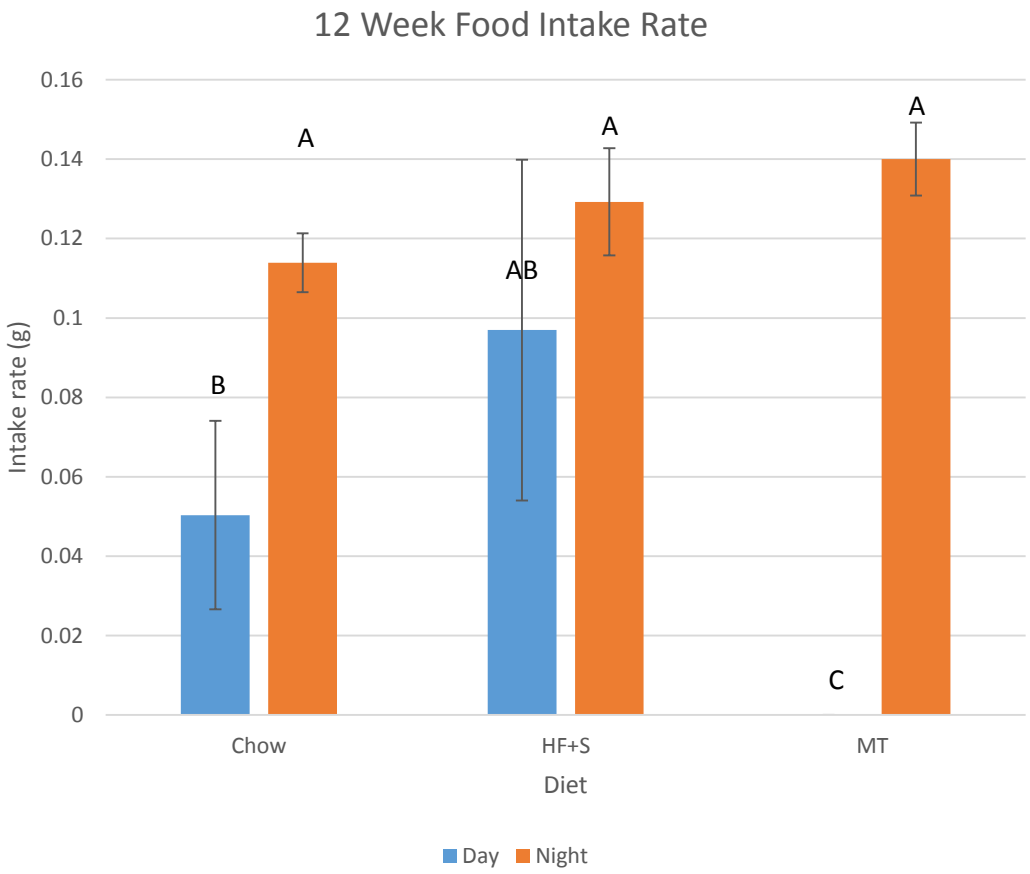

Figure 14: *Rate at which food was consumed at 12 weeks*

Chow-fed animals displayed consistent feeding behaviors as their intake amount, frequency, and rate are all greatest at night and significantly less during the day, illustrating the expected and more traditional eating habits seen in nocturnal animals of eating almost entirely at night. Although the frequencies and quantities of food consumed by animals on HF+S diet varied from the chow group, food intake rate during the day for both groups as well as nighttime HF+S were similar, suggesting that the amount of food consumed is not dependent entirely on intake rate and other parameters are also involved. The consistent food intake rate

at night, when the majority of food is consumed, across all diet groups indicates that although diet does influence the amount of food taken in, the rate at which it is consumed does not appear to be impacted. The invariable daytime food intake rate at both 7 and 12 weeks in both chow and HF+S diets supports this conclusion. Once again, MT did not impact the food intake parameter.

Food uptake duration measurements at seven weeks (Fig 15) generally did not differ across groups in that the 3.9 minutes spent interacting with the food hopper during the day for chow-fed animals was remarkably similar to the 3.8 and 3.6 minutes for animals on HF+S diet during the day and at night, respectively ($p < 0.05$). At night, the chow group spent a significantly greater amount of time feeding than other groups ($p < 0.05$), averaging 9.5 minutes interacting with the food hopper.

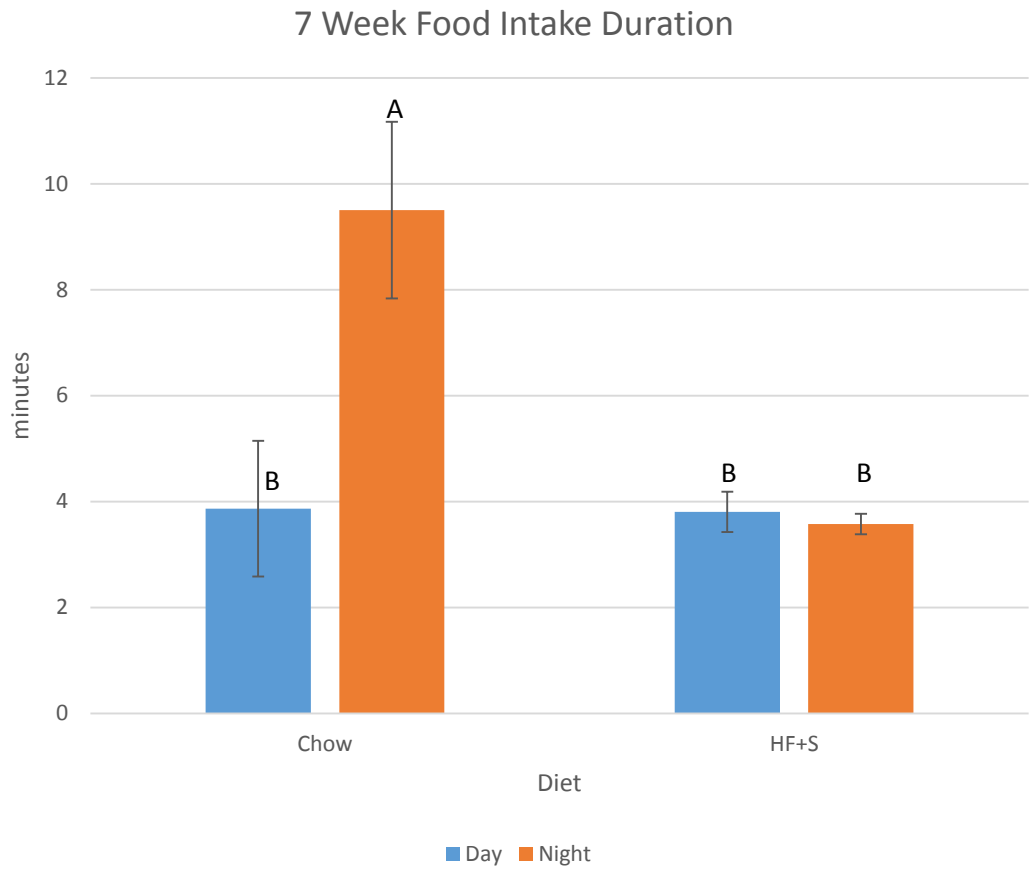

Figure 15: *Total amount of time spent feeding at 7 weeks*

The findings at 12 weeks (Fig 16) were similar in that there was very little difference in food intake duration between any of the diet groups, regardless of time of day. Meal timing did not have an effect on food intake duration, as the MT and HF+S groups displayed averaged nightly feeding durations of 3.6 and 3.5 minutes, respectively. These values did not significantly differ from the 2.6 and 4.5 minute-long periods spent interacting with the food hopper for the HF+S and chow diet groups during the day. However, all of these average times spent feeding were not only significantly greater than MT animals that did not have access to their food hoppers during the day, but they were all significantly less than the 8.9 minutes on average chow-fed animals spent feeding at night ($p < 0.05$).

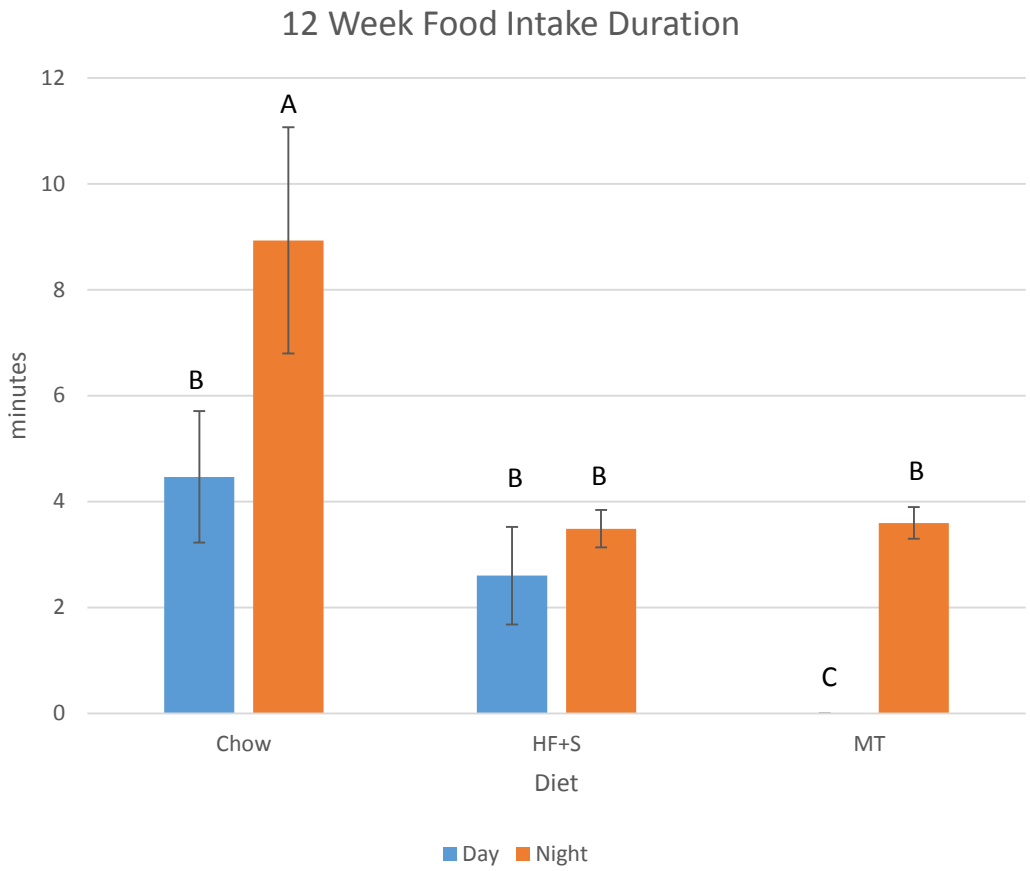

Figure 16: *Total amount of time spent feeding at 12 weeks*

With the exception of the chow group at night, there is no difference in food intake duration at 7 weeks or 12 weeks, suggesting that food composition does not impact the amount of time spent feeding. Meal timing did not alter the amount of time animals spent feeding. Although the durations at night for MT and HF+S fed animals were incredibly similar, animals fed a HF+S diet did spend more time overall feeding as MT animals did not have access to their food hoppers during the day. This signifies that limited or restricted access to food does not influence the rate at which food is consumed, whenever it is present.

Overall, little difference was seen at 12 weeks between MT and HF+S fed animals. Meal timing did not appear to have any impact on feeding habits or tendencies. Despite the inability to access food during the day, MT animals consumed food in comparable quantities, rates, durations, and frequencies to HF+S animals at night. The food intake amounts over 24 hours were also not different, indicating the access to food during the day is not necessary and providing food only at night does not alter feeding habits. As expected, animals on the chow diet displayed traditional eating habits seen in nocturnal animals at both 7 and 12 weeks. Their food consumption was limited almost entirely to the night with minimal interaction with the food hopper during the day. Because of this propensity to eat exclusively at night, their intake quantities, rates, durations, and frequencies were greatest at this time. HF+S animals did not display these classical eating habits. Rather, HF+S animals illustrated decreased inclination for nighttime feeding relative to chow-fed animals. However, the HF+S group did not display greater daytime feeding as expected as there was little difference between the two groups, thus failing to account for the greater food intake seen in chow-fed animals compared to HF+S animals over a 24 hour period. It is unclear to what extent the tendency of animals fed HF+S diet to remove abnormally large portions of food from their hopper at once influenced the collected food intake data. Analysis of covariance found no significant differences between the body mass, diet, and food intake amount parameters, and determined that body mass was driving the differences observed in food consumption at both 7 and 12 weeks across all dietary groups.

Manual Food Uptake

At seven weeks animals fed a chow diet consumed 0.15 g of food during the day and 3.40 g at night, totaling 3.55 g over a 24 hour period (17.4 kcal) (Fig 17). Animals on a HF+S diet also consumed a disproportionate amount of their food at night (2.17 g) compared to the day (1.0 g), totaling 3.17 g (19.02 kcal) over a 24 hour period. Surprisingly, nearly all of these values were significantly different from one another ($p < 0.05$). Although the miniscule amount of food consumed during the day for the chow group was significantly less than all other intakes, the nighttime consumption of the same dietary group was not significantly different than the total amount of food consumed for the chow or HF+S groups. Interestingly enough though, the total amount of HF+S food consumed was significantly less than the total amount of chow food ingested. Despite elevated daytime consumption in the HF+S group, this quantity of food was significantly less than the amount of HF+S food consumed at night. ANCOVA calculations revealed no significant differences in daytime ($p = 0.82$), nighttime ($p = 0.76$), or total consumption ($p = 0.95$) when comparing animals on chow diet to those fed HF+S, implicating body mass as a key determinant in food uptake.

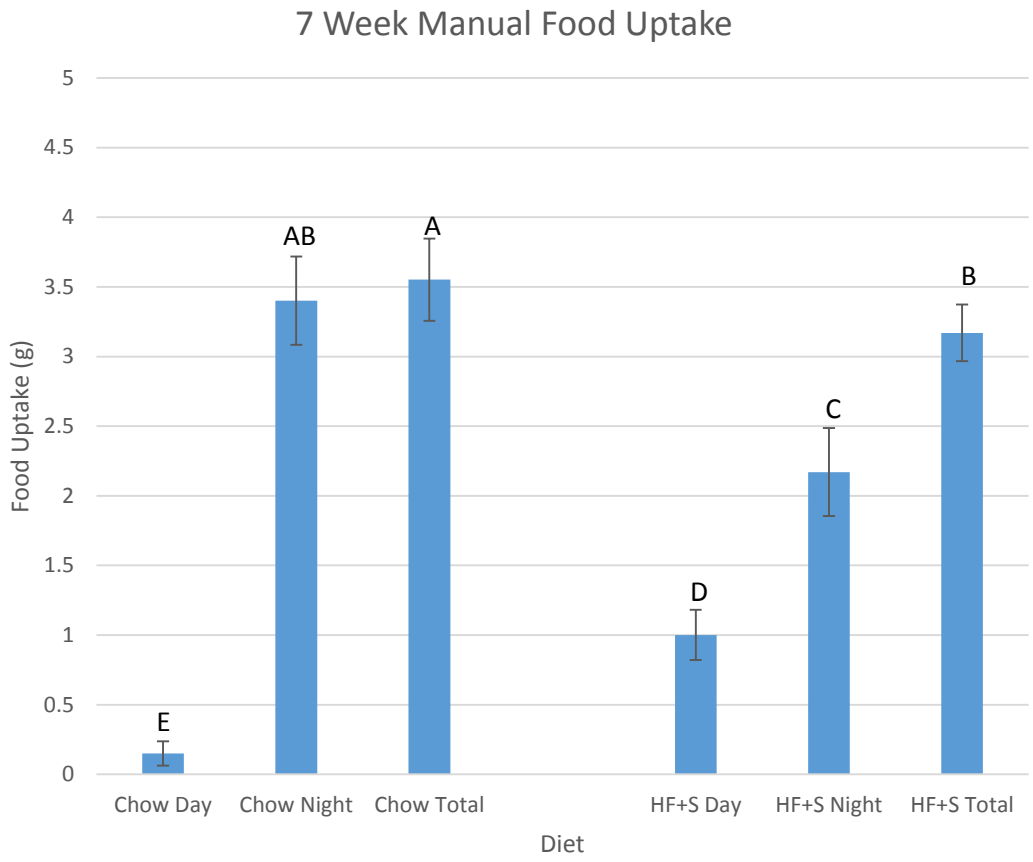

Figure 17: *Food uptake amount measured manually at 7 weeks*

Similar to the measurements at 7 weeks, there were very few similarities between food intake quantities at 12 weeks (Fig 18). Consuming 0.73 g during the day and 3.49 g at night for a total of 4.22 g, chow-fed animals had a greater total consumption amount (20.7 kcal) than the HF+S (2.638 g, 15.8 kcal) and MT (2.938 g, 17.4 kcal) groups ($p < 0.05$). Despite the absence of food during the day, MT animals did not have a significantly different total uptake amount compared to HF+S animals. However, this intake amount at night of 2.94 g (which is also the total) for MT animals was significantly greater than the nighttime consumption of 2.64 g for HF+S animals ($p < 0.05$). The 3.49g of chow diet consumed at night was not significantly different than the total intakes for the HF+S and MT groups. The 0.73 g of chow diet taken in

during the day was also not significantly different than the 0.72 g of HF+S diet consumed during the day. Twelve week ANCOCA results discovered a significant difference in daytime food uptake when comparing chow vs MT animals ($p < 0.05$), demonstrating that body did not influence food intake in this specific group. Statistical analyses also illustrated no significant differences in chow vs HF+S ($p = 0.30$) and HF+S vs MT ($p = 0.91$) daytime food intakes or chow vs HF+S ($p = 0.42$), chow vs MT ($p = 0.28$), or HF+S vs MT ($p = 0.37$) nighttime food intakes. Comparisons of total food intakes also revealed no significant differences (chow vs HF+S $p = 0.60$, chow vs MT $p = 0.69$, HF+S vs MT $p = 0.39$).

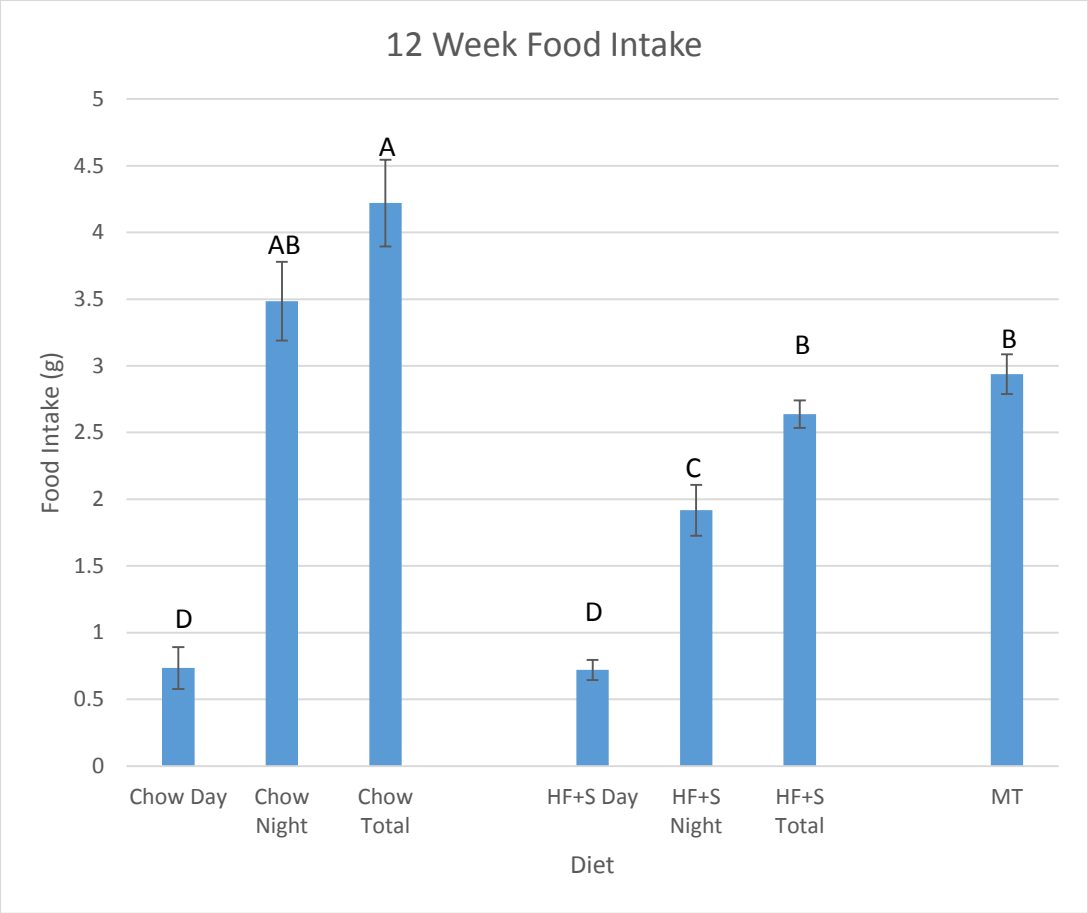

Figure 18: *Food uptake amount measured manually at 12 weeks*

The findings at seven weeks for the chow group were remarkably similar to the food intake amount results from the metabolic cages as the total amount of food consumed was nearly identical. This indicates that the environmental change from the microisolator cage to the metabolic cage did not impact the feeding habits of animals on a chow diet at seven weeks. Chow-fed animals demonstrated an overwhelming preference for eating at night (96% of their food), a behavior that was confirmed by the data from metabolic cages. In fact, chow-fed animals ate so little during the day that statistically there was not a difference between the amount of chow diet consumed at night compared to the total amount. Regardless of age, chow-fed animals ate more than HF+S or MT animals. This was consistent across both methods

of assessing food intake amount, indicating that animals will consume a greater amount of chow diet than HF+S irrespective of the type of cage in which they're housed. This also suggests that the removal of large chunks of food seen in the HF+S groups in the metabolic cages did not significantly impact the overall amount of HF food consumed. According to the metabolic cages, at 12 weeks animals on the HF+S diet had recorded uptakes of 1.81 g of food at night and 0.46 g during the day, totaling 2.27 g of HF food over a 24 hour period. Manual measurement of the food uptake in these same animals the day prior to their being transferred to metabolic cages yielded a total intake 2.63 g. This similarity illustrates the consistent feeding habits of the animals despite changes in their environments. Also consistent with the metabolic cage data, MT did not have an effect on total food intake. Animals on the HF+S diet did not appear to have increased daytime feeding relative to chow-fed animals. However, this cannot be said at seven weeks as daytime consumption of HF+S diet was significantly elevated. The analysis of covariance results were also in agreement with the metabolic cage findings as it was discovered in all but one comparison (daytime chow vs MT at 12 weeks) at both 7 and 12 weeks that body mass was the driving factor in the differences in daytime, nighttime, and total food intake amounts.

Water Intake

Similar to food, the amount, frequency, duration and rate at which water was withdrawn from the hopper in the metabolic cages was measured and analyzed. Data for each of these parameters were collected at 7 and 12 weeks of age and categorized based on diet type and time of day. The chow group contained normal drinking water while the HF+S and MT groups both had sugar added to the drinking water (42 g/L fructose/sucrose 55%/45%). Meal timing did not affect the accessibility or access to water. The presence or absence of sugar in the drinking water did not affect the way in which this data was collected or analyzed.

The water intake results very strongly resemble the food intake data. Assessment of water intake amounts at 7 weeks revealed the 1.9 g of water consumed at night by animals on the chow diet were not only significantly greater than the 0.1 g consumed during the day, but were also significantly greater than the 0.8 g nightly and 0.3 g daily intakes from animals on the HF+S diet ($p < 0.05$) (Fig 19). The daytime water intakes for both groups were not significantly different. Analysis of covariance determined there were no significant differences between chow and HF+S diets during the day ($p = 0.42$) or at night ($p = 0.12$), suggesting that body mass was responsible for the differences in water consumption.

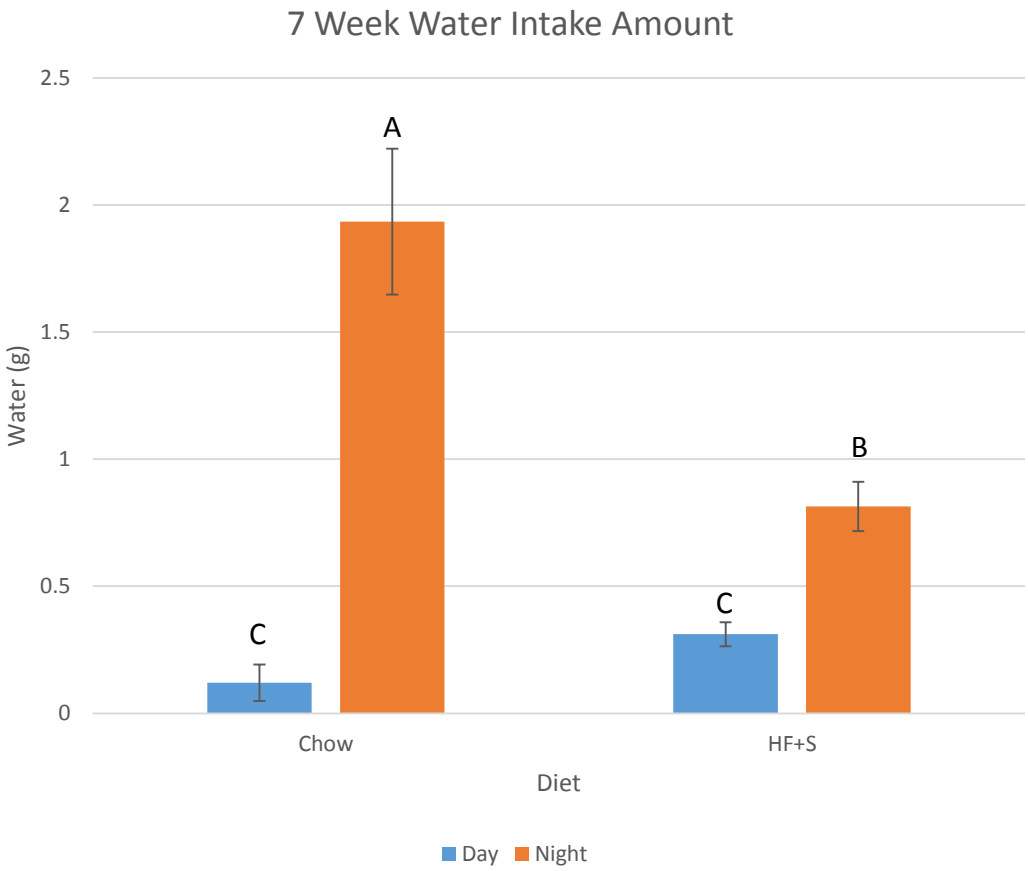

***Figure 19**: Total water intake at 7 weeks*

Assessment of the same parameter at 12 weeks yielded slightly different results (Fig 20). At night, the intake amount of 1.3 g for the chow group, 1.0 g for HF+S, and 1.2 g for MT were not significantly different from one another. Similarly, the daytime intake quantities for all three dietary groups were significantly less than the nighttime intake amounts but were statistically similar to one another as no significant difference existed between the 0.1, 0.2, and 0.1 g intake amounts for the chow, HF+S, and MT diet groups, respectively ($p < 0.05$). Analysis of covariance to assess the impact of body weight on diet and water intake amount yielded no significant differences during the day (chow vs HF+S $p = 0.17$, chow vs MT $p = 0.64$, HF+S vs MT

p =0.13) or at night (chow vs HF+S p = 0.91, chow vs MT p = 0.42, HF+S vs MT p =0.20), implicating body mass as the driving force in the various water intake amounts observed.

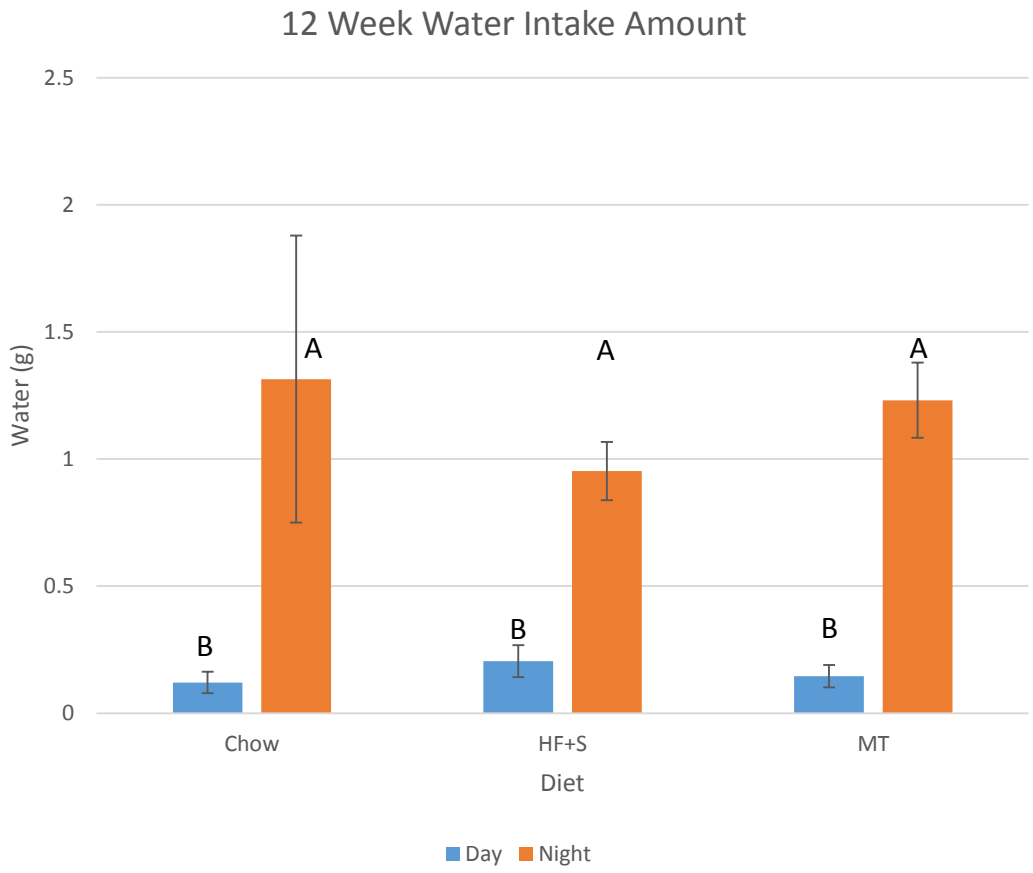

***Figure 20**: Total water intake at 12 weeks*

Although a significant difference existed at night, inclusion of sugar in the drinking water did not affect consumption during the day at seven weeks. At 12 weeks MT did not impact the amount of water consumed, suggesting that short-term access to food does not influence the amount of drinking water consumed. There was also no difference in the amount of water consumed between the chow and HF+S or MT groups during the day or at night, indicating that sugar content in the drinking water did not affect the water intake amount. The

disproportionate amount of water ingested at night compared to the day reflects the findings from the food intake measurements and illustrates that water consumption mirrors food consumption.

There was little difference between groups at seven weeks when examining water uptake rate (Fig 21). The 0.05 g during the day and 0.05 g at night of the HF+S group were not significantly different than the uptake rate of 0.05 g seen at night for the chow group. All three of these uptake rates were significantly greater than the 0.02 g rate seen during the day in the chow group ($p < 0.05$).

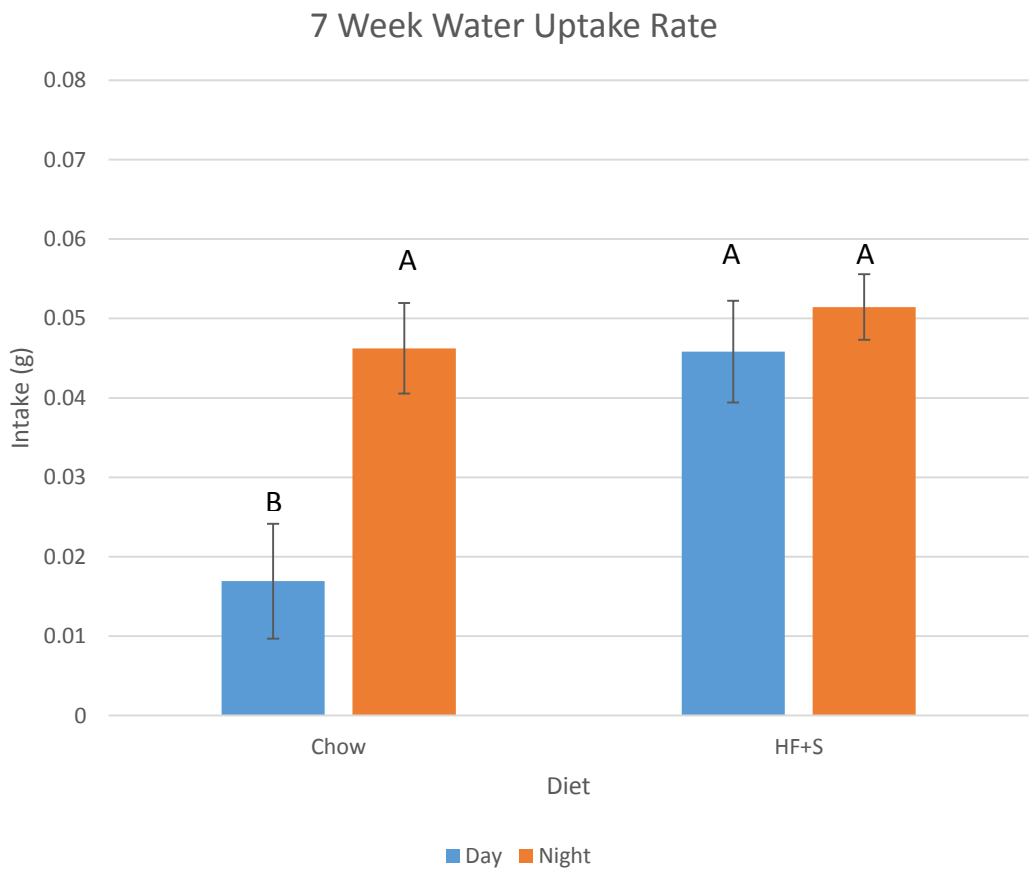

***Figure 21**: Rate of water consumption at 7 weeks*

Shockingly, at 12 weeks, all six of the different groups were statistically similar to each other (Fig 22). The daytime intake rates of 0.04, 0.06, and 0.04 g seen in the chow, HF+S and MT groups were not significantly different from the 0.04, 0.06, and 0.05 g nighttime intake rates in animals on chow, HF+S and MT diets ($p < 0.05$).

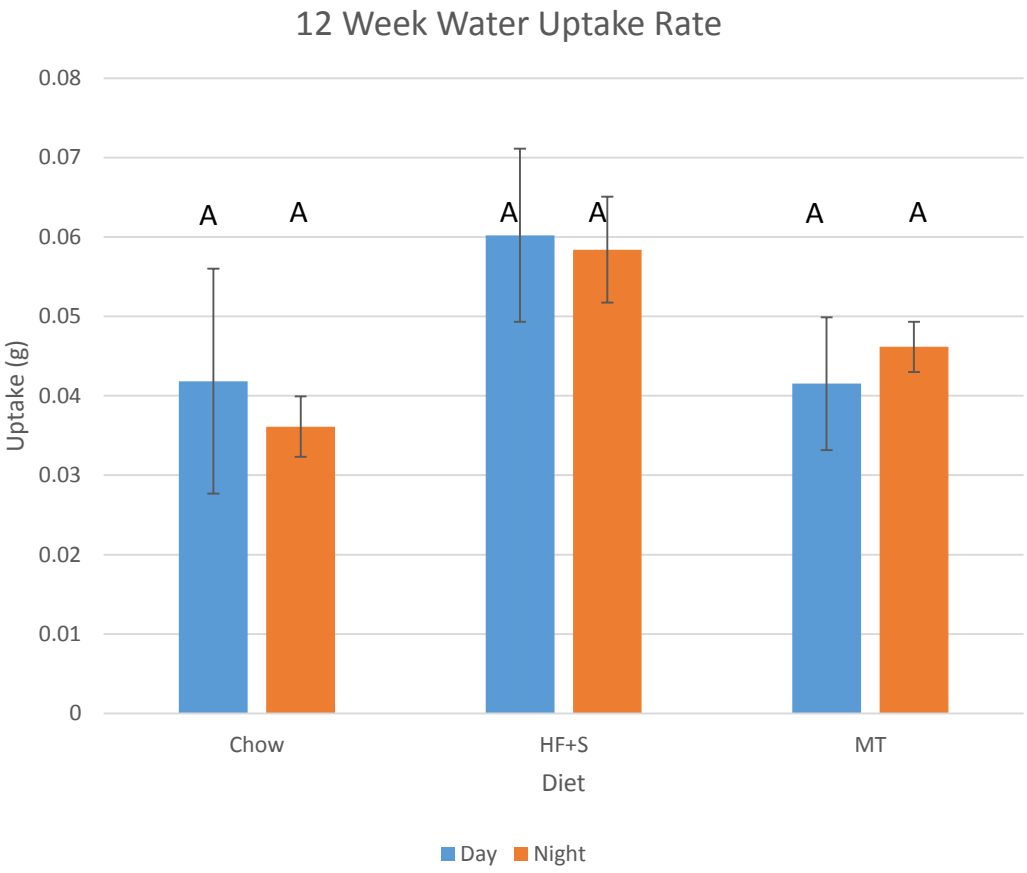

***Figure 22**: Rate of water consumption at 17 weeks*

With exception to the daytime intake rate seen in the chow group at 7 weeks, none of the other water uptake rates at either 7 or 12 weeks were significantly different. This leads to the conclusion that neither the time of day, composition of diet, or inclusion of sugar in the

drinking water affects the rate at which water in taken up. Meal timing did not have an impact on the water intake rate.

Several differences did emerge amongst groups at both 7 and 12 weeks regarding water intake frequency. At 7 weeks the 42.4 drinking bouts seen at night (Fig 23) in animals on a chow diet significantly exceeded the number of drinking events seen in all other groups ($p < 0.05$). The frequency at which animals consumed water during the day did not vary by a large amount, as the 5.6 drinking bouts for the chow group were not far from the 7.3 drinking event seen in the HF+S diet. Both of these frequencies were significantly less than the 18.0 nighttime drinking bouts in the HF+S group ($p < 0.05$).

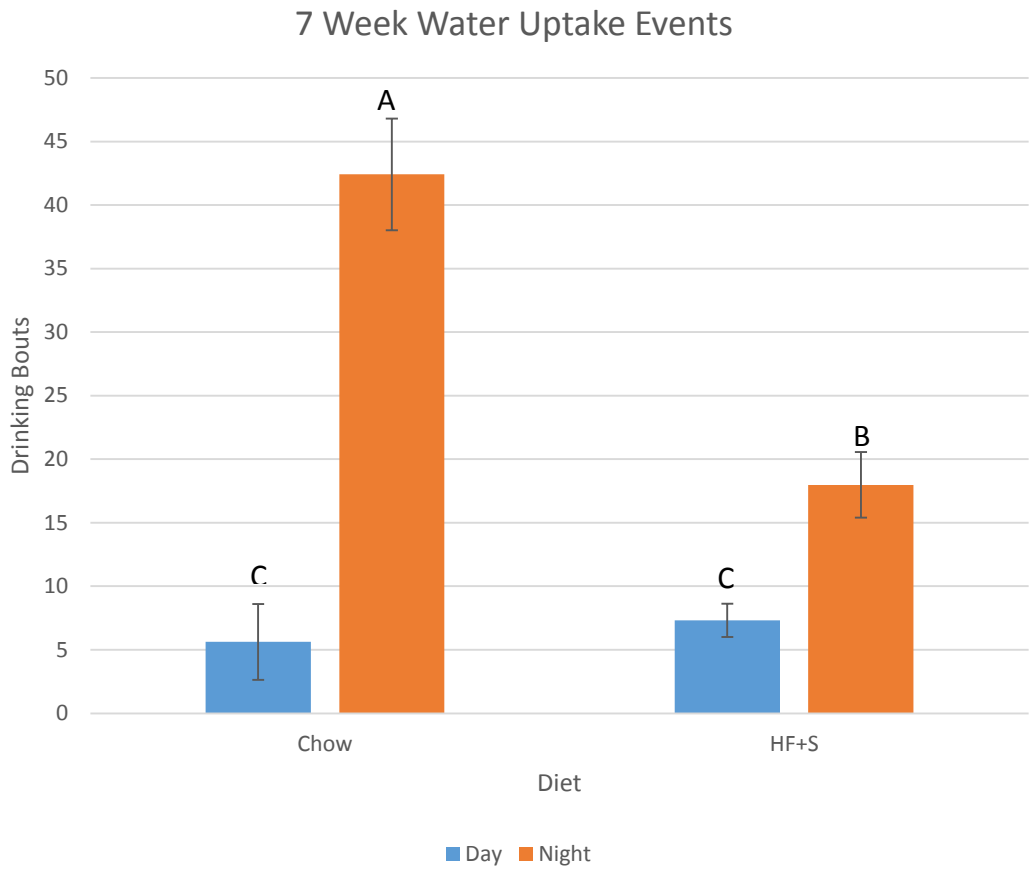

***Figure 23**: Frequency of water consumption at 7 weeks*

Similarly, at 12 weeks the daytime water intake frequencies of 3.6, 3.0, and 3.5 drinking bouts for the chow, HF+S, and MT groups, respectively, were not significantly different from each other but were significantly less than any of the groups at night (Fig 24) ($p < 0.05$). The 34.3 and 28.4 nightly drinking bouts seen in chow and MT animals, respectively, were not significantly different from each other, but were both significantly greater than the 16.9 drinking bouts seen in the HF+S group ($p < 0.05$).

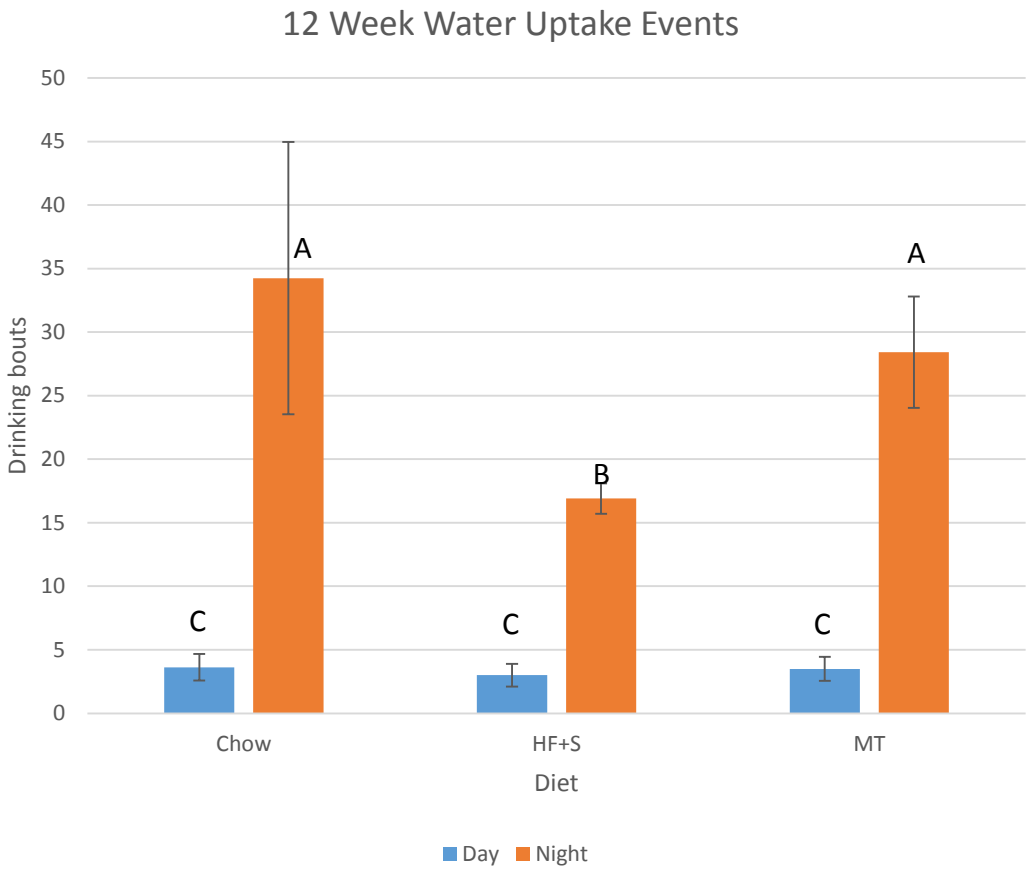

***Figure 54**: Frequency of water consumption at 12 weeks*

The water intake frequency data mirrored the water intake amount data. This is not at all surprising given that the water intake amount is calculated by the formula UptakeW_Sum = UptakeW_g * UptakeW_N. As the water intake rate data indicated there was no difference in the rate at which water was consumed across groups or time and therefore constant, it makes sense that the number of drinking bouts directly relates to the water intake amounts. However, although the nighttime water intake amounts and intake rates were similar at 12 weeks across the 3 diet groups, the frequency of drinking was less in the HF+S group compared to chow and MT. All three groups had similar amounts of daytime drinking bouts so it's unclear from where this discrepancy arises. Nevertheless, MT did increase the number of drinking bouts

at night compared to HF+S diet. Also, the drinking bouts for MT animals were not elevated during the day despite the lack of access to food, once again suggesting that drinking behavior is not impacted during short-term restrictions on food availability.

Little difference in water intake duration existed between groups at seven weeks (Fig 25). The amount of time spent interacting with the water hopper was greatest at night in the HF+S group, averaging 0.7 minutes. Water intake durations of 0.6 minutes at night for chow-fed animals, 0.4 minutes during the day for chow-fed animals, and 0.5 minutes during the day for animals on a HF+S diet were all statistically similar to one another and significantly less than the nighttime water intake duration for the HF+S group ($p < 0.05$).

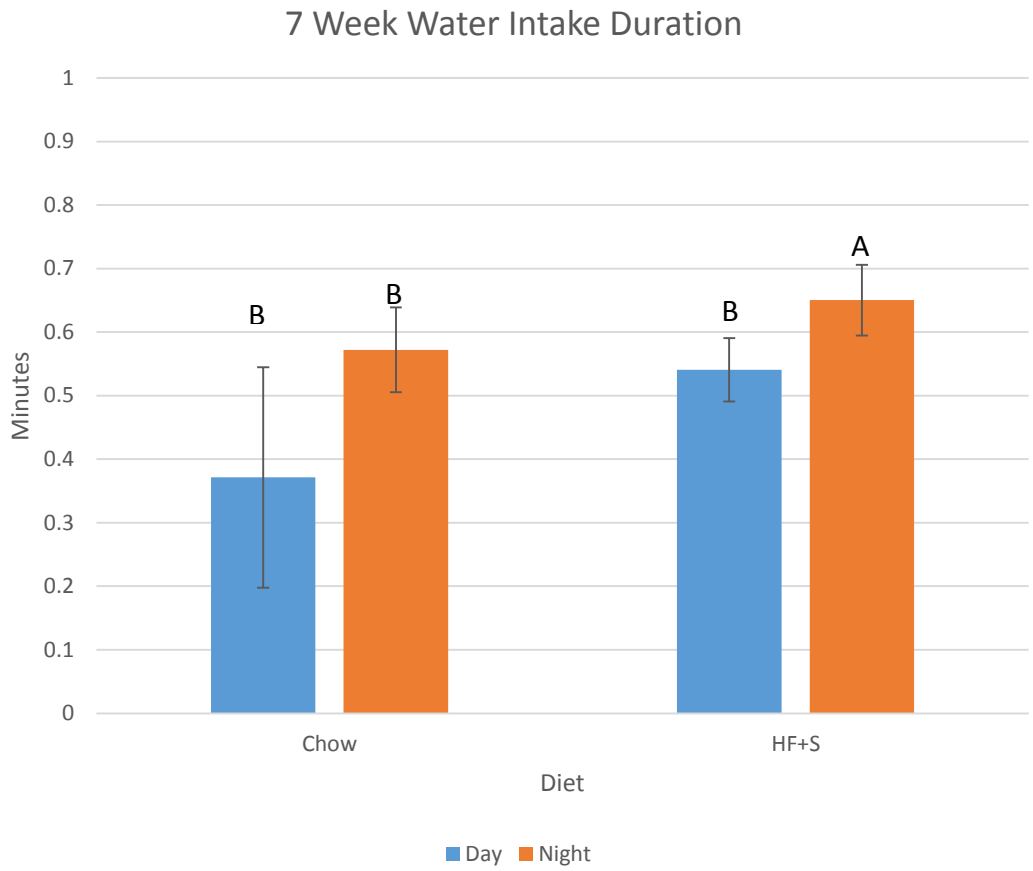

***Figure 25**: Time spent drinking water at 7 weeks*

There were no significant differences in daytime water intake duration at 12 weeks for the 3 diet groups (Fig 26). The 0.4 minutes in the chow group, 0.3 minutes in the HF+S group, and 0.4 minutes in the MT group were all statistically similar to one another ($p < 0.05$). Although the daytime HF+S and MT intake durations were similar to the chow group, these two diet groups were not similar to nighttime intake duration of 0.7 minutes seen in the MT group, as the daytime chow group was. This nightly intake duration in the MT group also was not significantly different than the 0.8 minute long interaction seen nightly in the HF+S diet or the 0.5 minutes observed at night in the chow diet ($p < 0.05$). Interestingly, the water intake duration of 0.5 minutes from the chow group at night was not significantly different from any

group, regardless of diet or time of day. The nighttime intake duration for the HF+S group was significantly greater than all daytime intakes.

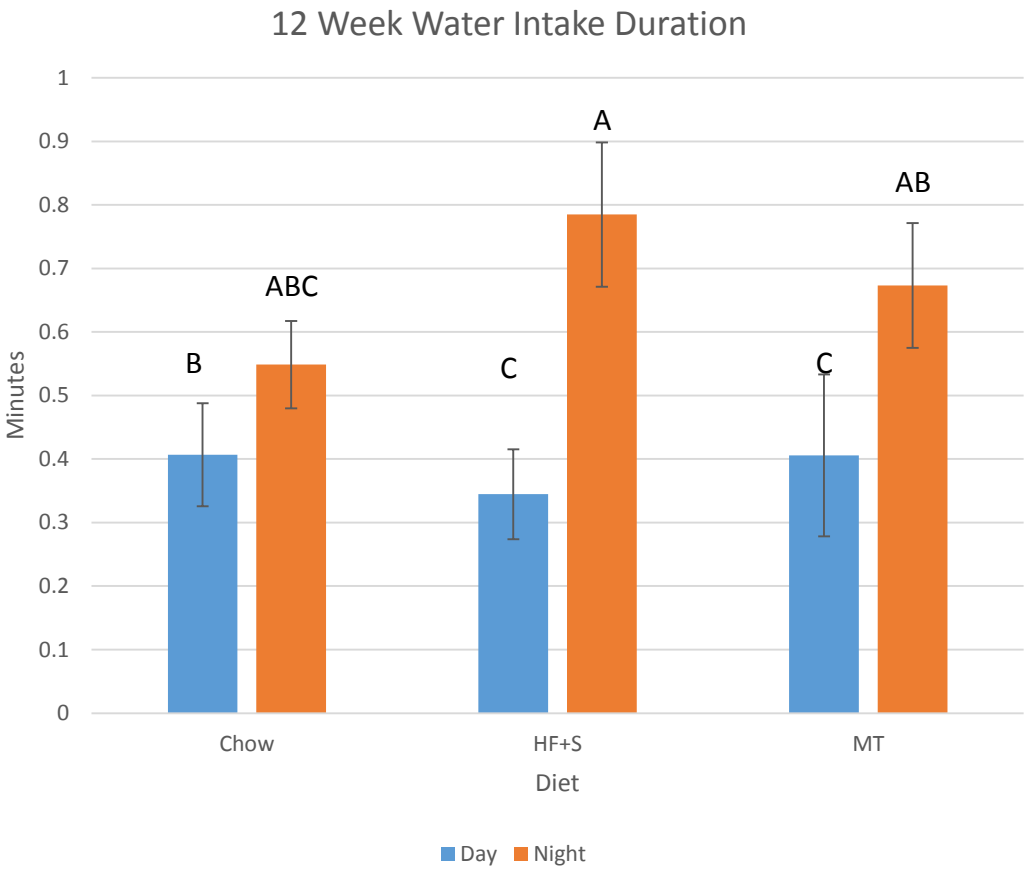

***Figure 26**: Time spent drinking water at 12 weeks*

The increased water intake duration seen in HF+S animals at night was only marginally greater than the nighttime intake duration seen in the chow group or the HF+S group during the day. Although a significant difference does exist, at seven weeks it appears the fluctuation in water intake duration between diet groups and time of day is minimal. At 12 weeks, consistent with other water intake parameters, the intake durations during the day were not dissimilar. During the night, the three diet groups also did not have profoundly different intake

durations from one another, although the MT group was related to the daytime chow group and the nighttime chow group was related to every other group, including all three dietary groups during the day. This considerable amount of overlap between dietary groups and times suggests there are few differences in the amount of time spent drinking water. Generally, the duration at night does appear to exceed the typical intake duration during the day. The presence or absence of sugar in the drinking water did not appear to impact water consumption or drinking habits. Meal timing also did not appear to have an effect on water intake duration.

Overall, the inclusion of sugar in the drinking water did not significantly affect water consumption or drinking habits. At night, when the majority of water was consumed, no significant difference existed between MT and HF+S groups in water intake amount, rate, or duration. The difference in water intake frequency between the two groups was minimal. There were no differences between the MT and HF+S water intake parameters during the day. Similar to food uptake, MT does not appear to impact overall consumption. The access to or restriction from food does not influence water consumption.

Behavior

Special Methods

This data required the use of a unique macro within the ExpeData system (Macro 10) to obtain behavioral quantifications. The data was also transformed to display a normal distribution by performing a logarithmic transformation on each behavioral quantification.

As previously described, the behaviors of the animals immediately following interaction with the food hopper and water hopper were observed and analyzed to determine the most likely activity or behavior following an eating or drinking event. Over a 24 hour period the probability of each event taking place immediately following a feeding or drinking event were calculated and recorded. This analysis provides a better understanding of how diet affects behavior. As this data was collected over a 24 hour period, animals on MT diet only had access to their food hopper from 8:15 pm to 5:15 am, accounting for only 9 hours (37.5% of the 24 hour period).

The subsequent behaviors immediately after interaction with the food hopper in which significant uptake was found was assessed in both chow and HF+S groups at 7 and 12 weeks. At seven weeks in chow-fed animals, lounging was the preferred activity after an eating event (Fig 27). Specifically, after eating an animal took a short lounge 63% of the time, and lounged for an extended period of time (> 60 seconds) 25% of the time, indicating that an animal would lounge after eating 88% of the time. Interaction with the water hopper only occurred 9% of the time

following feeding (5% with significant water uptake and 4% no significant uptake) while other activities, such as interaction with the habitat, with or without a stable mass reading, accounted for the reaming 3% of activities following eating.

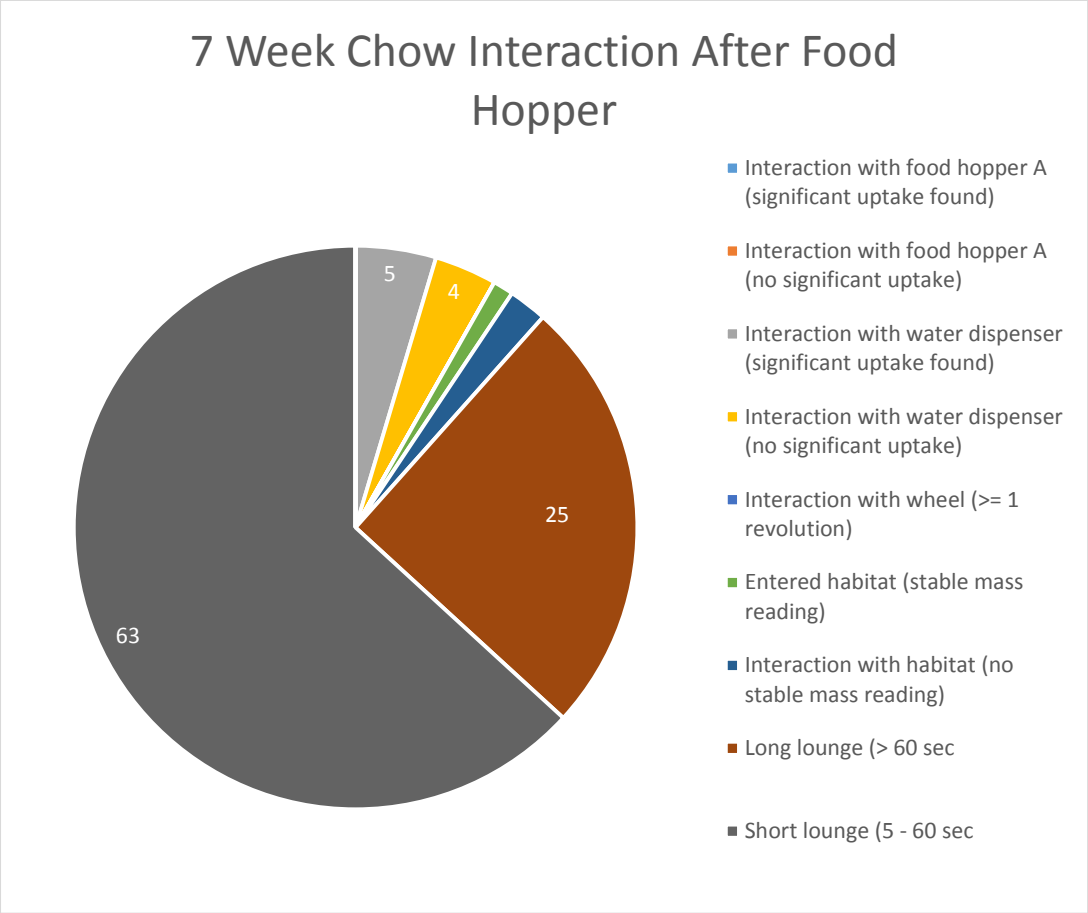

***Figure 27**: Behavior following interaction with food hopper in animals on chow diet at 7 weeks*

The results of animals fed a HF+S diet at 7 weeks were remarkably similar in that lounging was the preferred activity (92%) after eating, with animals taking a short lounge 53% of the time and a long lounge 39% of the time (Fig 28). Water hopper interaction was the next most probable event (7%) with significant water uptake found 4% of the time and interaction

with the water hopper without significant uptake occurring 3% of the time. Interaction with the habitat made up the remaining one percent.

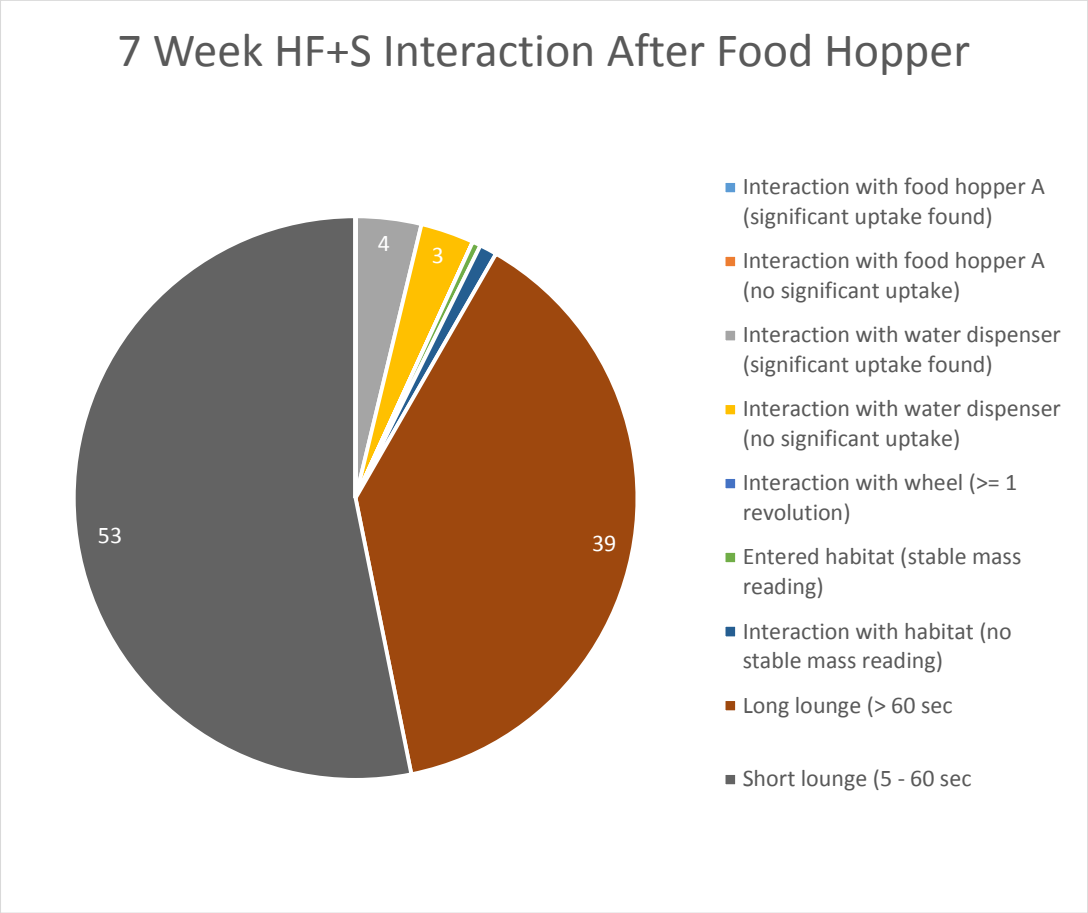

***Figure 28**: Behavior following interaction with food hopper in animals on HF+S diet at 7 weeks*

Animals on a HF+S diet demonstrated an increased likelihood to lounge following a feeding event. Although the probability of lounging in general was only marginally increased in the HF+S diet, animals in this group illustrated a 14% increased predictability of lounging longer than 60 seconds. This suggests that HF food increases sedentary behavior when compared to chow diet.

Transformation of the data to yield a normal distribution via logarithmic transformation demonstrated animals on HF+S diet had a significantly greater probability of taking a long lounge compared to chow-fed animals (least square means 1.6 HF+S, 1.4 chow). Unsurprisingly, chow-fed animals illustrated a significantly greater propensity for short lounges versus animals on HF+S diet (least square means 1.8 chow, 1.7 HF+S). There were no significant differences between dietary groups concerning interaction with the water hopper or habitat following feeding.

At 12 weeks, a similar propensity for lounging following a feeding event persisted across the diet groups. Chow-fed animals lounged 91% of the time after eating (69% short and 22% long lounges), while only interacting with the water hopper 6% of the time (4% significant uptake and 2% not significant uptake) and interacting with the habitat the reaming 3% (Fig 29).

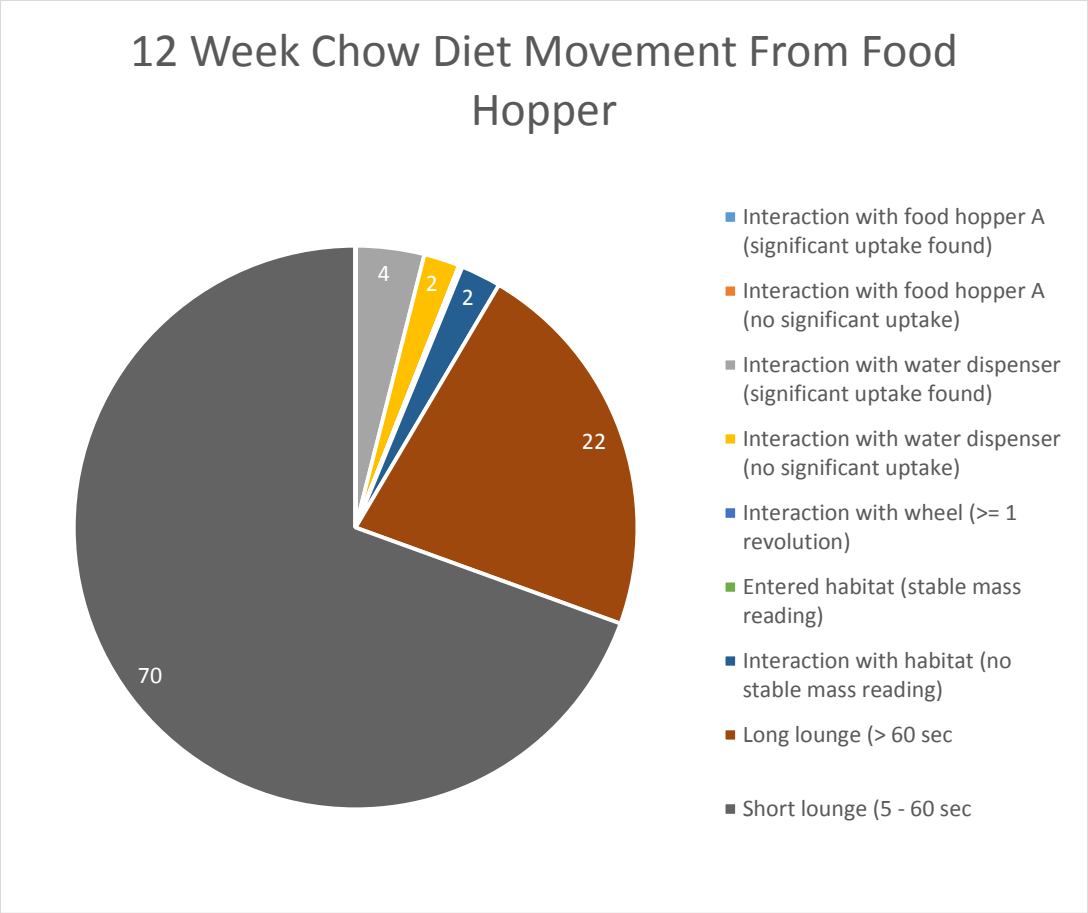

***Figure 29**: Behavior following interaction with food hopper in animals on chow diet at 12 weeks*

Animals on a HF+S diet also demonstrated a strong inclination for lounging after eating, taking a short lounge 49% of the time and enjoying a long lounge 44% of the time, revealing a tendency to lounge 93% of the time after eating (Fig 30). No interaction, significant or otherwise, with the water hopper or habitat accounted for greater than 3% of the remaining activities after eating.

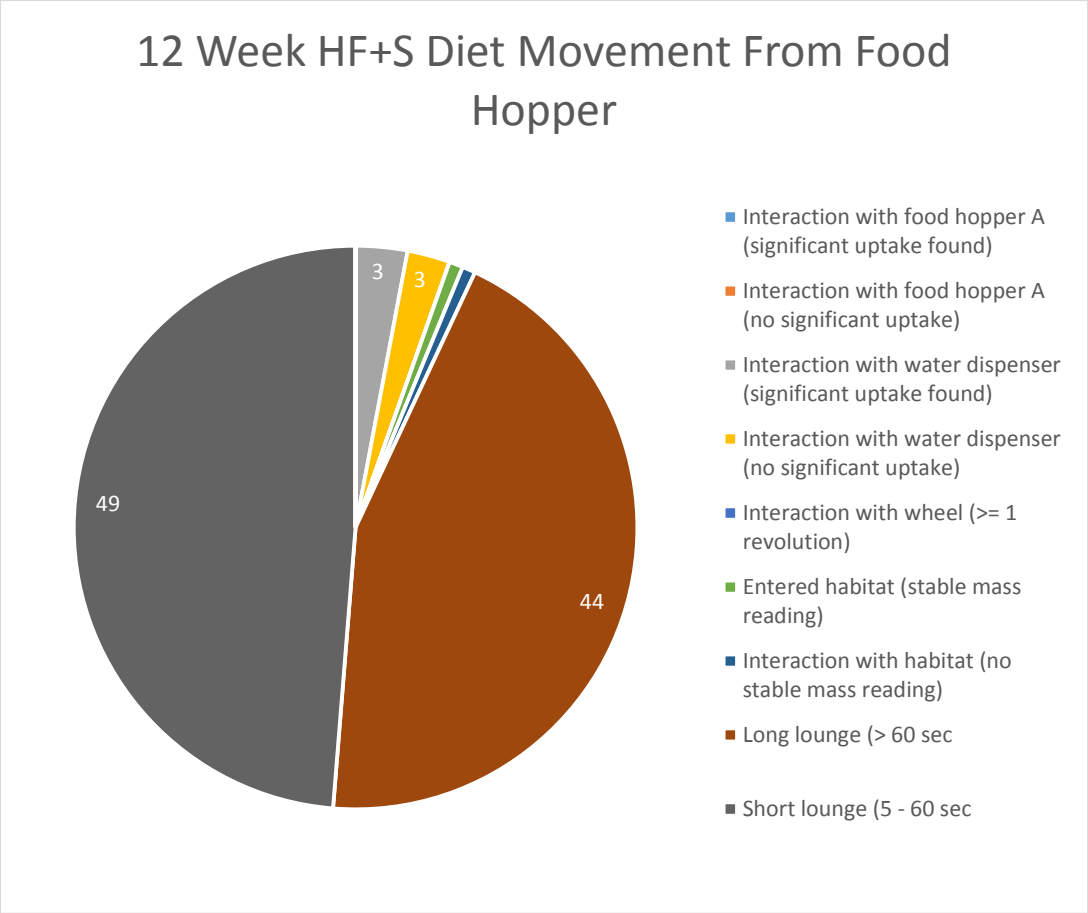

***Figure 30**: Behavior following interaction with food hopper in animals on HF+S diet at 12 weeks*

Meal timed animals exhibited an equally high preference for lounging (94%) following interaction with the food hopper, opting for a short lounge 53% of the time and a long lounge 41% of the time (Fig 31). Interaction with the water hopper with significant uptake accounted for an additional 4% of possible activities following feeding, while the remaining interactions were responsible the other 2 percent.

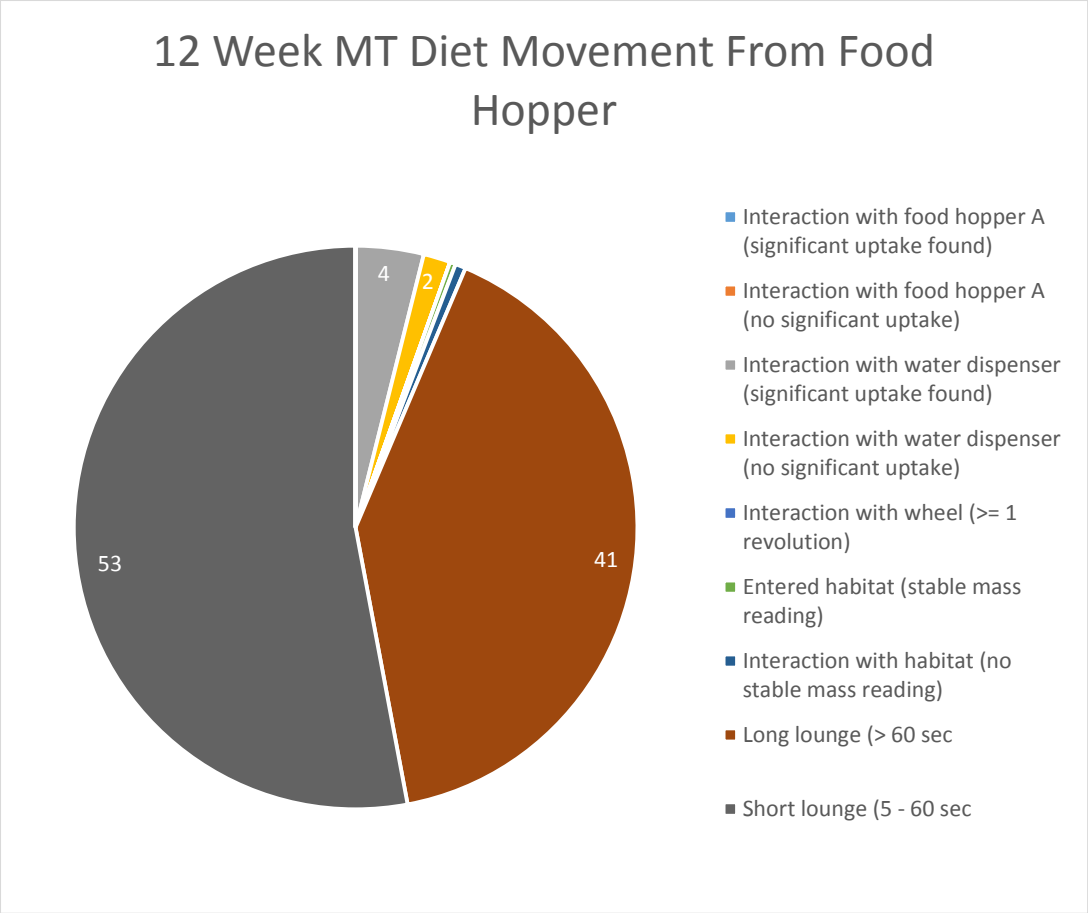

***Figure 31**: Behavior following interaction with food hopper in animals on MT diet at 12 weeks*

Animals fed a HF+S diet showed an increase in lounging occurrence relative to chow-fed animals, similarly to the data collected at seven weeks. HF+S animals also exhibited an increased likelihood of taking an extended lounge compared to chow-fed animals as the probability of a short lounge effectively doubled from 22% to 44%, also in agreement with the findings at 7 weeks. Meal timed animals lounged essentially the same amount as the HF+S group, however animals fed MT diet took a long lounge slightly less often (3% less) than HF+S animals. There was little difference in interactions with the water hopper or habitat between MT and HF+S groups. Meal timing did not appear to affect the behavior of animals following a feeding event. Due to the removal of the food hopper from 5:15 am to 8:15 pm, these

behavioral observations are based entirely on the 9 hour window at night when food is present rather than the complete 24 hour period observed with the other groups.

Logarithmic transformation of the data confirmed these results. Although no significant differences existed between the three groups regarding interaction with the habitat or water hopper immediately after a feeding event, the chow group did not resemble the HF+S and MT groups lounging tendencies. Specifically, chow-fed animals had a significantly greater likelihood of taking a short lounge (least square means 1.8) relative to both the HF+S and MT groups (least square means 1.7 for both HF+S and MT), whose distributions were essentially identical. Similarly, both the HF+S and MT groups demonstrated indistinguishable inclinations for long lounges (least square means 1.6 for both groups), an amount that was significantly greater than that measured in chow-fed animals (least square means 1.3). These calculations confirm that meal timing did not have any effect on behavior immediately after interaction with the food hopper.

Behavior immediately following interaction with the water hopper with significant uptake recorded was assessed and analyzed. At 7 weeks immediately following a drinking event animals on a chow diet took a short lounge 50% of the time and a long lounge 35% of the time, indicating a strong preference (85%) for lounging (Fig 32). Interaction with the food hopper in which significant uptake was recorded accounted for 8% of activity while interaction with the food hopper without significant uptake accounted for 5%. The remaining 2% consisted of interacting with the habitat.

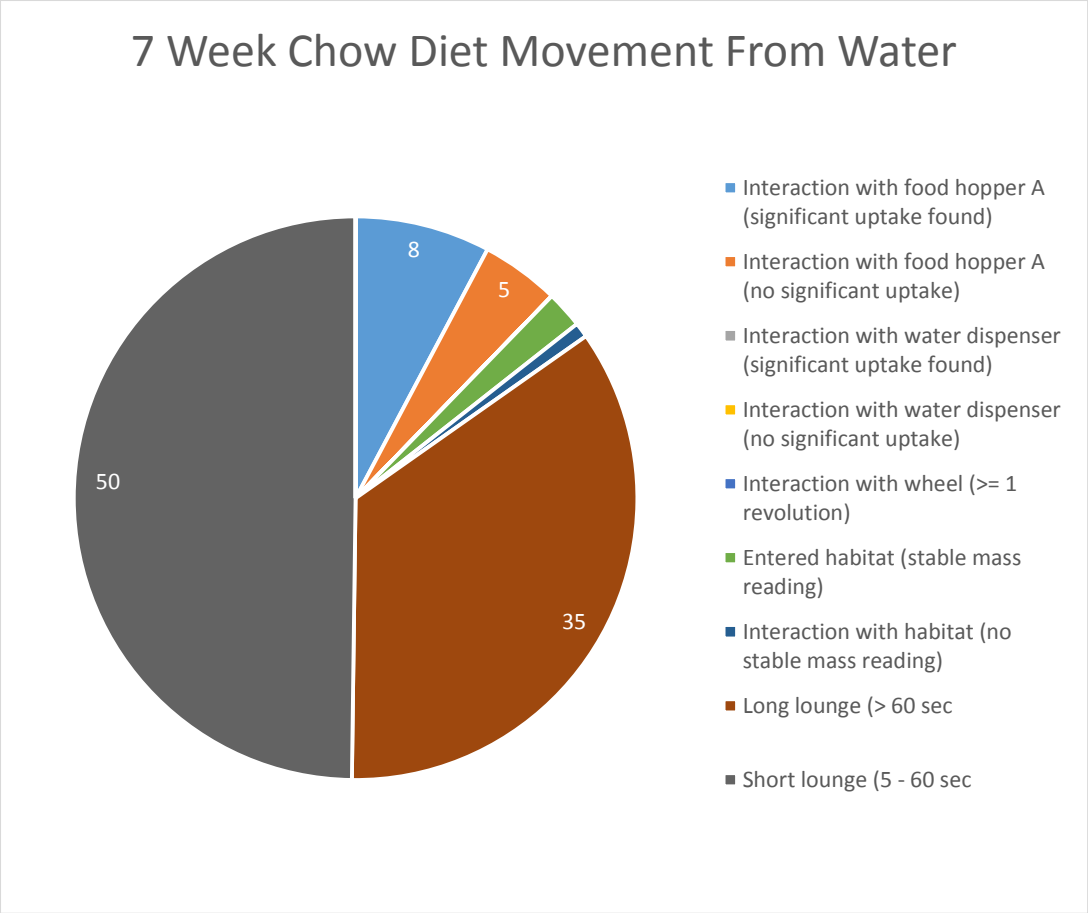

***Figure 32**: Behavior following interaction with water hopper in animals on chow diet at 7 weeks*

The results at seven weeks in the HF+S group (Fig 33) were nearly identical to the chow group. Lounging 82% of the time (49% short, 33% long), animals on a HF+S diet were likely to eat food only 7%, interact with the food hopper without any significant intake 5%, and enter the habitat 5% of the time after consuming water.

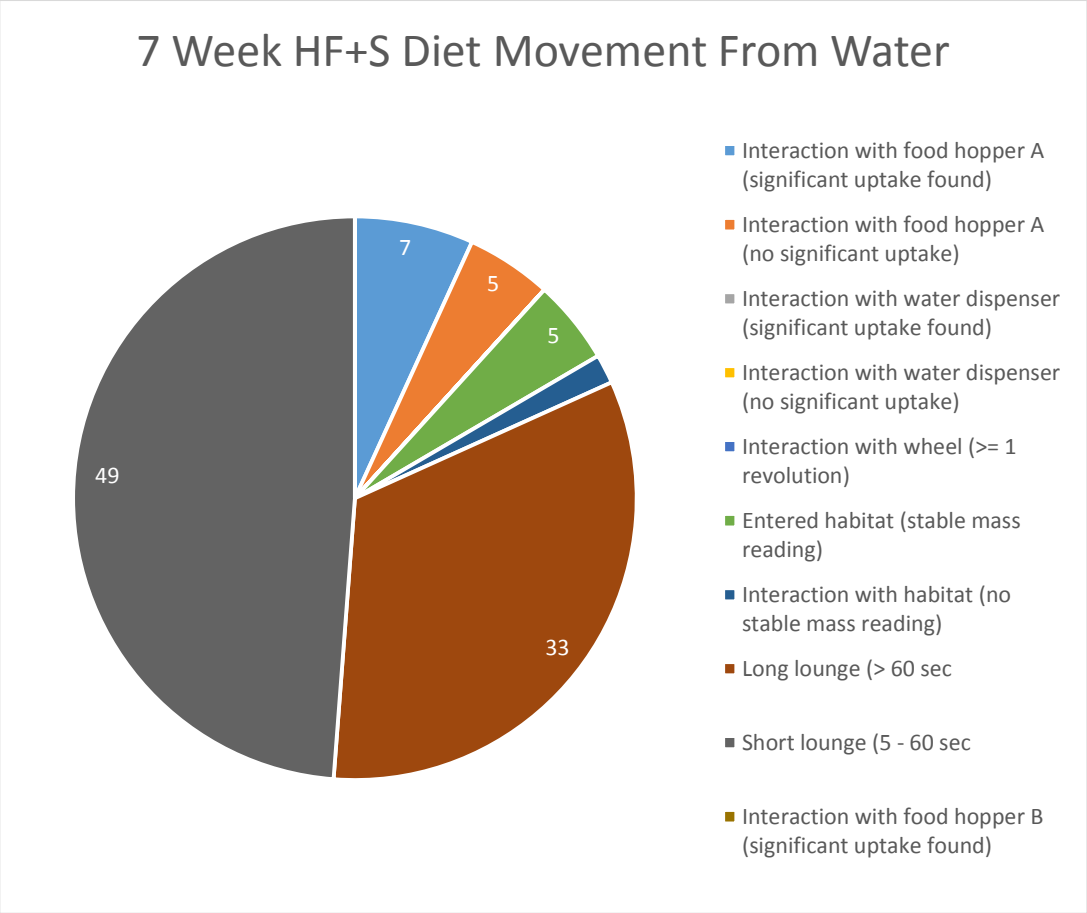

***Figure 33**: Behavior following interaction with water hopper in animals on HF+S diet at 7 weeks*

At seven weeks the movement from water data strongly resembles the movement from food data as both groups showed a strong inclination for lounging after drinking. Inclusion of sugar in the drinking water did not affect behavior. Logarithmic transformation of the both the chow and HF+S data revealed the only significant difference between dietary groups was the increased likelihood of animals on HF+S diet to interact with the habitat without achieving a stable mass reading compared to chow-fed animals. All other behavioral parameters did not significantly differ among groups.

At 12 weeks animals opted for a short or long lounge after interacting with the water hopper the vast majority of the time. The chow group took a short lounge 61% of the time and

a long lounge 20% of the time (Fig 34). Eating accounted for 10% of the group's activity, while interacting with the food hopper without significant uptake and entering the habitat were responsible for the remaining 5% and 4%, respectively.

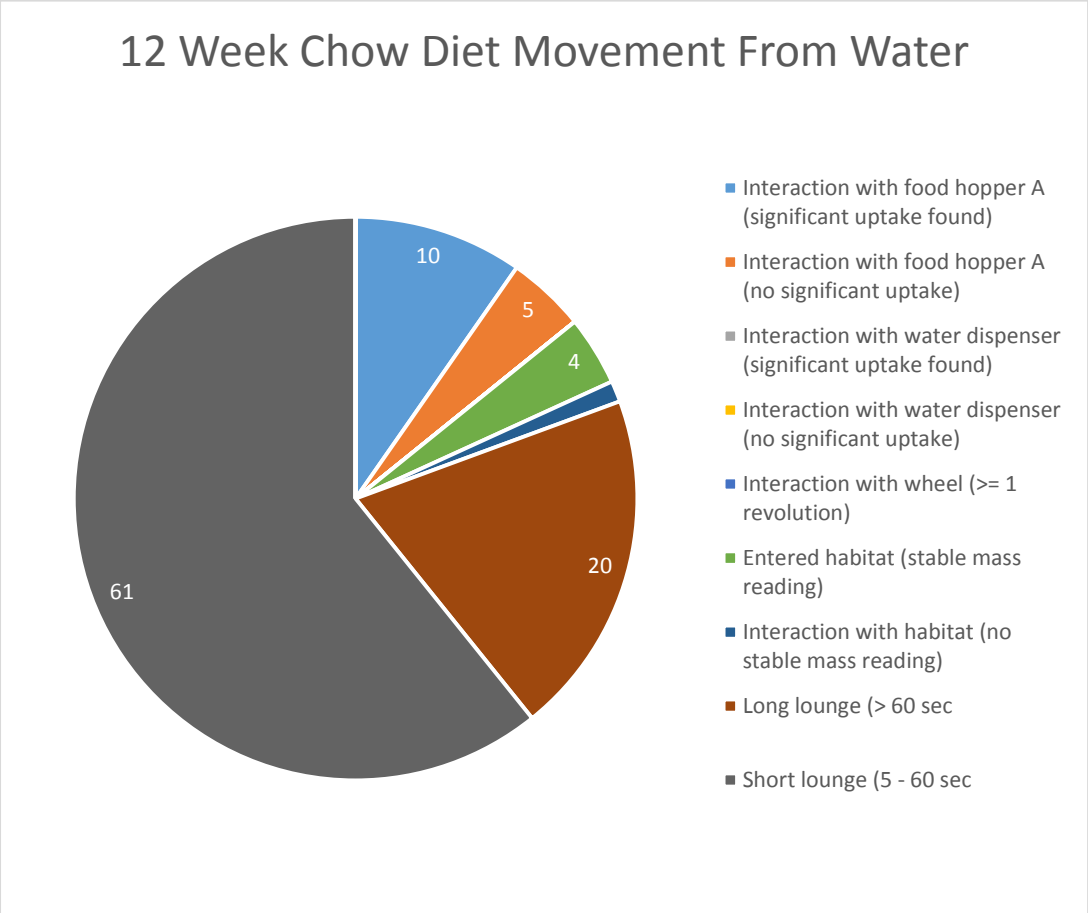

***Figure 64**: Behavior following interaction with water hopper in animals on chow diet at 12 weeks*

Animals on a HF+S diet demonstrated similar behaviors at 12 weeks as seen at 7 weeks, lounging 84% of the time (Fig 35). Specifically, short lounges accounted for 47% of their activity following a drinking event, long lounges 37%, interaction with the food hopper with significant uptake 7%, and interaction with the food hopper without any significant uptake 7%. Animals in this group very rarely interacted with the habitat, significantly or otherwise, immediately after drinking water.

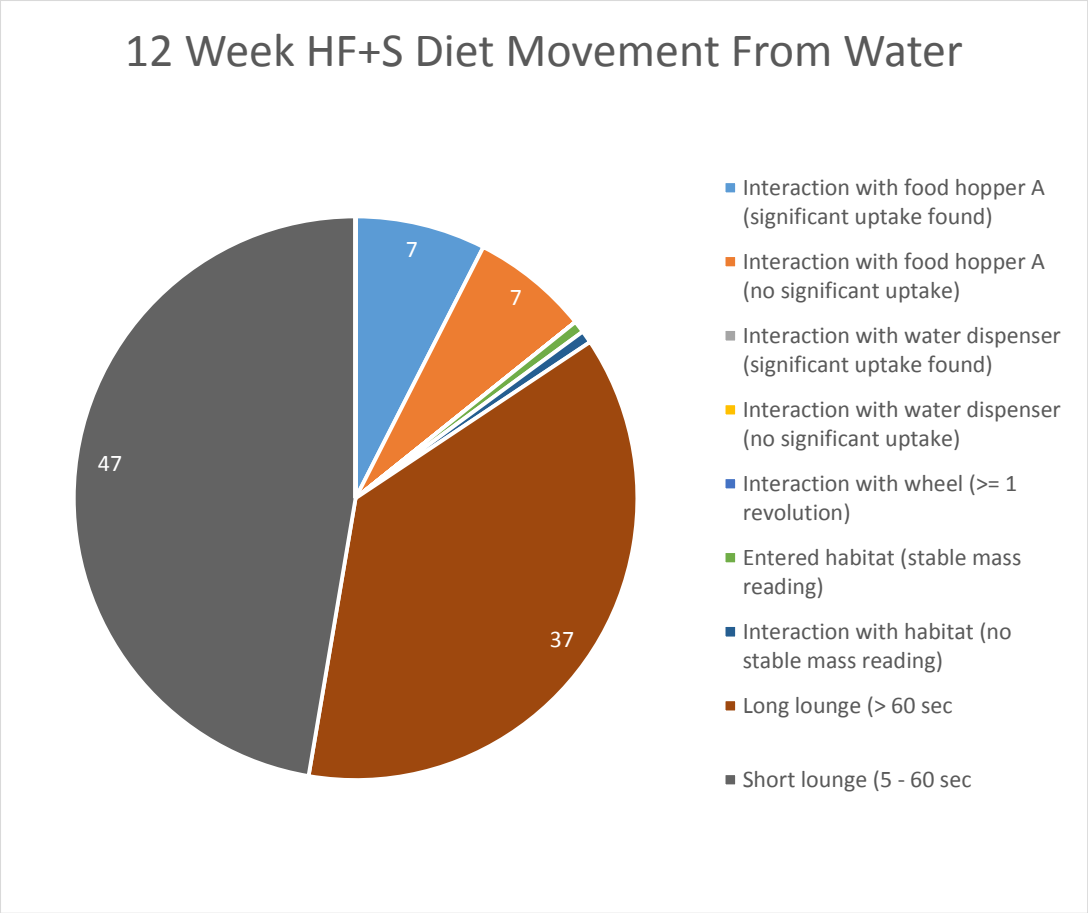

***Figure 35**: Behavior following interaction with water hopper in animals on HF+S diet at 12 weeks*

After interacting with the water hopper, animals on a MT diet opted for a lounge a staggering 91% of the time, taking a short lounge 47% of the time and a long lounge 44% of the time (Fig 36). Interaction with the food hopper with and without significant uptake each accounted for 3% of behaviors while entering the habitat and interacting with the habitat without a stable mass reading were responsible for the reaming 2 and 1 percent, respectively.

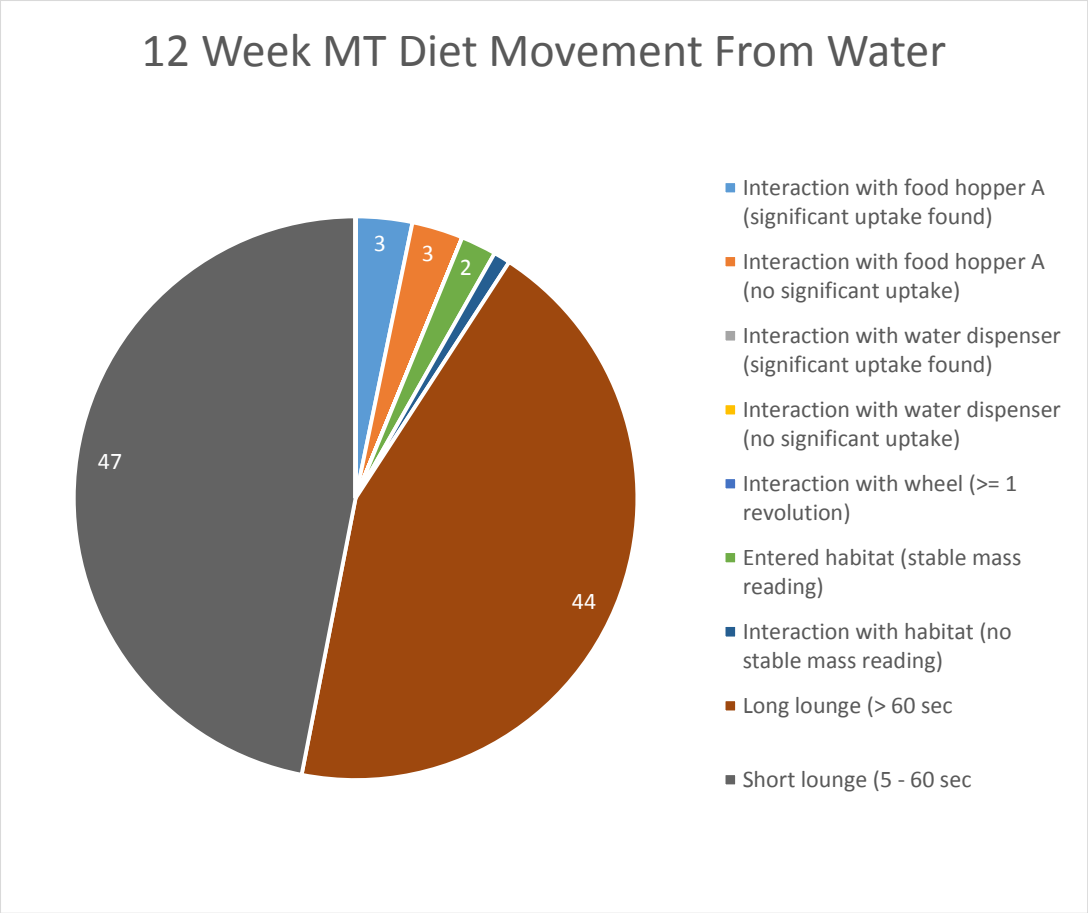

***Figure 36**: Behavior following interaction with water hopper in animals on MT diet at 12 weeks*

Animals on a chow diet showed an increased probability of short lounging compared to HF+S animals, without significantly impacting the likelihood of engaging in other activities, such as interacting with the food hopper or habitat. HF+S animals showed very little change between 7 and 12 weeks, with the exception of the minimal decrease in entering the habitat. Meal timing increased the inclination for long lounges without limiting the occurrence of short lounges. Animals on MT diet also displayed a decreased interaction with the food hopper after drinking which is not surprising given that the food hopper was only present in the cages for nine hours a day while the water hoppers were there constantly. Overall, MT did not appear to significantly impact behavior following interaction with the water hopper. Transformation of

the data confirmed these results but indicated that the observed reduction in food hopper interaction in the MT group was not statistically significant as all three dietary groups measured similar values (least square means 0.9 chow, 0.7 HF+S, and 0.5 MT). The likelihood of engaging in a long lounge after drinking water in HF+S animals (least square means 1.5) was not significantly different than the MT (least square means 1.6) or chow (least square means 1.3) groups, although these two groups were significantly different from one another.

Activity

The total distance traveled, or all meters, over a 24 hour period was recorded for each animal at both 7 and 12 weeks. At 7 weeks, chow-fed animals traveled the greatest distance, 300.1 m, at night, while only traveling 62.3 m during the day (Fig 37). This daytime activity was not significantly greater than the daytime movement of the HF+S group, which traveled 69.2 m, but was significantly less than the nighttime distance of 103.7 m traveled by the HF+S group ($p < 0.05$). Chow-fed animals traveled a significantly greater distance at night than HF+S animals.

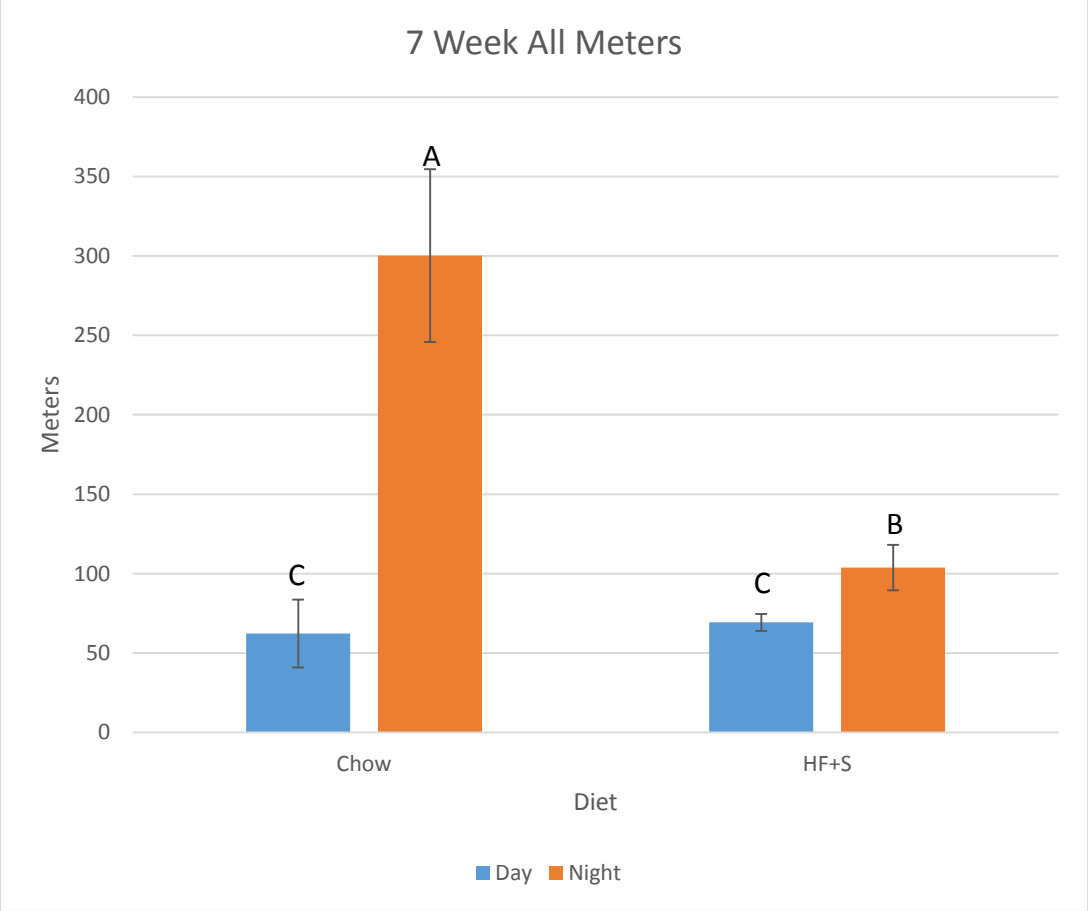

***Figure 37**: Total distance traveled at 7 weeks*

The results were similar at 12 weeks as the daytime distances of 59.3, 50.4, and 40.4 m for the chow, HF+S, and MT groups, respectively, were not significantly different from one another ($p < 0.05$) (Fig 38). Animals on a chow diet traveled 238.7 m at night, a distance significantly greater than the 141.1 and 163.8 m traveled by HF+S and MT animals, respectively, which did not differ significantly from each other ($p < 0.05$).

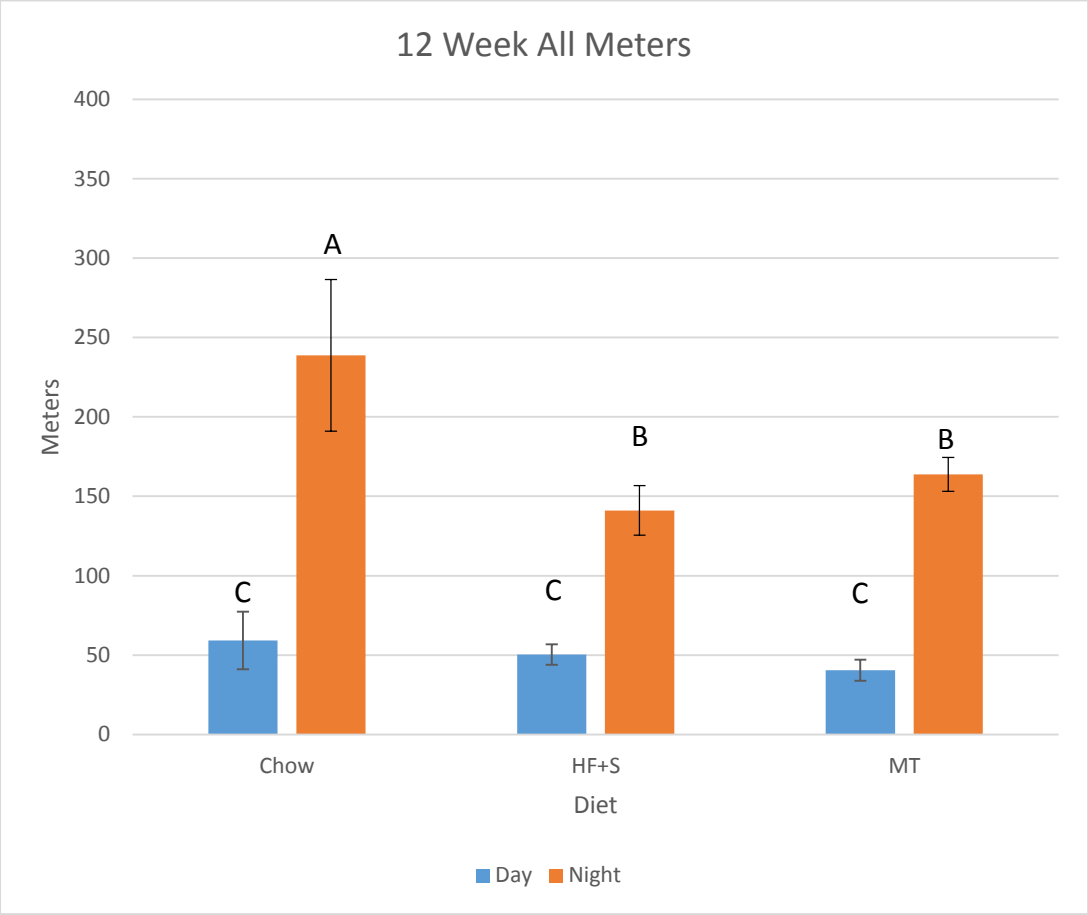

***Figure 38**: Total distance traveled at 12 weeks*

As expected in nocturnal animals, both diet groups were most active at night. However, chow-fed animals were an incredible three times more active than animals consuming a HF+S diet at seven weeks. The 12 week data mirrored the 7 week data in that no difference existed

between groups during the day and chow-fed animals were much more active at night than the HF+S and MT groups. Meal timing did not affect the total distance traveled by animals during the day or at night.

The amount of time spent sleeping, or sleep percentage, over a 24 hour period was also observed for the various dietary groups at 7 and 12 weeks. Chow-fed animals slept 84.3% of the time during the day, an amount not significantly different than the 83.6% seen in HF+S animals during the day at 7 weeks ($p < 0.05$) (Fig 39). Both of these amounts were significantly greater than the 78.2% sleep at night for HF+S animals, which in turn was significantly greater than the 47.9% sleep seen in the chow group at night ($p < 0.05$).

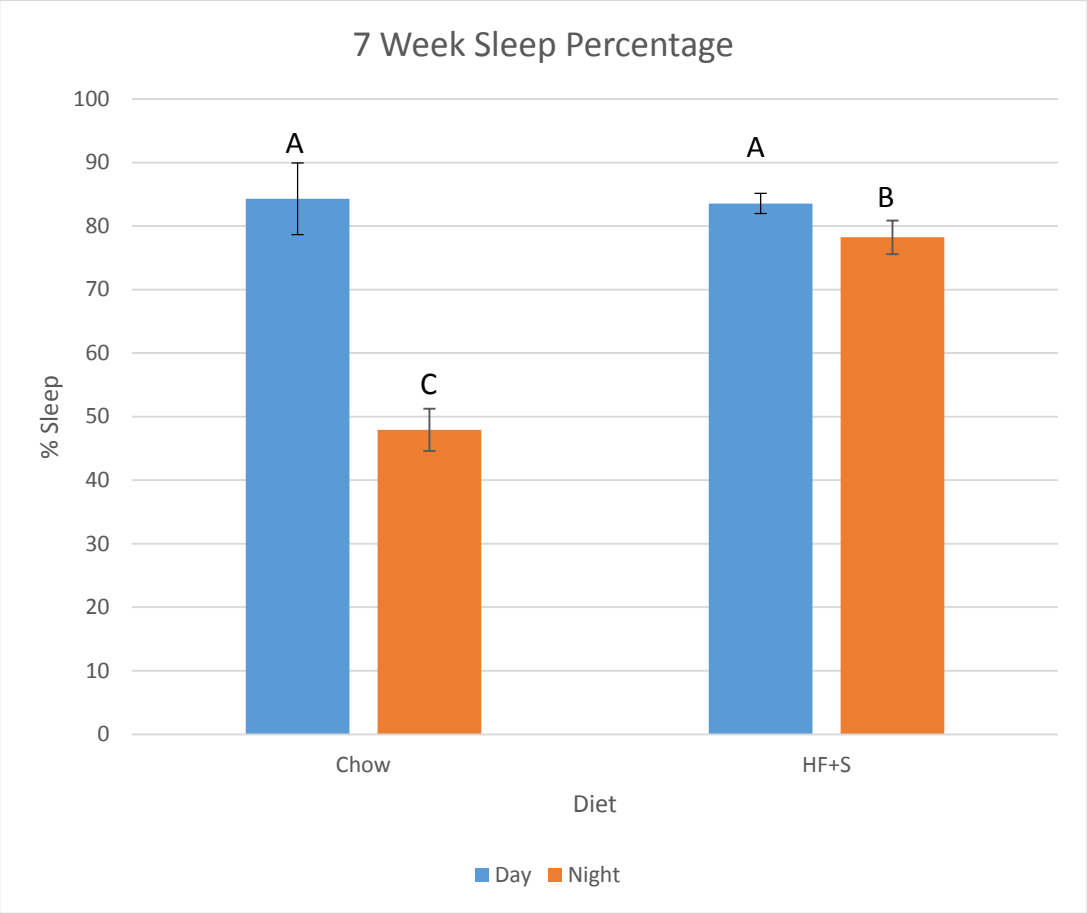

***Figure 39**: Percentage of time animals spent sleeping at 7 weeks*

The chow, HF+S and MT groups at 12 weeks all had similar sleep percentages of 87.1%, 84.8%, and 89.3%, respectively, during the day (Fig 40). Sleep percentage was significantly decreased at night, as HF+S animals slept 61.1% and MT animals slept 62.3% of the time ($p < 0.05$). These percentages were not significantly different from each other but were significantly greater than the 52.7% sleep observed in chow animals ($p < 0.05$).

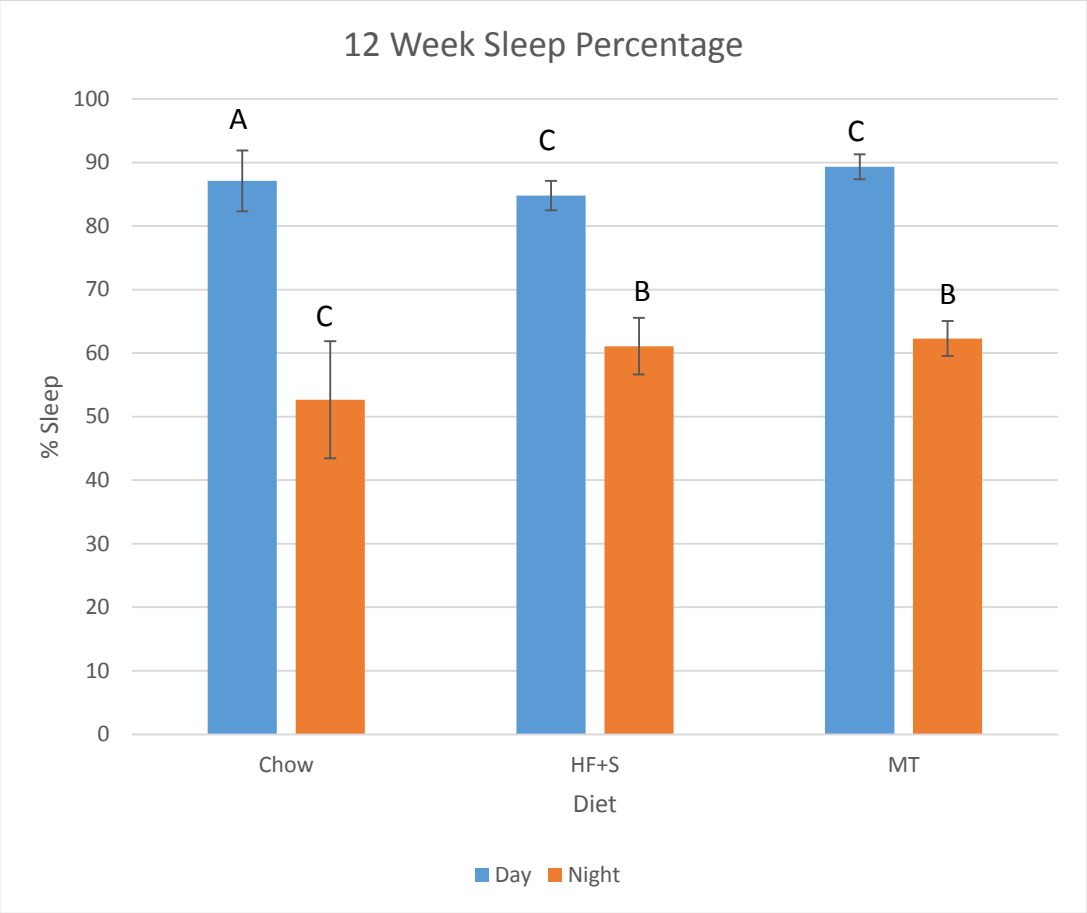

***Figure 40**: Percentage of time animals spent sleeping at 12 weeks*

Unsurprisingly, all animals spent the vast majority (over 80%) of their time during the day sleeping and were significantly more active at night. However, at 7 weeks HF+S animals slept greater than 1.6 times more than chow-fed animals. At 12 weeks this disparity was not observed. Meal timing did not affect sleep percentage compared to non-meal timed animals on HF+S diet during the day or at night. At night, chow-fed animals slept marginally less than the HF+S and MT groups.

The amount of time spent stationary, or still percentage, revealed results nearly identical to the sleep percentage data. At 7 weeks the 93.1% still in chow-fed animals during

the day was not significantly different from the 93.1% still in HF+S animals, but both were significantly greater than the 91.1% still observed in HF+S animals at night ($p < 0.05$) (Fig 41). This, in turn, was a significantly greater still percentage than the 76.36% observed in chow-fed animals during the day ($p < 0.05$).

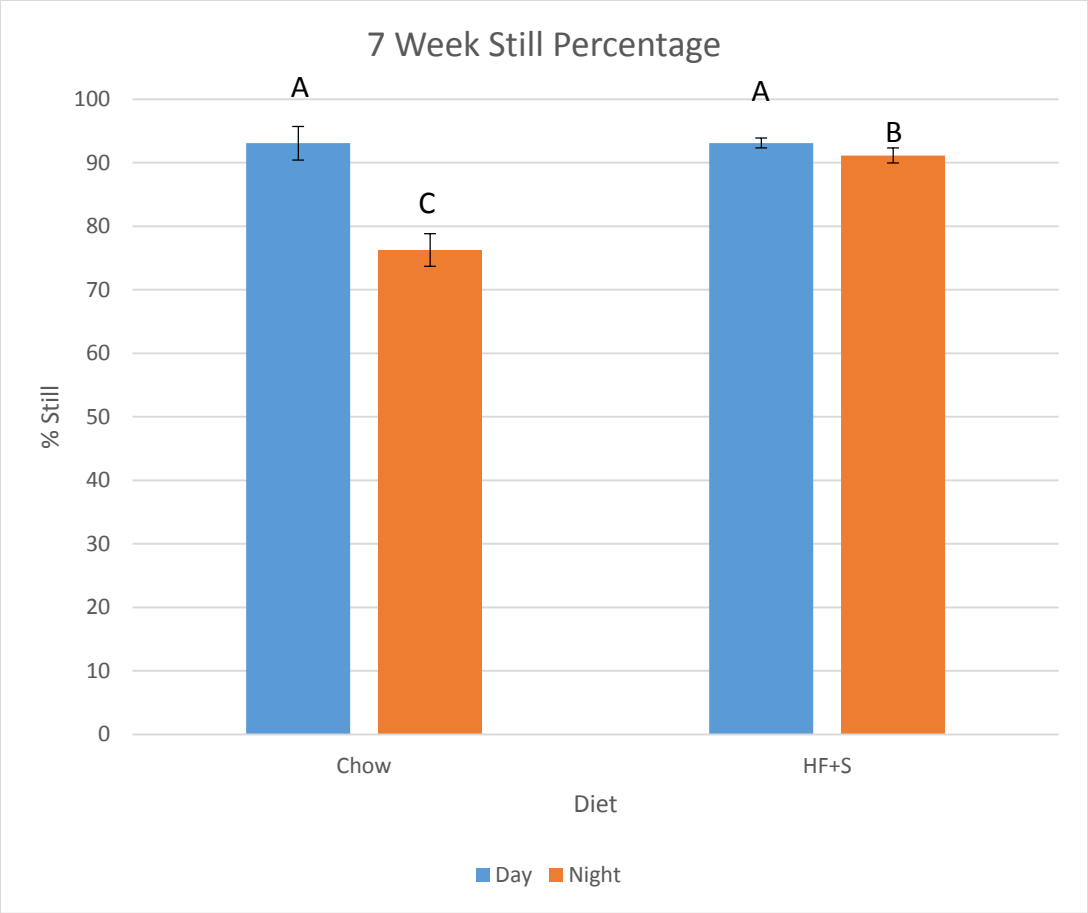

***Figure 41**: Percentage of time animals spent still at 7 weeks*

The results at 12 weeks revealed chow-fed animals at night are still only 79.5% of the time, an amount significantly less than the 83.5% and 84.5% observed in HF+S and MT animals at the same time ($p < 0.05$) (Fig 42). All 3 diet groups, with nightly still percentages of 94.1% for chow, 93.9% for HF+S, and 95.8% for MT were not significantly different from one another but

were significantly greater than the still percentages observed by animals during the day ($p < 0.05$).

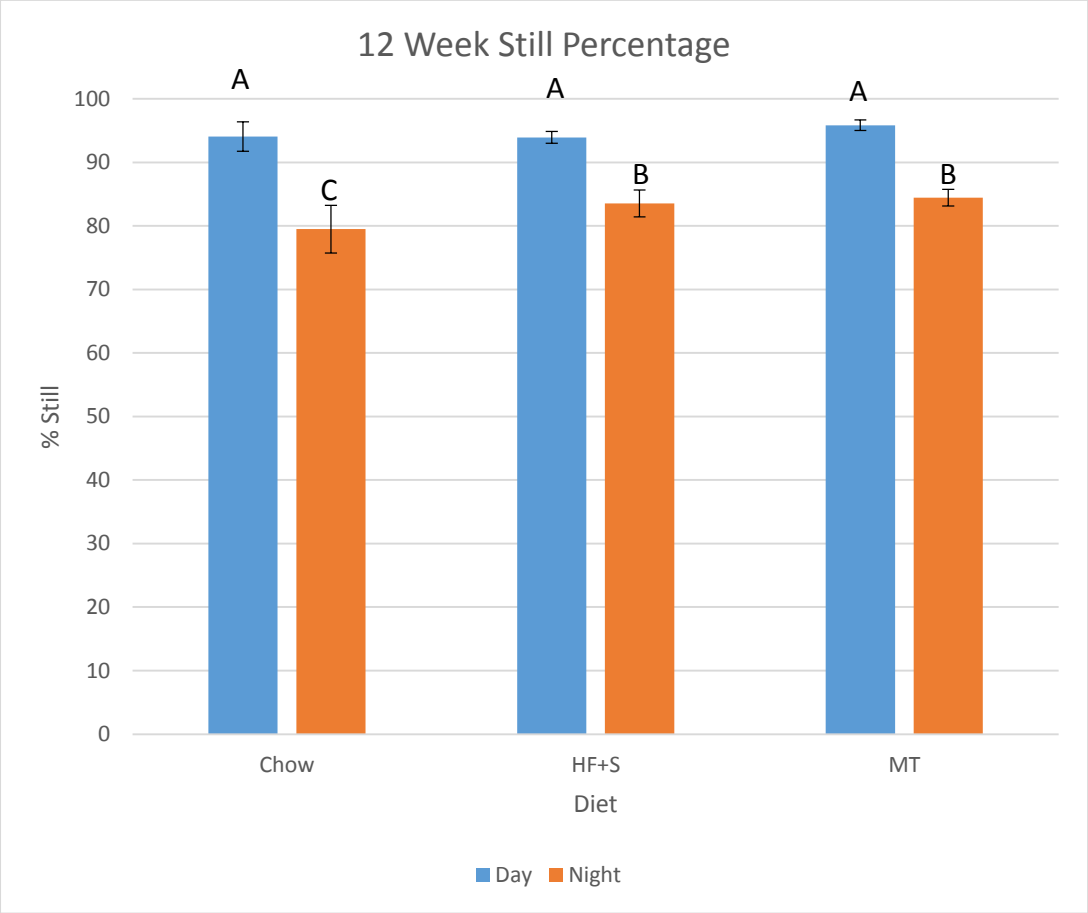

***Figure 42**: Percentage of time animals spent still at 12 weeks*

The still percentage results naturally agree strongly with the sleep percentage results in all groups at both 7 and 12 weeks as the absence of a running wheel significantly limits the animals' options for activity. Consistent with the sleep percentage data, animals were most stationary during the day and chow-fed animals were less sedentary than HF+S and MT animals at night.

The mean speed during pedestrian locomotion, or ped speed, was measured for every movement made within the metabolic cage. At 7 weeks the ped speed of 0.02 m/s for the chow group at night was significantly greater than the 0.01 m/s traveled by the HF+S group at night ($p < 0.05$) (Fig 43). The daily locomotion rate of 0.02 m/s by the chow group and the 0.01 m/s by the HF+S group in the daytime were not statistically different from the nightly speed of the HF+S group, and therefore were significantly slower than the chow-fed group at night ($p < 0.05$).

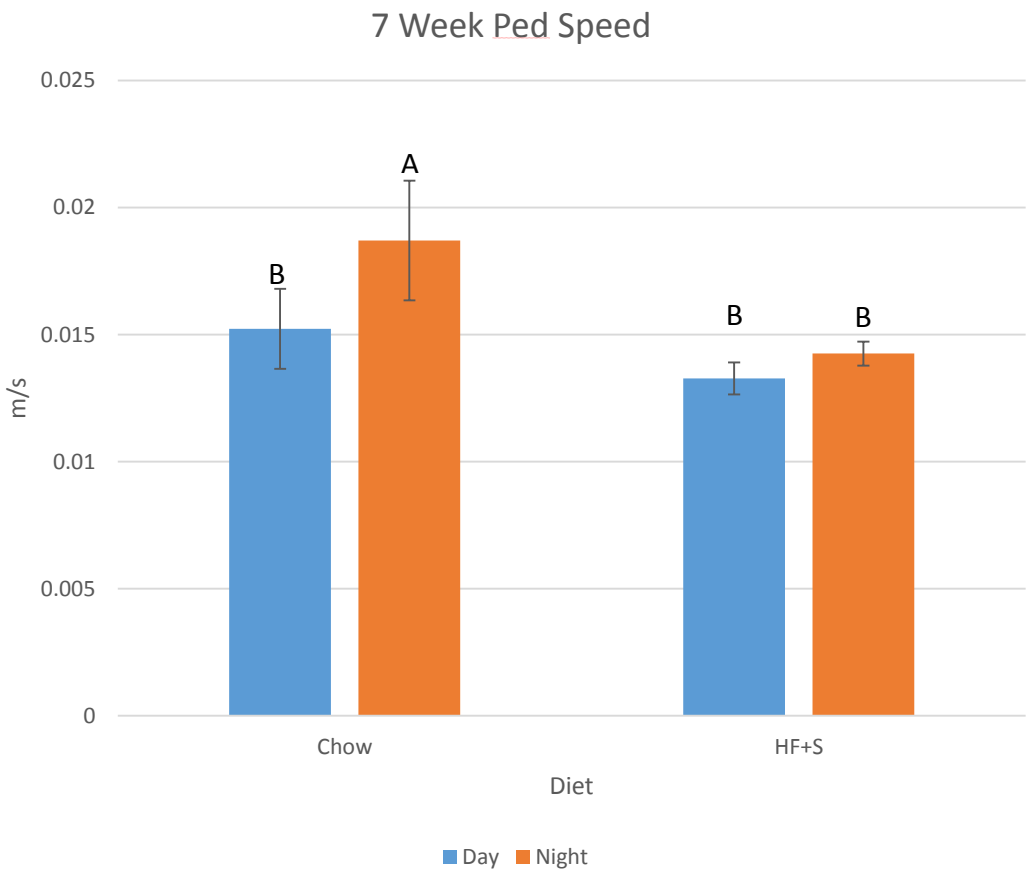

***Figure 43**: Mean speed during pedestrian locomotion at 7 weeks*

At 12 weeks the chow-fed animals had a nightly ped speed of 0.02 m/s, a rate that was significantly greater than all others except the chow groups' daily speed of 0.02 m/s ($p < 0.05$) (Fig 44). This daily speed was not significantly dissimilar than the nightly ped speed of 0.02 m/s observed in the MT group, but both surpassed the 0.01 m/s locomotion rate from the HF+S group at night ($p < 0.05$). The MT and HF+S groups had daily ped speeds of 0.01 m/s and 0.01 m/s, respectively, both of which were significantly slower than that of the HF+S nightly speed and all other groups ($p < 0.05$).

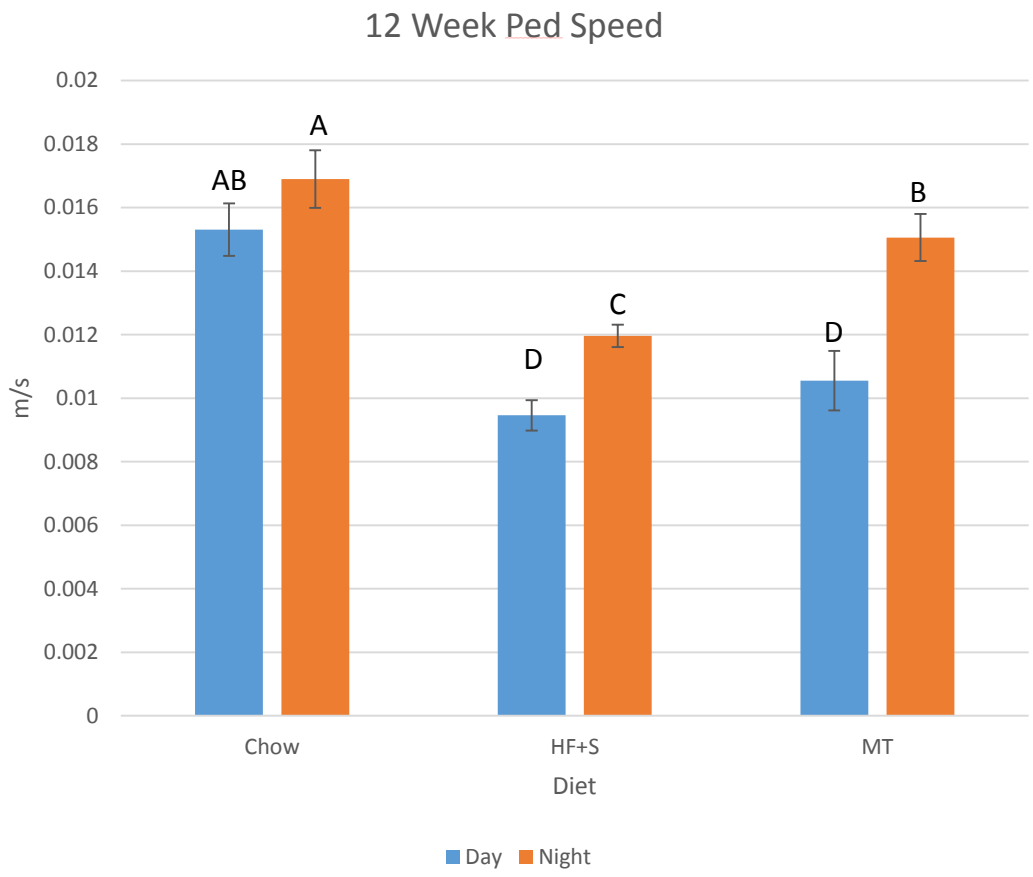

***Figure 44**: Mean speed during pedestrian locomotion at 12 weeks*

Similar to the distances traveled, the HF+S group at both time points and the chow group during the day traveled at approximately the same speed. Much like the significantly greater distance traveled at night by the chow animals, the speed at which this group of animals moved was significantly greater than the others. This may be due in part to the lower body masses seen in chow-fed animals, potentially allowing them to move at greater speeds than the heavier animals on HF+S diets. The chow group at night still had the greatest ped speed, but by a much smaller margin. The nightly speed seen in MT animals resembled the chow group. Although the MT nightly ped speed was marginally less than the chow group at night, it was significantly greater than the HF+S group. This indicates that MT did have an effect on locomotion speed compared to non-meal timed animals on a HF+S diet. Given that the MT group also had decreased body mass relative to the HF+S group, the postulation that decreased body mass is inversely related to locomotion speed is substantiated. Although not significantly different, MT animals during the day displayed a ped speed that trended upwards of the daily speed in HF+S animals.

Distance traveled in pedestrian locomotion, or ped meters, was also measured. Animals in both the chow and HF+S groups were significantly less active during the day, traveling 49.7 m and 53.7 m, respectively, compared to the 81.3 m traveled at night by animals on HF+S diet ($p < 0.05$) (Fig 45). Chow-fed animals traveled significantly more at night than HF+S animals, recording 254.4 m ($p < 0.05$).

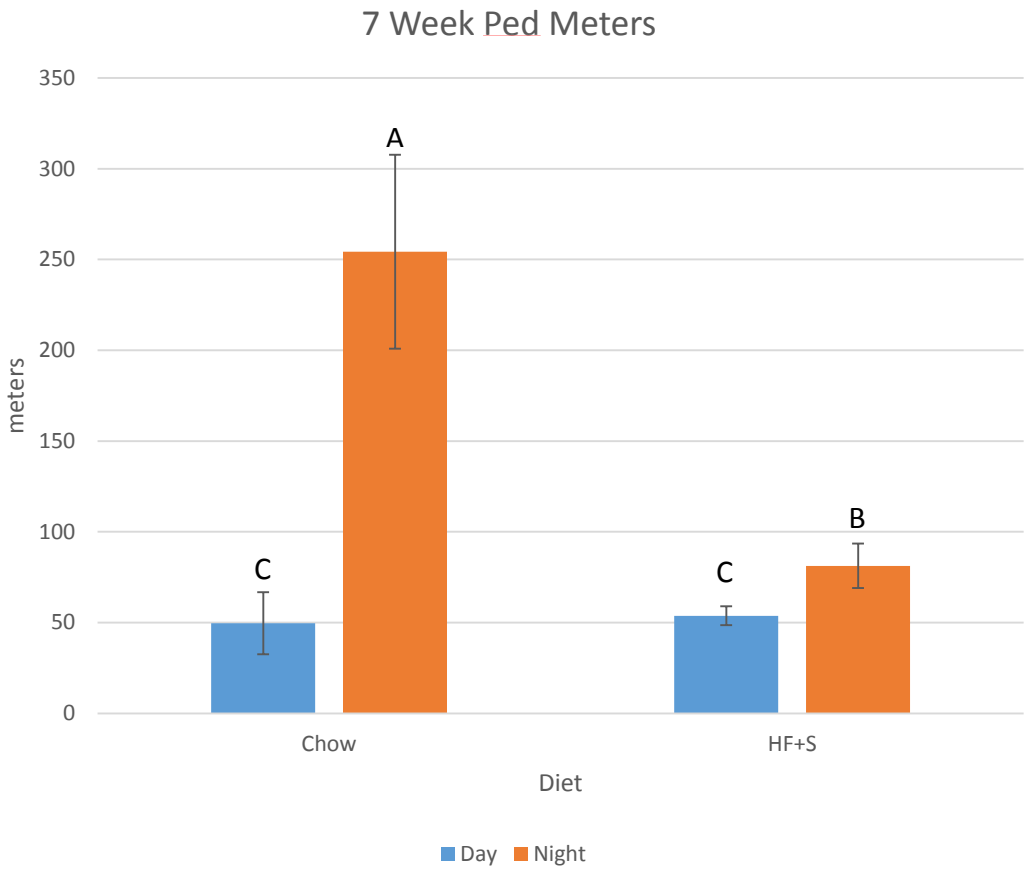

Figure 45: *Distance traveled in pedestrian locomotion at 7 weeks*

Daytime activity was also significantly less than nightly activity at 12 weeks (Fig 46). Although the 107.8 m and 126.3 m traveled at night by HF+S and MT animals, respectively, were statistically similar, these distances were significantly greater than the 49.6 m covered by chow, 36.3 m by HF+S, and 26. 0 m by MT groups during the day ($p < 0.05$). Chow-fed animals, travelling 195.1 m at night, were significantly more active than any other group ($p < 0.05$).

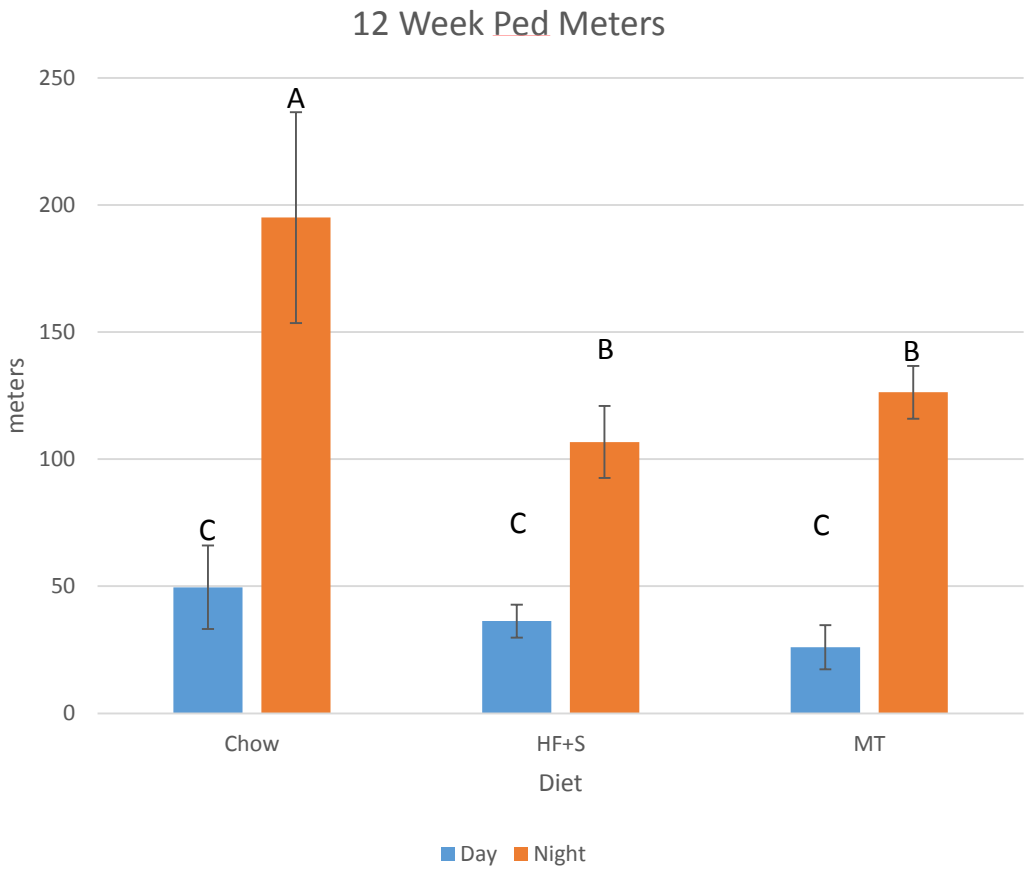

***Figure 46**: Distance traveled in pedestrian locomotion at 12 weeks*

Analysis over a 24 hour period for all dietary groups at both 7 and 12 weeks was conducted (Fig 47 and 48). Plots of every activity event for each diet group were then overlay on top of each other for comparison. Repeated measures ANOVA compared the data across dietary groups at each of the corresponding 181 time points. Analysis at 7 weeks discovered 23 significant differences between the chow and HF+S groups (time points 4, 49, 58, 62, 87, 102, 107, 109, 123, 125, 131, 132, 140, 142, 143, 145, 152, 155, 160, 167, 170, 171, and 176). Repeated measures ANOVA at 12 weeks also found numerous differences when comparing the three differet diet groups. Comparison of activy between chow-fed and HF+S animals revealed differences at times 1, 13, 22, 86, 96, 102, 103, 111, 115, 131, 133, 138, 139, 148, 149, and 167

while comparions between the chow and MT groups illustrated differences at time points 1, 13, 22, 86, 96, 98, 100, 111, 115, 133, 138, 139, 148, 167 and 170. Comparison of activty between HF+S and MT animals yielded significant differences at times 97 and 170.

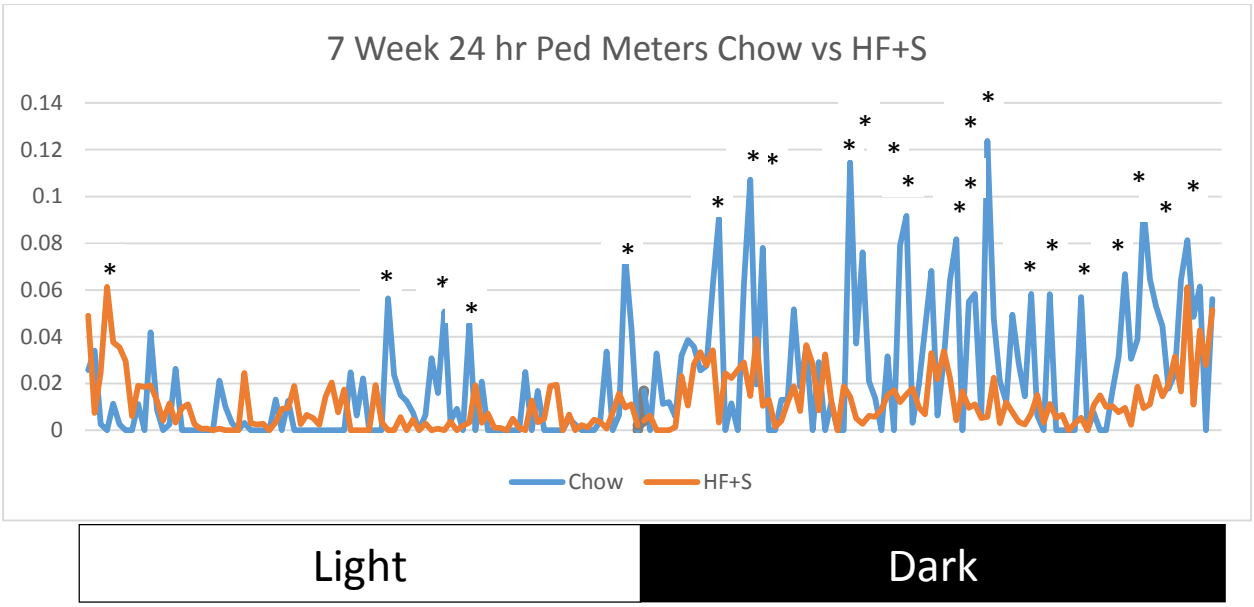

***Figure 47**: Distance traveled in pedestrian locomotion (m) over a 24 hour cycle in animals on both chow and HF+S diets at 7 weeks*

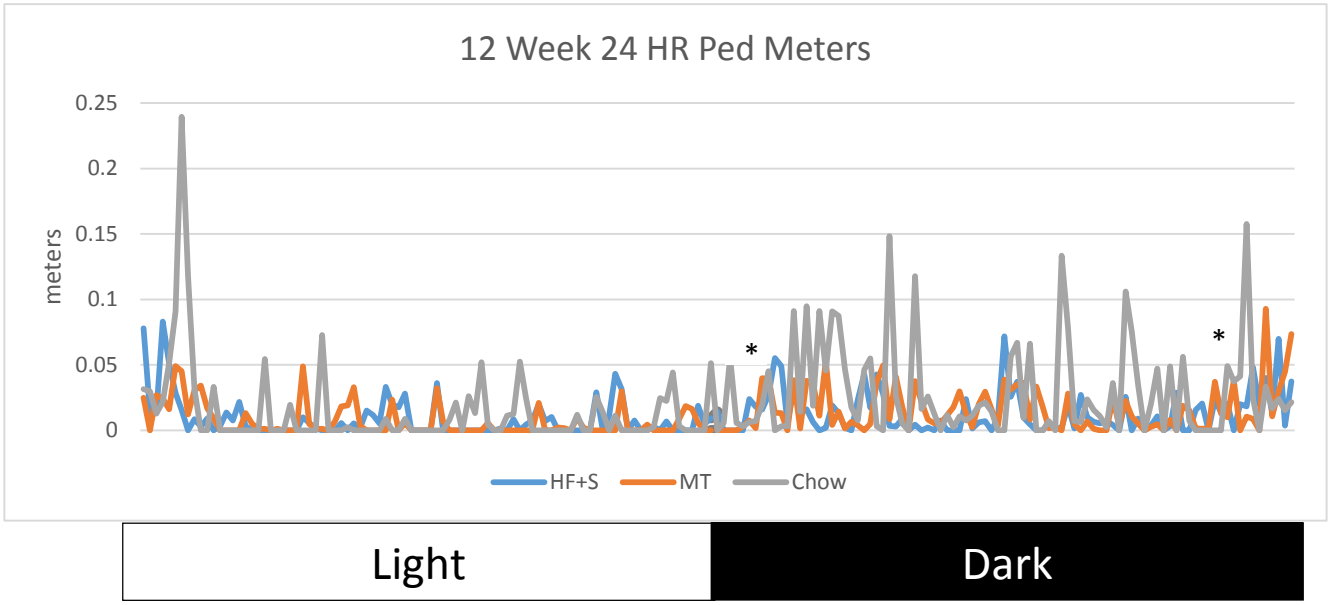

***Figure 48**: Distance traveled in pedestrian locomotion (m) over a 24 hour cycle in animals on chow, HF+S, and MT diets at 12 weeks. Due to overcrowding marks for significance (*) where only included for comparison of HF+S & MT groups.*

Unsurprisingly, the distribution of the ped meters data is the inverse of the sleep percentage and still percentage data, illustrating less activity during the day and more activity during the night. Daytime ped meters at both 7 and 12 weeks did not differ between diet groups. At 7 and 12 weeks chow-fed animals were significantly more active than HF+S animals at night, a result consistently seen across multiple activity parameters. Meal timing did not have an impact on pedestrian locomotion as MT and HF+S activity were not significantly different.

Horizontal movement across the cage, or X breaks, was calculated by the number of laser beam breaks on the X axis. This activity parameter strongly resembled the all meters data as the 5,101 X breaks during the day in the chow group were not statistically different from the 4,984 beam breaks observed in the HF+S group during the day (Fig 49). Both of these values

were significantly less than the 7,742 nightly X breaks in HF+S animals, which in turn was significantly less than the 16,144 beam breaks from chow-fed animals at night ($p < 0.05$).

***Figure 49**: Beam breaks along the X axis at 7 weeks*

Although a significant difference existed between all of the daily X breaks compared to the nightly x breaks, there were no differences between the dietary groups at 12 weeks (Fig 50). The 4,170, 4,815, and 4,580 X breaks observed during the day in the chow, HF+S, and MT groups, respectively, were all significantly less than the 13,239 chow, 13,150 HF+S, and 13,780 MT nightly beam breaks ($p < 0.05$).

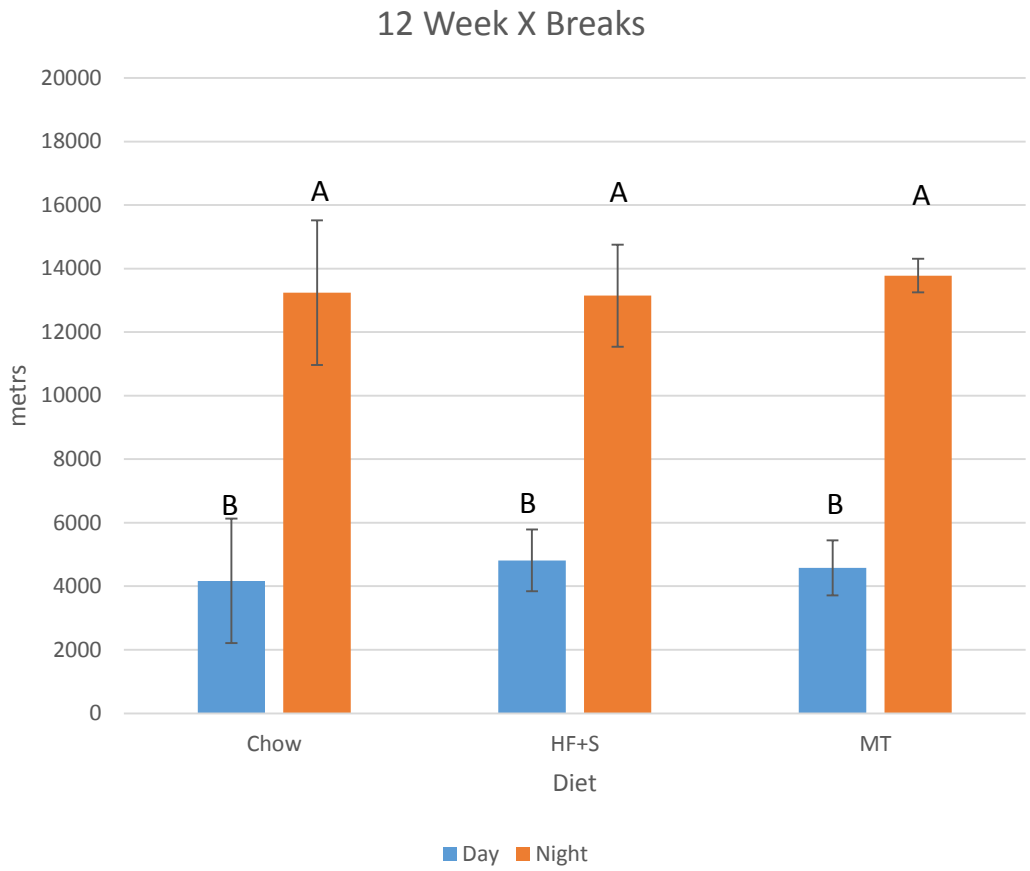

***Figure 50**: Beam breaks along the X axis at 12 weeks*

Given that horizontal movement is one of the parameters used to determine the total distance traveled by animals (all meters), it is not surprising the data mirror each other. Animals were consistently more active at night at both 7 and 12 weeks and chow-fed animals displayed greater movement than HF+S animals at 7 weeks. At 12 weeks the number of X breaks at night did not vary significantly across the three diet groups. Therefore, MT did not affect horizontal movement.

Vertical movement across the cage, or Y breaks, determined the amount of forward and backward movement across the longer plane within the metabolic cage. The distribution of this

data was identical to the X breaks parameter in that the 6,599 and 8,586 daily Y breaks seen in the chow and HF+S groups, respectively, were significantly less than the 11,489 beam breaks in HF+S animals at night (Fig 51) ($p < 0.05$). The 26,025 nightly Y breaks in chow-fed animals were significantly greater than the HF+S group ($p < 0.05$).

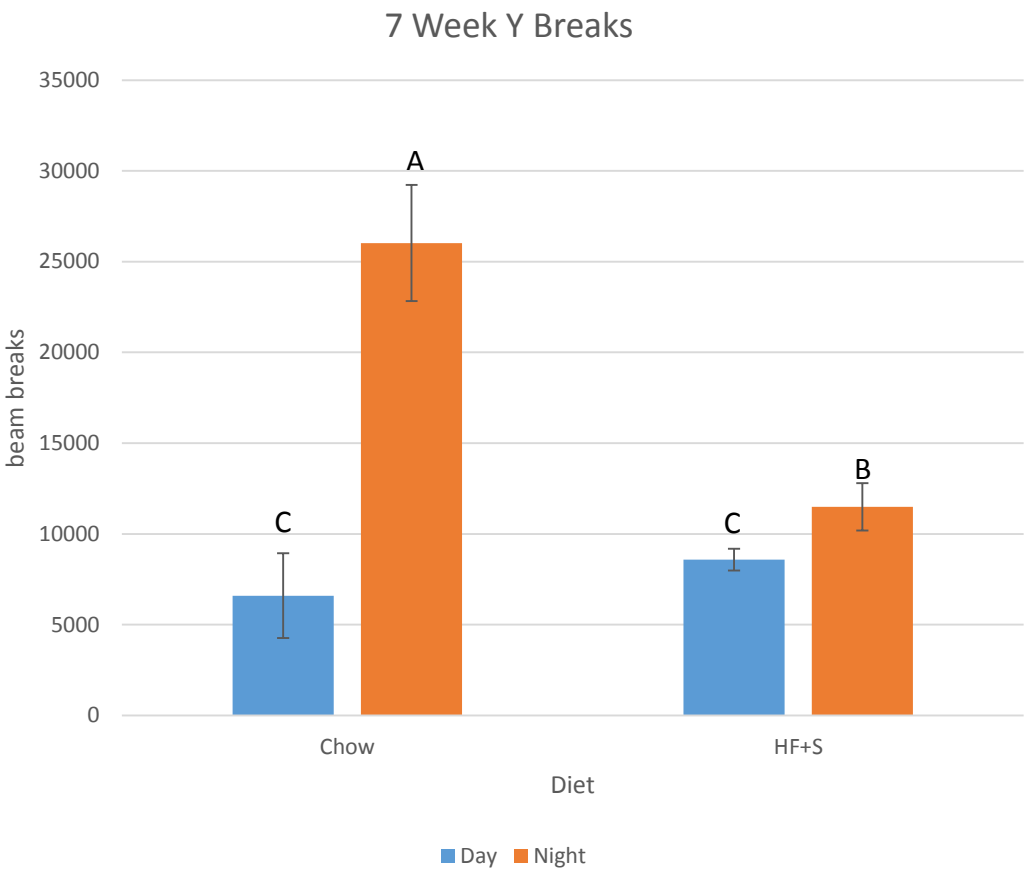

Figure 51: *Beam breaks along the Y axis at 7 weeks*

Similarly, at 12 weeks the 5,274 Y breaks for the chow, 7,340 for the HF+S, and 7,336 for the MT groups were not significantly different from one another but were significantly less than the 16,952 beam breaks observed at night for HF+S animals (Fig 52) ($p < 0.05$). Animals on MT diet were significantly more active at night than HF+S animals, accounting for 18,804 Y breaks

($p < 0.05$). Chow-fed animals were significantly more active at night, recording 24,508 beam breaks.

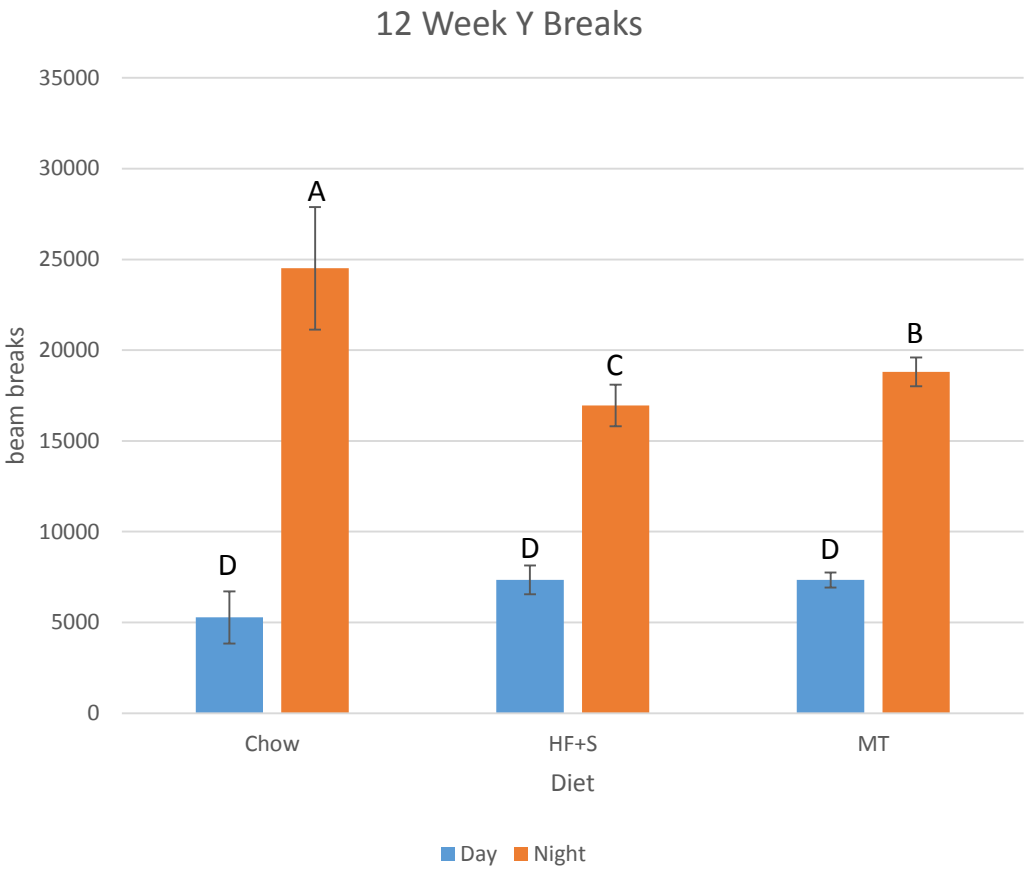

Figure 52: *Beam breaks along the Y axis at 12 weeks*

Y breaks are also used in the calculation of all meters, therefore, the seven week data is identical to the X breaks data and is in strong agreement with the other activity parameters. Although the daytime Y breaks are similar across all three groups, the nightly beam breaks all differ from one another. Consistent with other activity parameters, chow-fed animals are more active at night than the HF+S and MT groups. Meal timing increased the number of Y beam breaks compared to HF+S diet. It is possible the slight differences among groups seen in Y

breaks and not X breaks are influenced by the size of the area in which the animals can move. The metabolic cages are not a perfect square, and the area along the Y axis is much greater than the area along the X axis. This increased space to move about may be more representative of the animals' activity and thus account for the differences seen in both parameters.

Z breaks, vertical movement such as an animal standing of their hind legs or climbing, was also analyzed. The distribution at 7 weeks resembled the X breaks distribution in that the 868 Z breaks during the day for chow-fed animals was not significantly different than the 599 daily Z breaks measured in the HF+S group (Fig 53) ($p < 0.05$). These daily activity amounts were significantly less than the 1,187 nightly Z beaks in HF+S animals, which were significantly less than the 5,496 beam breaks observed in chow-fed animals at night ($p < 0.05$).

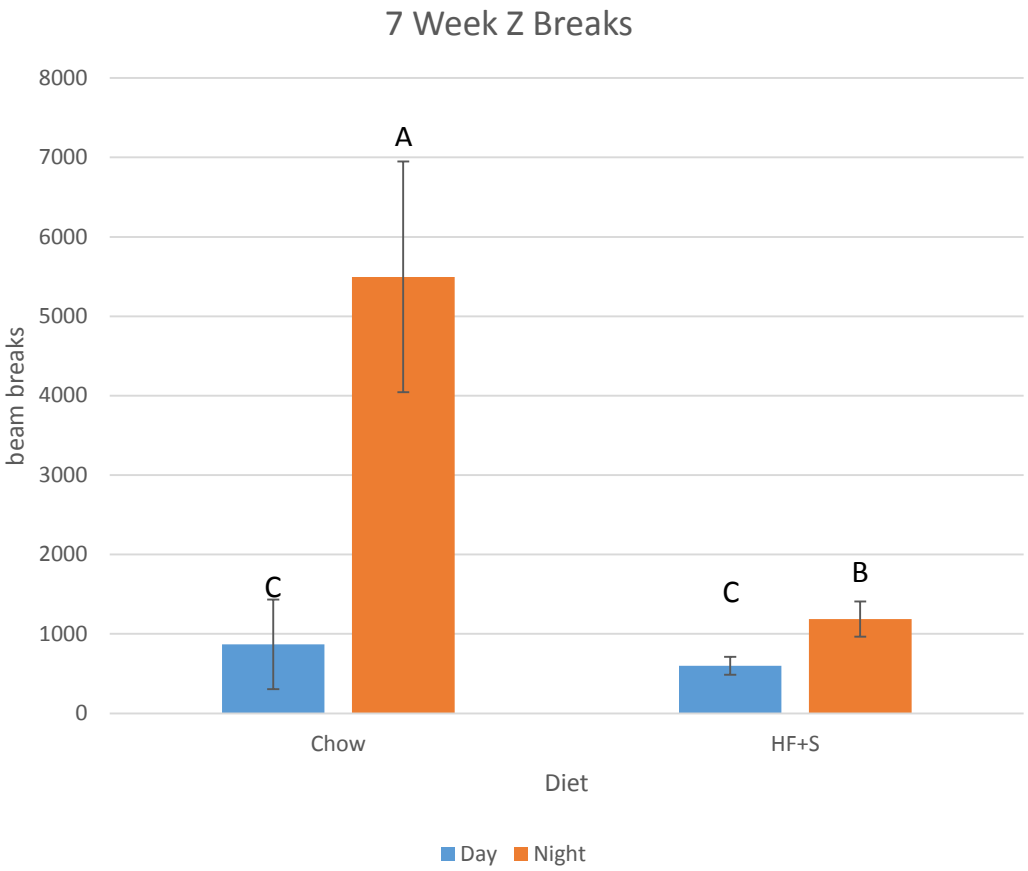

Figure 53: *Beam breaks along the Z axis at 7 weeks*

Animals on HF+S and MT diets had significantly fewer Z beam breaks (462 and 247, respectively) than the 1,866 observed in chow-fed animals during the day at 12 weeks (Fig 54) ($p < 0.05$). These daily Z breaks in chow animals were not significantly different than the 1,617 nightly breaks seen in the HF+S group or the 2,629 from the MT group. Activity for chow-fed animals at night was significantly greater than all other groups, registering 6,025 Z breaks ($p < 0.05$).

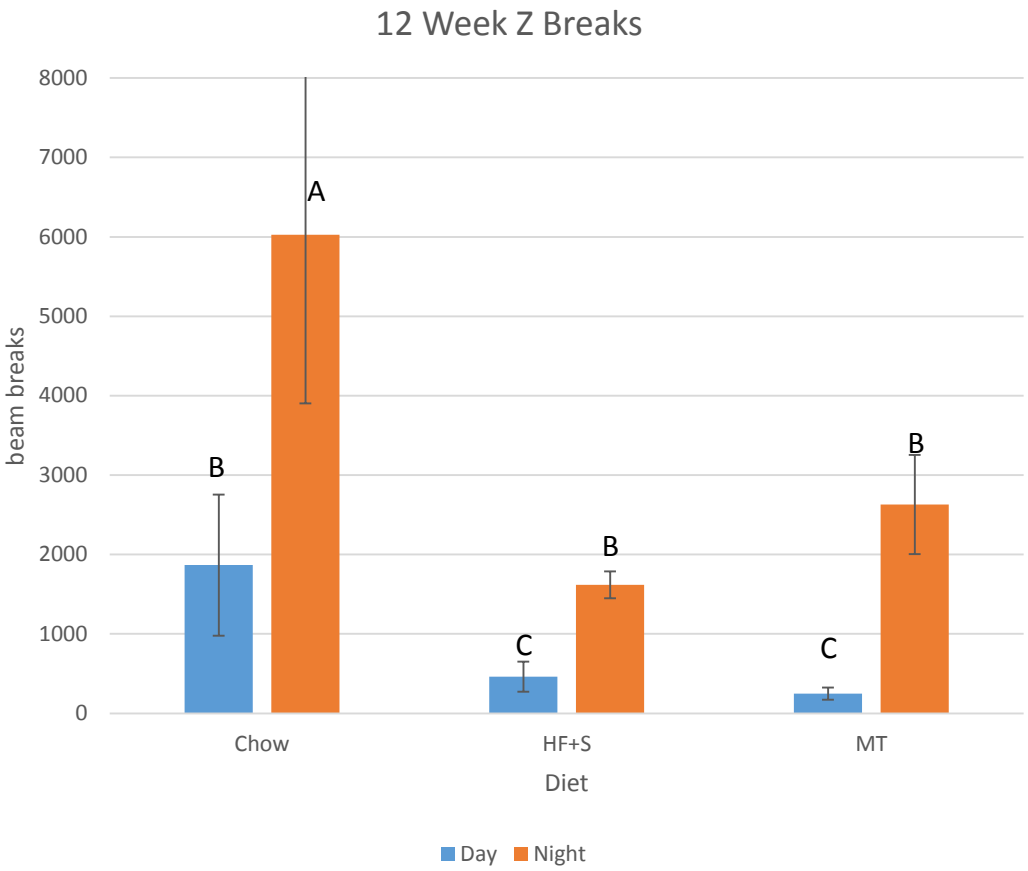

Figure 54: *Beam breaks along the Z axis at 12 weeks*

At seven weeks the chow group at night was significantly more active than HF+S animals, a result consistently found in all activity parameters. The similar distribution of the data regarding Z breaks with the X and Y breaks is expected as all three of these parameters are components of comprehensive activity parameters, such as all meters. At 12 weeks, daytime activity was significantly less than activity measured at night. Meal timing did not affect Z breaks as the daily and nightly activities were not significant different than those in the HF+S group. Chow animals were significantly more active than HF+S and MT animals during the day and at night.

Energy Expenditure

Assessment of energy lost to activity and resting energy metabolism was conducted, as the average, total, and resting energy expenditures for each dietary group were recorded. Although food uptake was similar between the HF+S and MT groups, MT animals had significantly less body mass. Given that greater body mass leads to increased energy demands, it was expected that HF+S animals would have greater total energy expenditure than MT animals to account for this difference in body mass. Despite similar daytime activity levels across all three groups, different energy expenditures, especially between chow and HF+S animals, were expected.

Average energy expenditure at seven weeks was significantly different between chow and HF+S groups both during the day and at night (Fig 55). Energy output was greatest at night in the HF+S group, averaging 0.486 kcal/hr. This was significantly greater than the nightly expenditure of 0.476 kcal/hr in the chow group or the daily output of 0.458 during the day in HF+S animals ($p < 0.05$). Both of those expenditures significantly eclipsed the 0.329 kcal/hr recorded in chow-fed animals during the day ($p < 0.05$). Analysis of covariance to assess the impact of body weight on diet and average energy expenditure revealed a significant difference at night ($p = 0.01$) while there was no significant difference during the day ($p = 0.18$). This asserts that although body mass was driving the differences in energy expenditure during the day, body mass was not responsible for the differences at night.

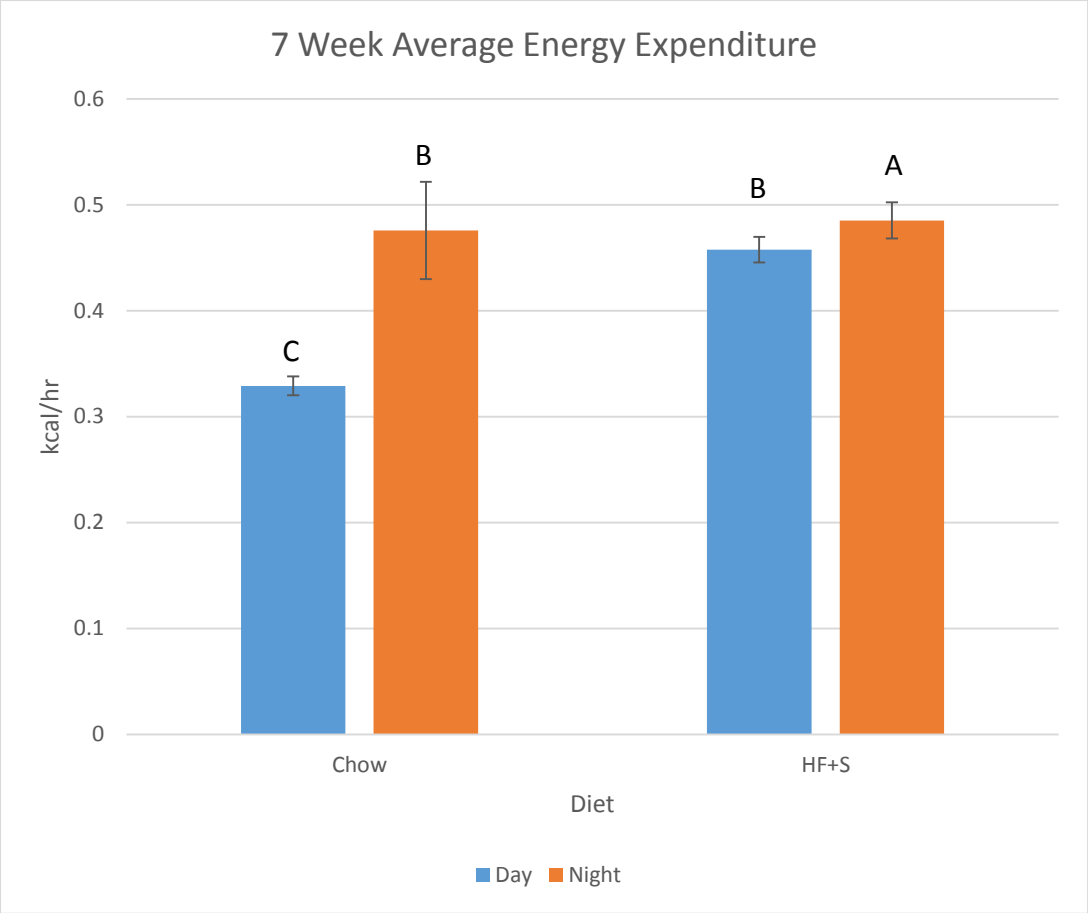

Figure 55: *Mean energy expenditure over 12 hour cycle at 7 weeks*

At 12 weeks, nightly energy expenditures of 0.487 kcal/hr in chow, 0.501 kcal/hr in HF+S, and 0.486 kcal/hr in MT animals were not significantly different from each other but were significantly greater than the daily 0.42 kcal/hr recorded in the HF+S group (Fig 56) ($p < 0.05$). This daytime expenditure was significantly greater than the 0.378 kcal/hr observed in MT animals during the day which, in turn, was significantly greater than the 0.342 kcal/hr expended during the day in the chow group ($p < 0.05$). ANCOVA results at 12 weeks determined that body mass was responsible for the differences in average energy expenditures across diet groups both during the day (chow vs HF+S $p = 0.08$, chow vs MT $p = 0.74$, HF+S vs MT $p = 0.08$) and at night (chow vs HF+S $p = 0.26$, chow vs MT $p = 0.62$, HF+S vs MT $p = 0.41$).

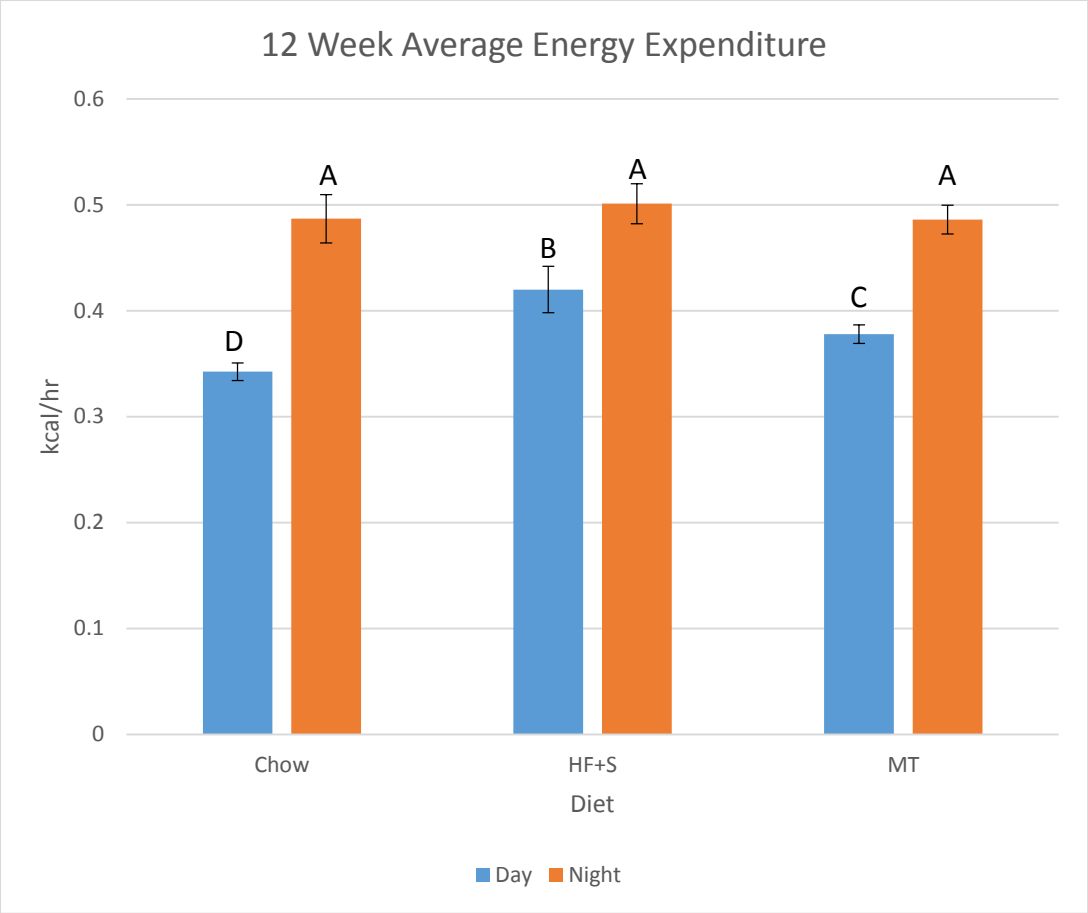

Figure 56: *Mean energy expenditure over 12 hour cycle at 12 weeks*

Given animals are primarily inactive during the day, energy expenditure at this time almost exclusively consists of resting metabolism. The findings that HF+S animals had significantly greater daytime average energy expenditures at both 7 and 12 weeks is not surprising given their increased body masses and the established association between elevated energy demands and greater body masses. The reduced daytime average energy expenditure in MT animals compared to HF+S animals demonstrates meal timing reduces energy expenditure, primarily when activity is minimal. At night, when animals are significantly more active, average energy expenditures were appropriately elevated across the board relative to during the day.

Total energy expenditure is the summed energy expenditure for an entire 12 hour cycle. At 7 weeks, the 5.8 kcal expended at night in the HF+S group was significantly greater than the 5.7 kcal at night in the chow group and 5.5 kcal during the day in HF+S animals (Fig 57) ($p < 0.05$). The 3.9 kcal utilized by chow-fed animals during the day were significantly less than any other time or dietary group ($p < 0.05$). A 24 hour plot illustrates the consistently elevated energy expenditure in the HF+S group compared to chow-fed animals over an entire day (Fig 58). Consistent with the average energy expenditure results at 7 weeks, ANCOVA identified body mass as the driving force in differences in energy expenditure across diet groups during the day ($p = 0.18$) but not at night ($p = 0.01$).

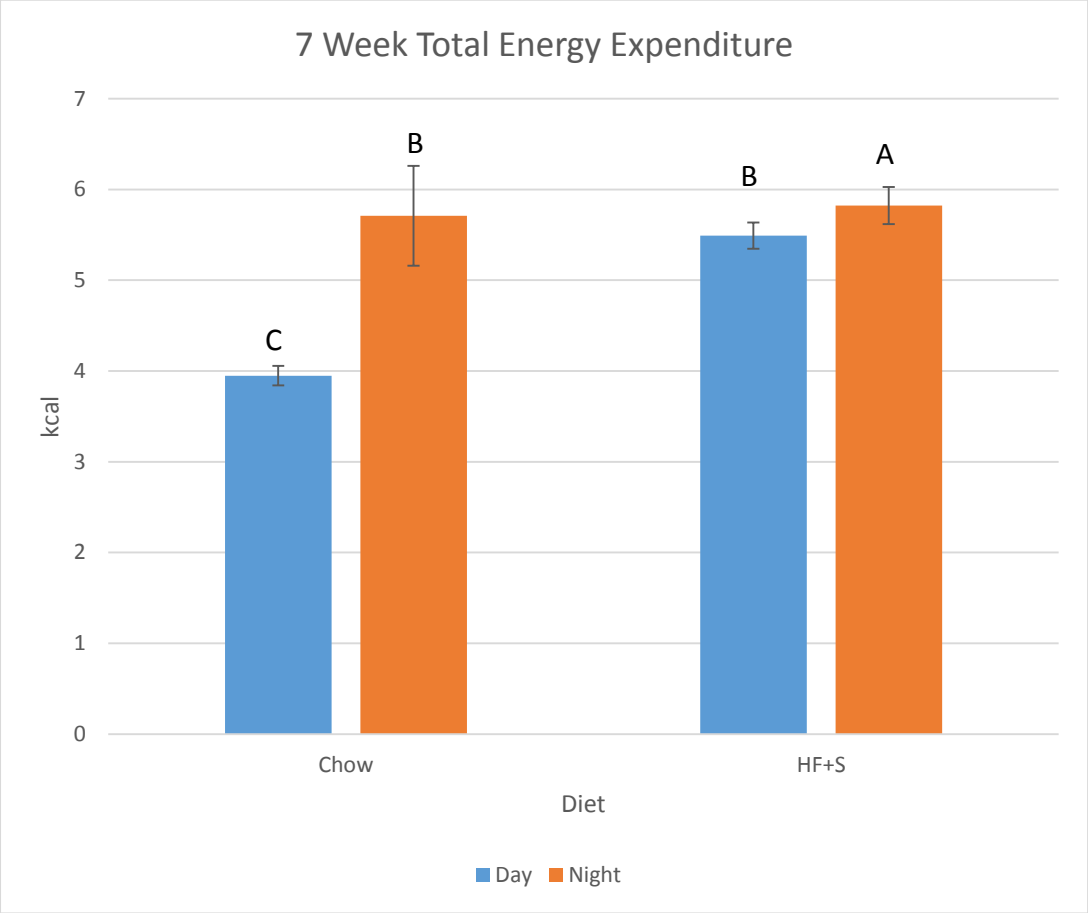

***Figure 57**: Summed energy expenditure for an entire 12 hour cycle at 7 weeks*

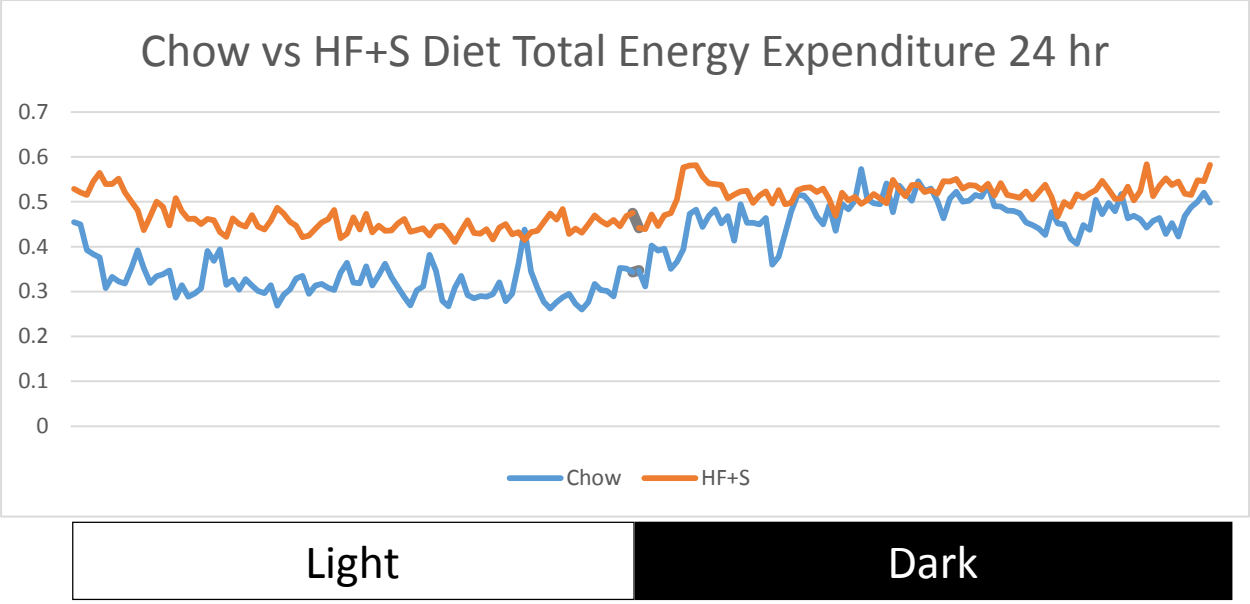

Figure 58: *Total energy expenditure over a 24 hour cycle in animals on chow and HF+S diets at 7 weeks*

At 12 weeks the nightly energy expenditures for the chow (5.8 kcal), HF+S (6.0 kcal), and MT (5.8 kcal) groups were all statistically similar (Fig 59) ($p < 0.05$). Total energy expenditure during the day for HF+S animals (5.0 kcal) was significantly less than any group at night, but was significantly greater than the 4.5 kcal expended in MT animals, which was significantly greater than the 4.1 kcal utilized in chow-fed animals during the day ($p < 0.05$). A plot over 24 hours illustrates the consistent energy expenditures across the 3 groups at night and the variable outputs seen during the day (Fig 60). Similar to the average energy expenditure results at 12 weeks, analysis of covariance to determine the impact of body mass on total energy expenditure across diet groups revealed no significant differences during the day (chow vs HF+S $p = 0.08$, chow vs MT $p = 0.74$, HF+S vs MT $p = 0.08$) or at night (chow vs HF+S $p = 0.26$, chow vs MT $p = 0.62$, HF+S vs MT $p = 0.41$), implicating body mass as a key determinant in total energy expenditure.

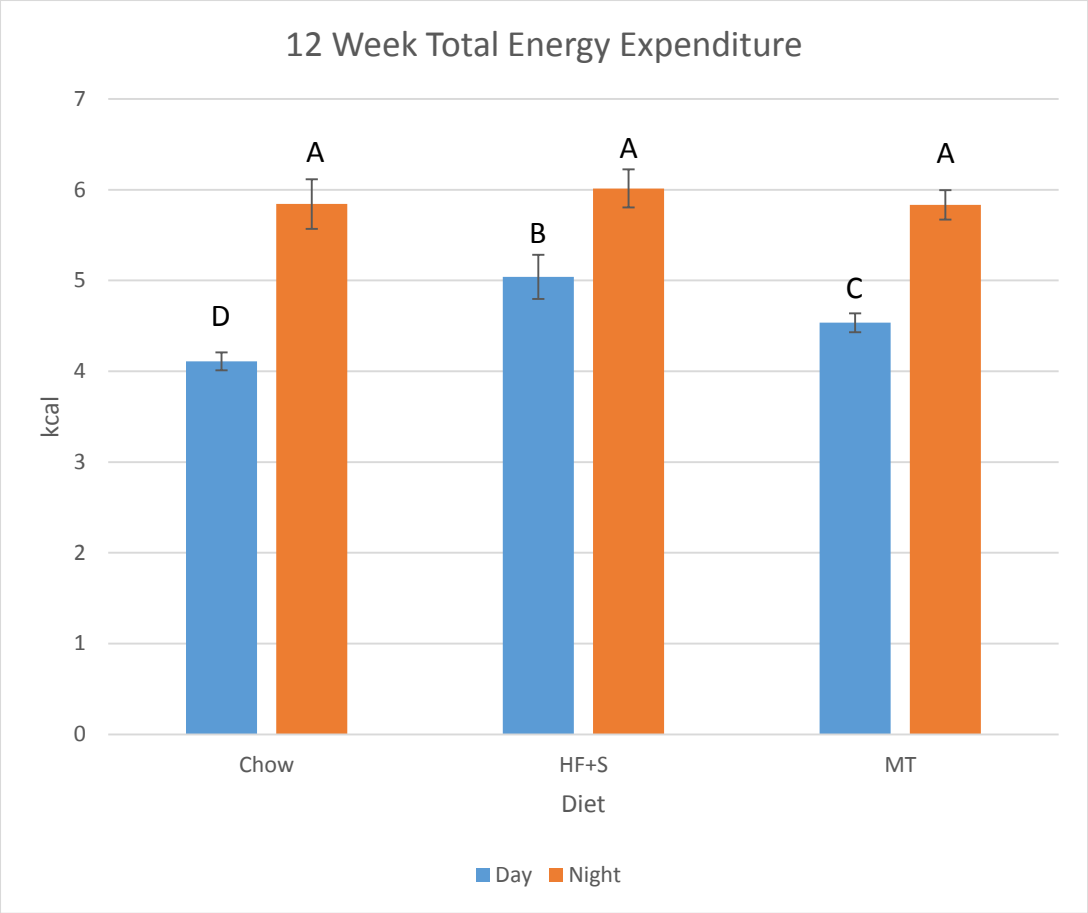

***Figure 59**: Summed energy expenditure over a 12 hour cycle at 12 weeks*

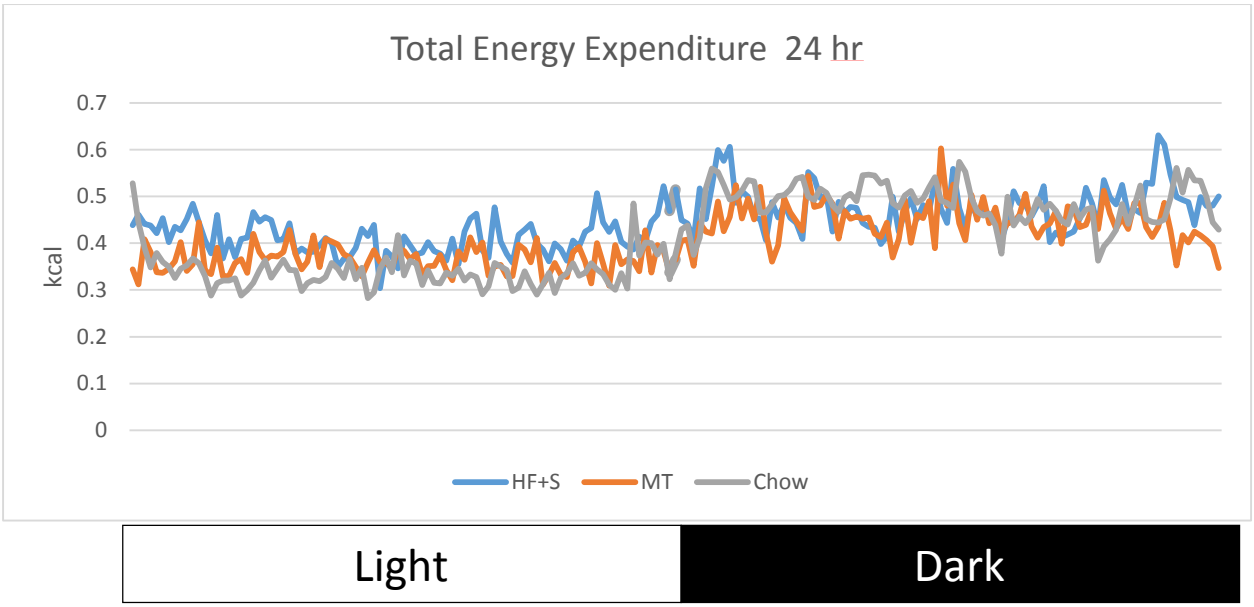

***Figure 60**: Total energy expenditure over a 24 hour cycle in animals on chow, HF+S, and MT diets at 12 weeks*

Total energy expenditure results strongly resembled the average energy expenditure findings, indicating that the average energy expenditure data was an accurate representation of the animals' energy output. Given that the average energy expenditure data is simply an hourly expression of total energy output over a 12 hour period (day and night) for each group, it is not at all surprising the two data sets look so much alike. As such, MT appears to decrease total energy expenditure during the day when activity is lowest. Repeated measures ANOVA compared the total energy expenditures for each dietary group against each other at each of the corresponding 181 time points. When comparing HF+S and chow groups significant differences were found at time points 14,15 19, 20, 21, 40, 41, 71, 78, 81, 82, 90, and 91. Analyses of total energy expenditure over a 24 hour period in MT versus chow-fed animals identified significant difference at time points 19, 40, 84, 174, and 176. Comparison of HF+S and MT groups revealed significant differences at time 77, 90, 91, 100, and 134. This suggests

that meal timing imposes little difference on total energy expenditure compared to HF+S animals.

Resting energy expenditure, defined as the mean value during the 30 minute period when activity scores were lowest, had no similarities between diet groups or times at seven weeks (Fig 61). Resting energy expenditure was greatest at night in HF+S animals (0.5 kcal) and lowest during the day in chow-fed animals (0.3 kcal). The chow group during the night had an average resting energy expenditure of 0.4 kcal, which was significantly greater that the same diet group during the day, but significantly less than the 0.4 kcal from the HF+S group during the day ($p < 0.05$). Analysis of covariance to determine the impact of body mass on resting energy expenditure across the diet groups revealed no significant differences during the day ($p = 0.67$) or at night ($p = 0.15$). This confirmed body mass as the driving factor behind the differences measured in resting energy expenditure.

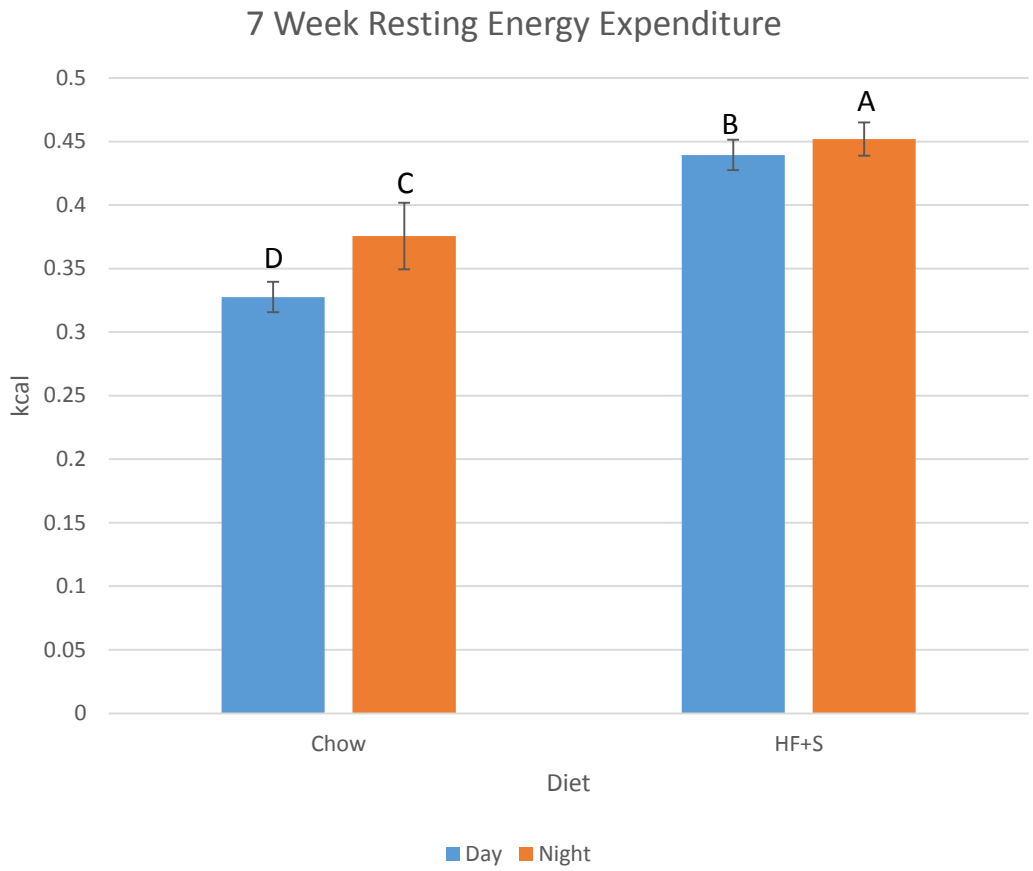

Figure 61: *Energy expenditure during the 30 minute period when activity scores were lowest at 7 weeks*

At 12 weeks the nightly resting energy expenditures of 0.4 kcal in chow, 0.5 kcal in HF+S, and 0.4 kcal in MT animals were not significantly different from one another or the daily expenditure of 0.4 kcal measured in HF+S animals, but were all significantly greater than the 0.3 kcal and 0.4 kcal recorded during the day for the chow and MT groups, respectively (Fig 62) ($p < 0.05$). Similar to the statistical analyses performed at 7 weeks, analysis of covariance to assess the impact of body mass on resting energy expenditure across dietary groups revealed no significant differences during the day (chow vs HF+S $p = 0.16$, chow vs MT $p = 0.58$, HF+S vs MT $p = 0.50$) or at night (chow vs HF+S $p = 0.11$, chow vs MT $p = 0.86$, HF+S vs MT $p = 0.27$),

indicating that body mass was responsible for the variations measured in resting energy expenditure.

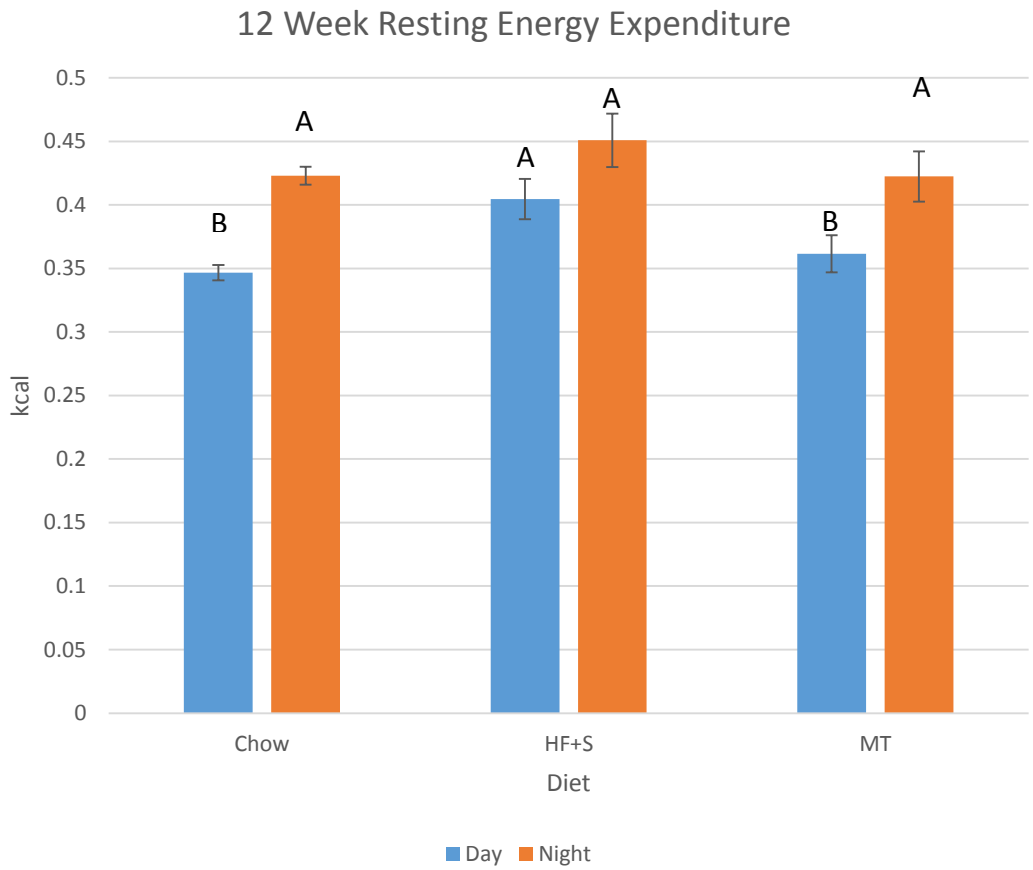

Figure 62: *Energy expenditure during the 30 minute period when activity scores were lowest at 12 weeks*

Resting energy expenditure data strongly agrees with body mass in that an inverse relationship is evident at both 7 and 12 weeks. Daytime energy expenditures in each dietary group were consistently less than at night. Although no significant difference was evident between MT and HF+S animals at night, resting energy expenditure in MT animals was significantly less than HF+S animals and strongly resembled the expenditure of chow-fed

animals, indicating that meal timing does decrease energy expenditure when there is little to no activity.

Overall, the energy expenditure data strongly agrees with the activity data. There was no difference in energy expenditures between the three groups at night. During the day, when animals are consistently less active, energy demand inversely corresponds with body mass. As such, meal timing consistently decreased energy expenditure across all parameters during the day compared to non-meal timed animals on HF+S diet. Analysis of covariance assessed the impact of body weight and diet on energy expenditure parameters. It was determined body mass significantly affected seven week total and average energy expenditures when comparing chow to HF+S diets at night, indicating that the heavier animals on HF+S diet had elevated energy expenditures relative to the lighter chow-fed animals during this time. Although animals are awake mostly at night, the activity data illustrated the animals are resting or stationary that vast majority of the time. Therefore, the decreased energy expenditure caused by meal timing may be more profound than originally presented.

Substrate Utilization

The RQ was measured to identify which substrate was primarily utilized for energy by the body. As previously mentioned, carbohydrates have an RQ of 1.0 and the RQ of fat is 0.7. The average RQ at 7 weeks was highest at night in the chow group at 0.96 and at its lowest in the same group during the day at 0.81 (Fig 63). The HF+S group had far less dramatic differences, with a nightly RQ of 0.84, a value that was significantly greater than the 0.84 RQ measured during the day ($p < 0.05$). The significant gap in RQ at night between the two diet groups is apparent in the 24 hour plot (Fig 64). Repeated measures ANOVA to compare RQ at all 180 time points revealed a significant difference between chow-fed and HF+S animals a staggering 96 times (Time points 1-4, 12, 15, 16, 33, 48, 75, 81, 100-157, 159-173, 176, 178 and 179.

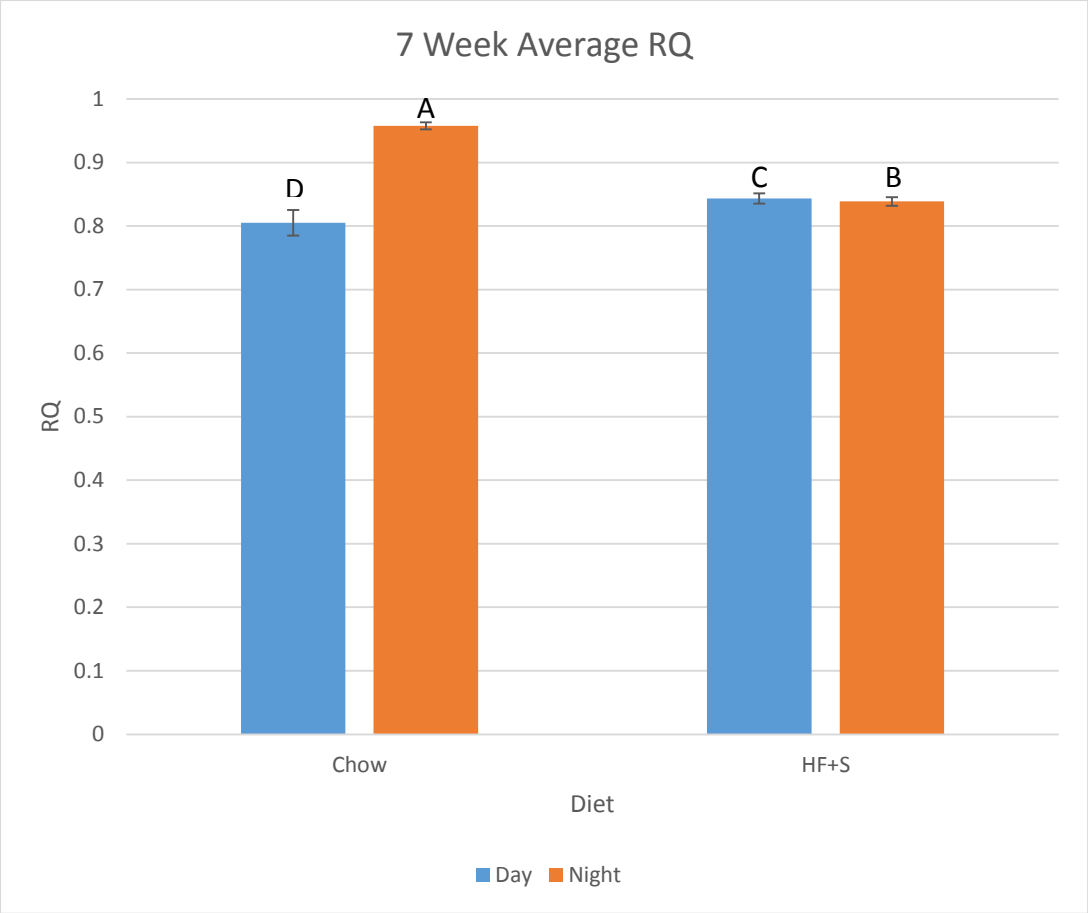

***Figure 63**: Mean respiratory quotient over a 12 hour cycle at 7 weeks*

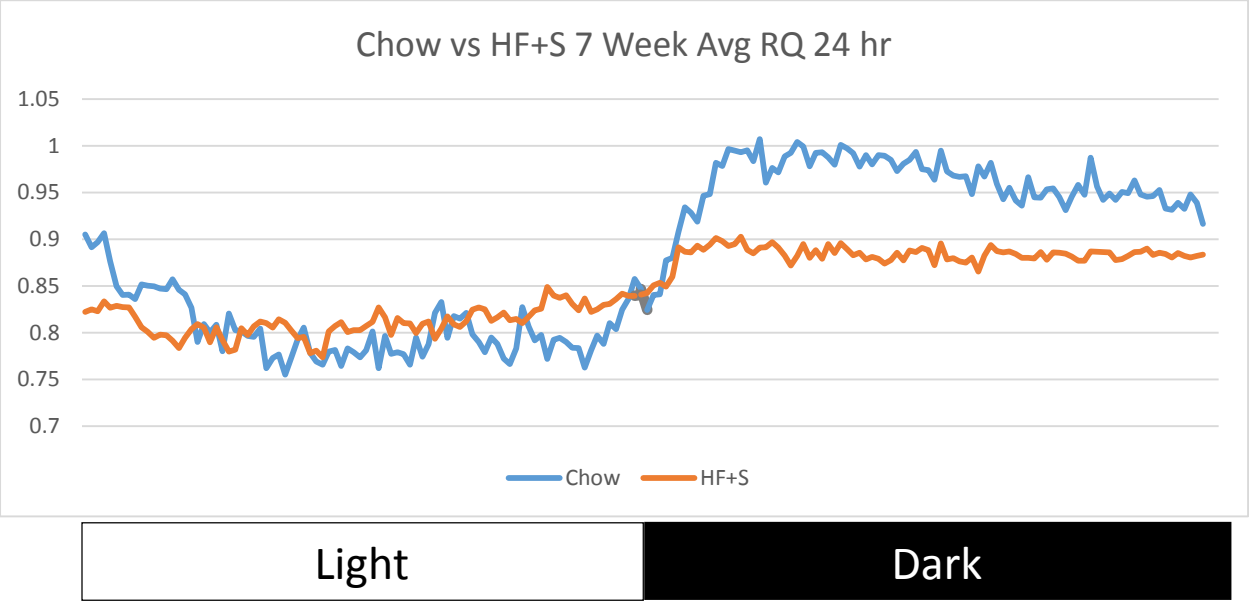

***Figure 64:** Respiratory quotient over a 24 hour cycle in animals on chow and HF+S diets at 7 weeks. Due to overcrowding marks of significance (*) were not included in the figure*

At 12 weeks the chow group at night had the highest RQ (0.96), followed by the MT group with a value of 0.91. (Fig 65) The nightly RQ measured in HF+S animals was significantly less than MT animals at 0.88, and the daily value for the same group was significantly less at 0.84 ($p < 0.05$). Although these two values for the HF+S group were significantly different from one another, they were both statistically similar to the 0.86 RQ observed in chow-fed animals during the day ($p < 0.05$). Animals on MT diet during the day had the lowest RQ of 0.8. The 24 hour plot not only illustrates the consistently elevated RQ in chow-fed animals at night versus the HF+S group, but the similar RQ spikes in both the chow and MT groups once the dark cycle begins are also illuminated (Fig 66). Repeated measure ANOVA at 12 weeks revealed numerous significant interactions between the three dietary groups. Comparison of chow-fed animals to HF+S found significant differences at time points 86, 87, 89, 92, 100, 102, 103, 104, 106-110, 112-114, 116-121, 123-131, 133, 134, 136-142, 144, 150, 151, 153, 154, 157, 158 and 160 while comparison of the chow group to MT animals revealed significant differences at time points 60, 66, 70, 72, 77-80, 82-84, 86-93, 96-103 and 106. Significant differences between the HF+S and MT groups were also found at time points 89, 93, 97-102, 123, 125, 126, 139, 142, 150, 151 and 153.

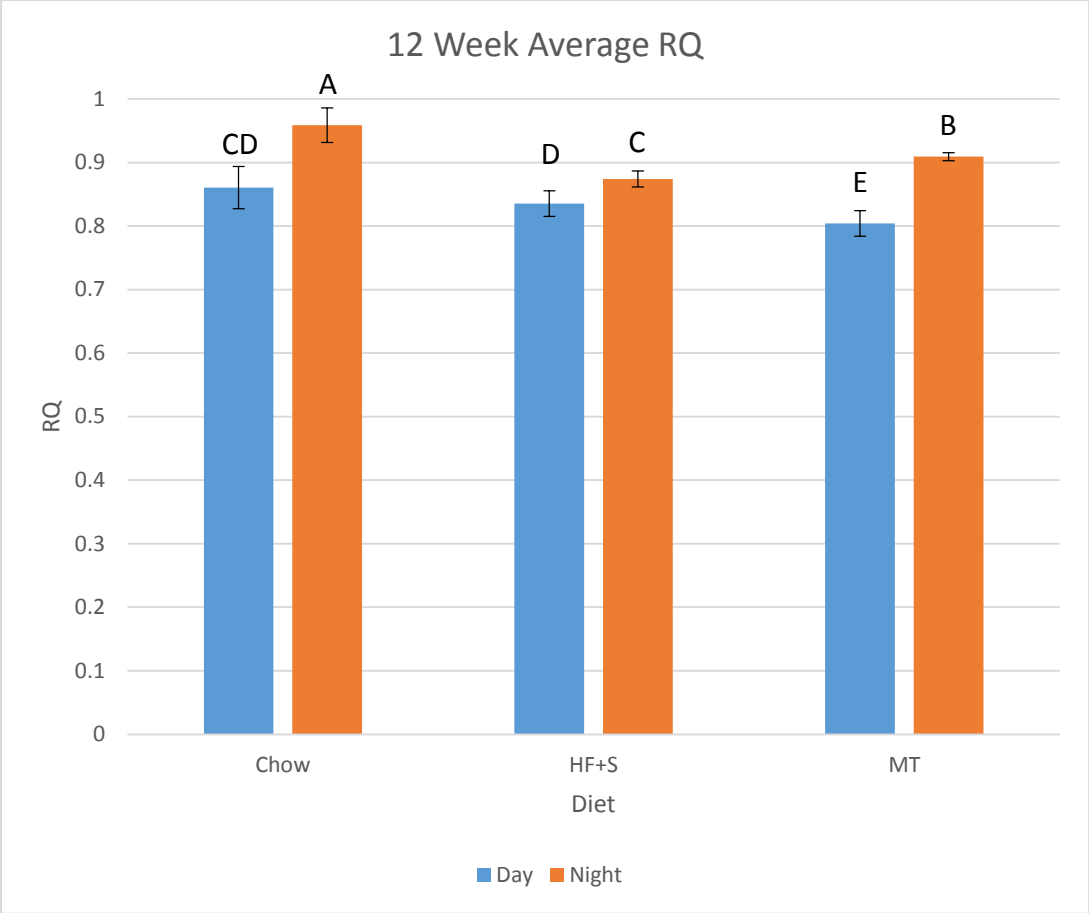

***Figure 65**: Mean respiratory quotient over a 12 hour cycle at 12 weeks*

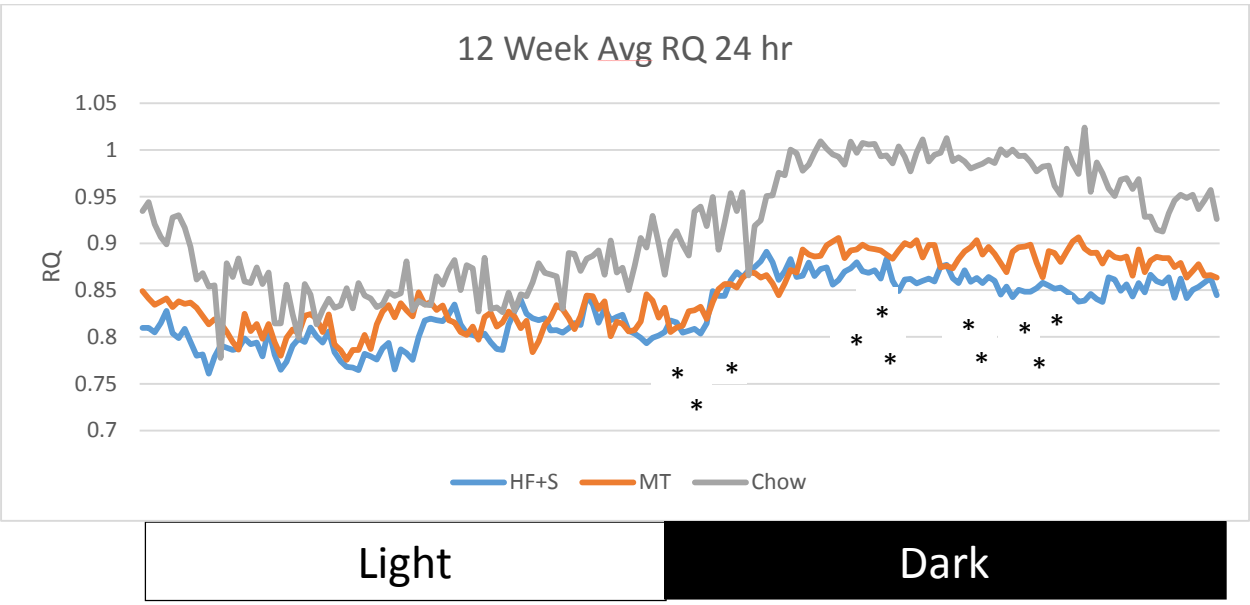

***Figure 66**: Respiratory quotient over a 24 hour cycle in animals on chow, HF+S, and MT diets at 12 weeks. Indicators of significance (*) reflect significant differences between the HF+S and MT groups. Significance found at time points 89, 93, 97-102, 123, 125, 126, 139, 142, 150, 151 and 153*

The highest RQ value at both 7 and 12 weeks occurring at night in chow-fed animals is not surprising given the food intake data. The chow group consumed their food almost exclusively at night, justifying the utilization of primarily carbohydrate energy sources at night and relying on fat stores during the day. This emphasis on fat utilization was also evident at 12 weeks in MT animals during the day when their food hopper was not present. The profound increase in RQ from day to night in MT animals strongly resembles the chow group and illustrates the dramatic effects of meal timing compared to the HF+S group. Examination of the 24 hour plots reveal dramatic increases in RQ in both the chow and MT groups as soon as the lights are turned off and the dark cycle begins, reinforcing their similarities with each other and juxtaposition to the HF+S group. There was very little difference between day and night in HF+S animals. This minimal change compared to the abrupt transition in RQ observed in MT animals at night when food is available indicates that when an animal is eating, not the presence of sugar in the drinking water, has a dramatic effect on substrate utilization. This also reinforces the power of meal timing and its ability to impact respiratory quotient.

Resting RQ measured the RQ during the 30 minutes when energy expenditure was lowest. At 7 weeks there was little difference between groups and time of day (Fig 67). The highest RQ, 0.85 recorded in the chow-fed group at night, was not significantly greater than the nighttime RQ of 0.81 measured at night in HF+S animals ($p < 0.05$). The HF+S, but not chow, group nighttime RQ was significantly greater than the 0.82 observed during the day in HF+S animals, which was not significantly different than the daytime chow group RQ of 0.79 ($p < 0.05$).

Figure 67: *Respiratory quotient during the 30 minutes when energy expenditure was lowest at 7 weeks*

Very little difference between groups or time of day was evident at 12 weeks (Fig 68). Chow-fed animals at night had the highest RQ of 0.91. Daytime and nighttime resting RQ of the HF+S (0.82 and 0.86) and MT (0.81 and 0.85) were not significantly different from each other or the resting RQ of 0.83 recorded in chow-fed animals during the day ($p < 0.05$).

Figure 68: *Respiratory quotient during the 30 minutes when energy expenditure was lowest at 7 weeks*

At seven weeks there was very little difference between groups or time of day concerning resting RQ. Values were slightly lower during the day when animals are usually asleep. The resting RQ was at its highest at night in the chow group at both 7 and 12 weeks. Considering resting RQ is determined solely from a 30 minute window of inactivity, it is not surprising there is little difference between daytime and nighttime RQ. Meal timing did not affect resting RQ at night or during the day compared to non-meal timed animals on a HF+S diet.

Overall, meal timing did appear to promote fat utilization during the day and more closely resemble the chow group. This corresponds with the food intake data in that chow-fed animals consumed their food almost entirely at night and MT animals only had access to their food hoppers at night. The RQ was at its highest in both groups at night, indicating the utilization of carbohydrate for energy, and significantly lower during the day, representing the utilization of fat stores for energy. HF+S animals showed an increased tendency to eat throughout both the day and night. Thus, the RQ's of this group were not astoundingly different when comparing the two times, but were consistently elevated during the day relative to chow-fed and MT animals.

Physiological

Blood samples were collected during the harvesting of tissues at 12 weeks. Fasting glucose levels (chow 158 mg/dl, HF+S 164 mg/dl, MT 171 mg/dl) (Fig 69) and triglyceride levels (chow 64.2 mg/dl, HF+S 62.4 mg/dl, MT 73 mg/dl) (Fig 70) were not significantly different among dietary groups ($p < 0.05$). The average cholesterol level in chow-fed animals (108.4 mg/dl) was significantly less than the HF+S (241 mg/dl) and MT (172.5 mg/dl) groups (Fig 71) ($p < 0.05$).

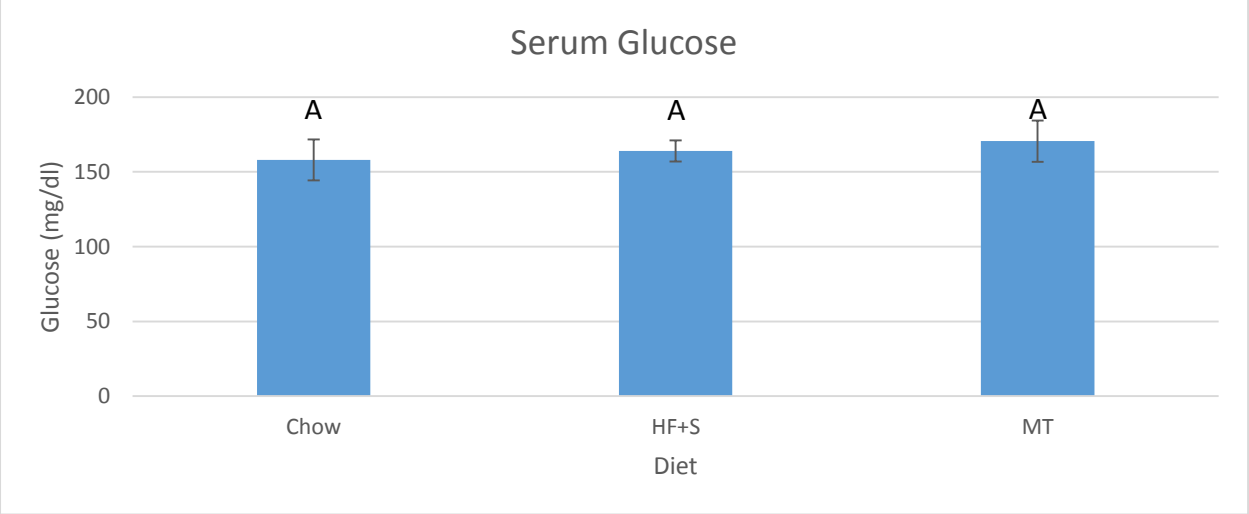

Figure 69: *Mean fasting serum glucose concentrations in animals on chow, HF+S, and MT diets*

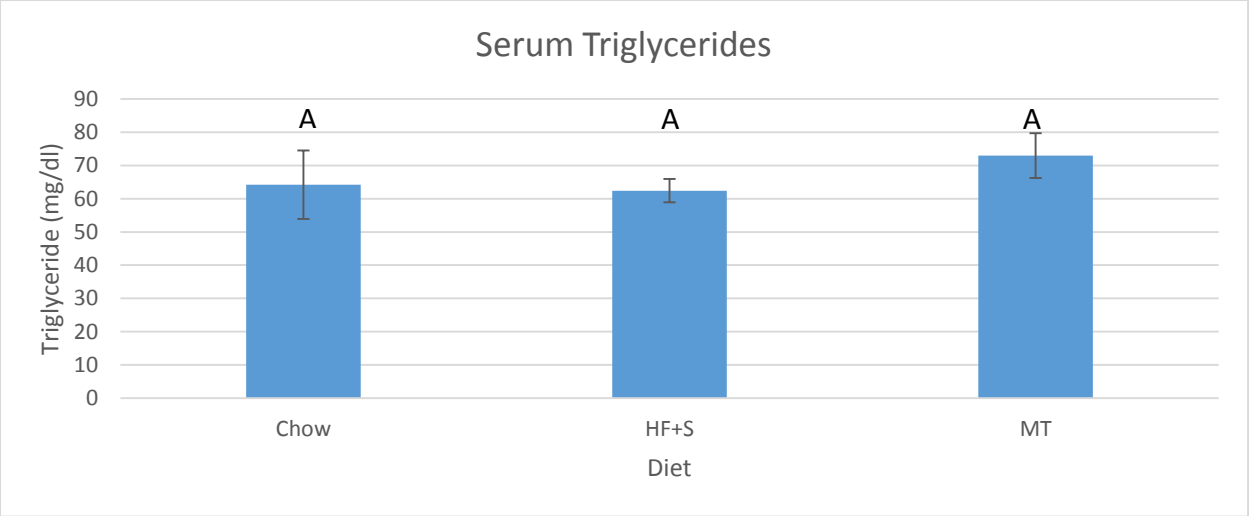

***Figure 70**: Mean fasting serum triglyceride concentrations in animals on chow, HF+S, and MT diets*

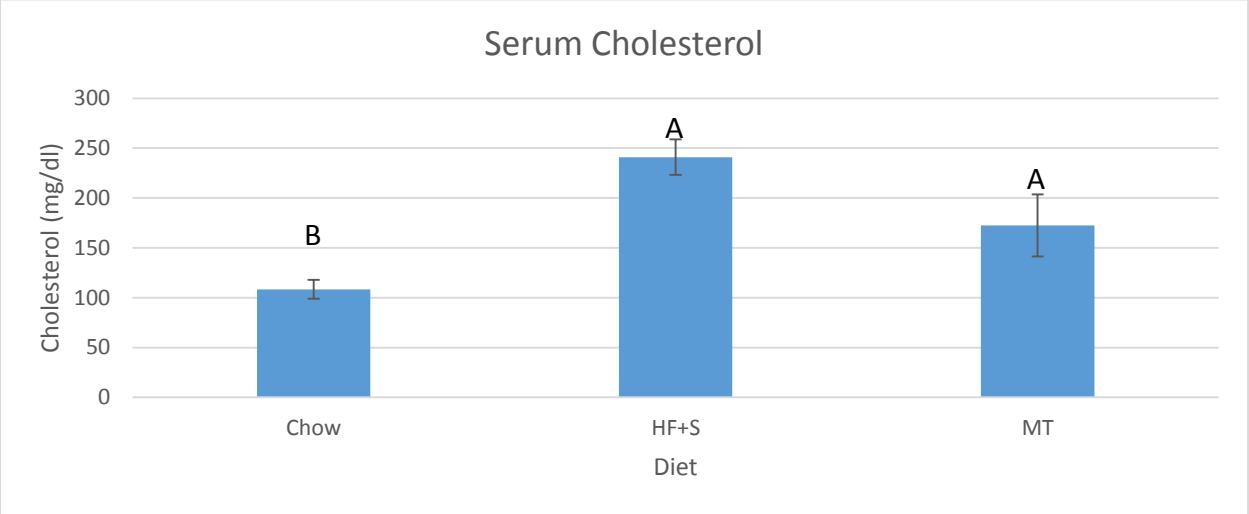

***Figure 71:** Mean fasting serum cholesterol concentrations in animals on chow, HF+S, and MT diets*

Although the HF+S and MT cholesterols technically were not significantly different, MT animals' cholesterol on average was 68 points lower than the HF+S group and actually were closer to the average cholesterol measured in chow-fed animals. Statistical analysis comparing the HF+S and MT groups revealed a significant difference at $p < 0.1$ ($p = 0.07$).

Liver weight was obtained during tissue harvest and normalized to body mass (Fig 72). The normalized liver weight was greatest in HF+S animals, averaging 0.06 g. Animals on MT diet

had a significantly lower normalized liver weight of 0.05 g, which was significantly greater than the 0.04 g measured in chow-fed animals ($p < 0.05$).

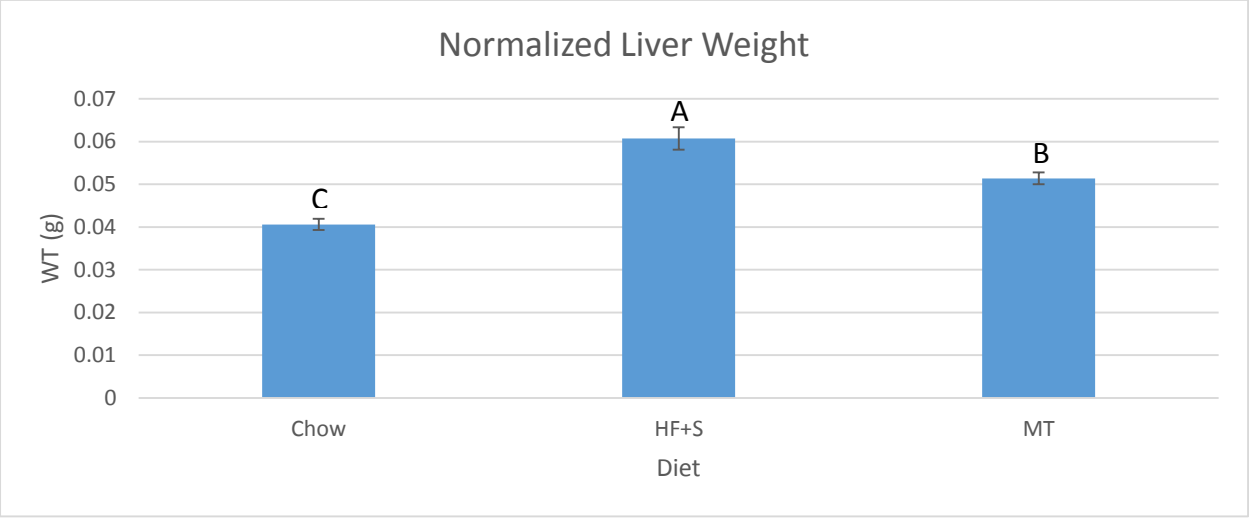

***Figure 72**: Liver weight normalized to body mass in animals on chow, HF+S, and MT diets*

After normalizing the liver weight to body mass, animals on HF+S diet had significantly elevated liver weights, suggesting an increased susceptibility to steatosis and NAFLD development. Meal timed animals had significantly lower liver weights, illustrating the ability of meal timing to inhibit the development and progression of liver disease and its hallmark symptoms. Both MT and HF+S groups had significantly greater normalized liver weights compared to chow-fed animals, suggesting that a high fat diet combined with sugar added to the drinking water facilitates NAFLD manifestation. However, the significant reduction in liver weight observed in MT animals relative to the HF+S group demonstrates the efficacy of meal timing and suggests a reversal and/or delay in the progression of NAFLD.

Epididymal, retroperitoneal, and inguinal fat pads were removed and weighed to assess adipose tissue expansion. Chow-fed animals had significantly less epididymal fat pad weight

(0.02 g) compared to HF+S (0.06 g) and MT (0.06 g) animals, which did not significantly differ from each other (Fig 73) ($p < 0.05$). Similarly, the 0.03 g and 0.03 g retroperitoneal fat pad weights in HF+S and MT animals, respectively, were significantly greater than the 0.01 g weight recorded in chow-fed animals (Fig 74) ($p < 0.05$). The inguinal fat pads had different results as the 0.03 g fat pad in the MT group was significantly less than the 0.04 g fat pad measured in HF+S animals (Fig 75) ($p < 0.05$). Chow-fed animals continued to have a fat pad weight (0.01 g) significantly less than the other groups ($p < 0.05$).

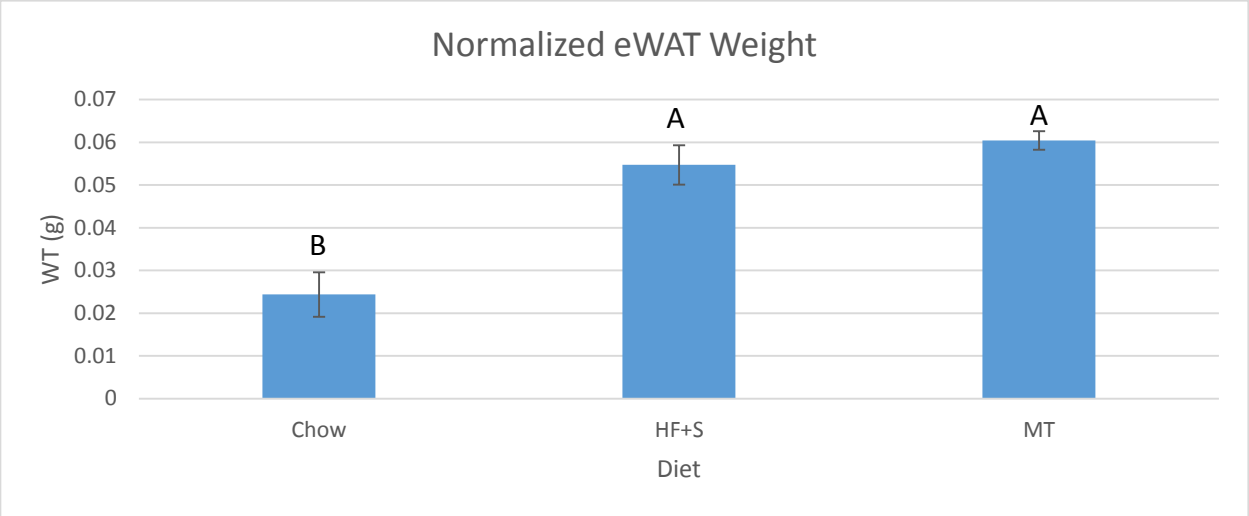

***Figure 73**: Epididymal fat pad weight normalized to body mass in animals on chow, HF+S, and MT diets*

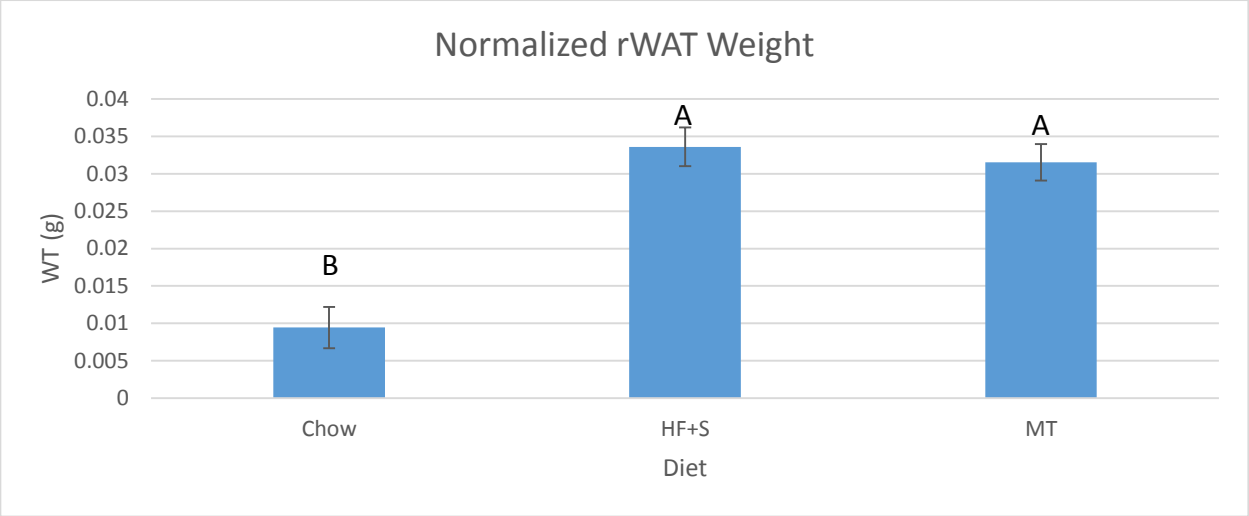

***Figure 74**: Retroperitoneal fat pad weight normalized to body mass in animals on chow, HF+S, and MT diets*

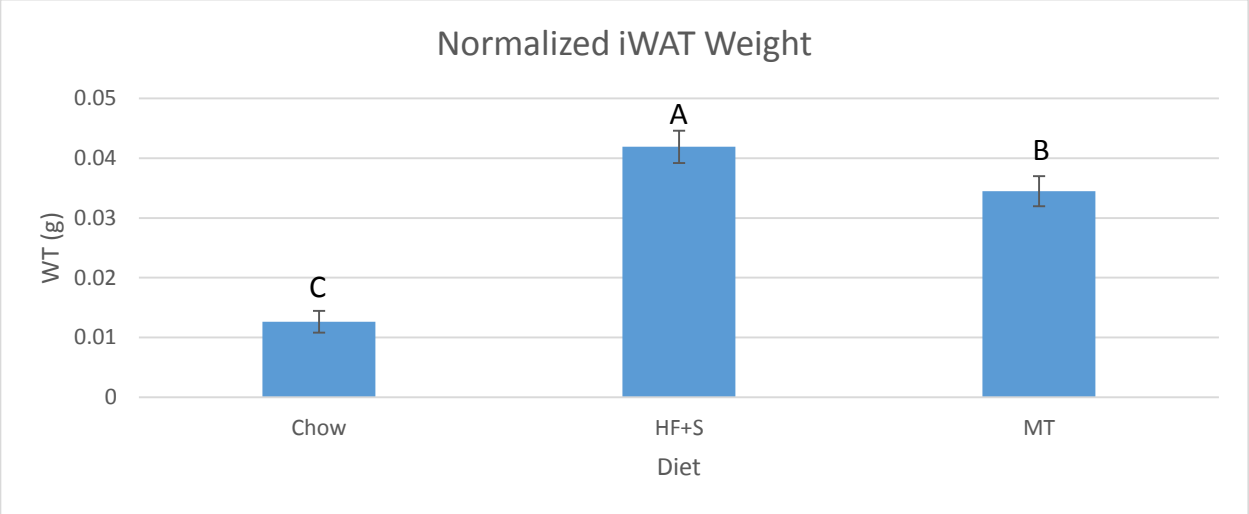

***Figure 75**: Inguinal fat pad weight normalized to body mass in animals on chow, HF+S, and MT diets*

Animals in the chow group consistently had lower fat pad weights compared to HF+S and MT animals. Given the significantly lower fat content in their diet and lesser body mass this is not surprising. Epididymal and retroperitoneal fat pad weight was not different between the HF+S and MT groups but MT animals did have a significantly lighter inguinal fat pad weight compared to HF+S animals. Although the epididymal and retroperitoneal fat pads had similar weights, this significant difference in inguinal weight not only indicates MT animals have less subcutaneous fat, but also illustrates that MT animals have smaller fat depots and store less

lipid. Thus, despite the same composition of the HF+S and MT diets, meal timing decreases overall adipose deposition compared to non-meal timed animals on HF+S diet and suggests that the decreased body mass associated with meal timing is due to decreased body fat.

Three days before animals were placed in the metabolic cages at the 12 week mark glucose tolerance tests were performed to determine how quickly glucose was cleared from the blood and potentially identify any chronic hyperglycemia or insulin resistance within the animals (Fig 76). The fasting glucose concentrations for all diet groups were relatively similar before glucose injection (chow 139 mg/dl, HF+S 166 mg/dl, MT 118 mg/dl) and expectedly showed comparable spikes in glucose levels 15 minutes after injection (chow 409 mg/dl, HF+S 411 mg/dl, MT 393 mg/dl). However, 30 minutes after injection the chow and MT groups exhibited minimal increases in glucose concentration (chow 436 mg/dl, MT 413 mg/dl) while the levels in HF+S animals continued to dramatically rise (506 mg/dl). HF+S animals continued to show increasing glucose concentrations after 60 minutes (528 mg/dl) while MT animals displayed a marginal decrease (392 mg/dl) while the chow group revealed drastic reductions (314 mg/dl). One hundred and twenty minutes after injection both the chow and MT groups showed dramatic declines from the previous time point and similar serum glucose concentrations (chow 223, MT 256 mg/dl). Although animals on HF+S diet exhibited a slight reduction (465 mg/dl), their average glucose concentration remained extremely elevated and 2.8 fold greater than their initial value. Quantification of the area under the curve (AUC) revealed the chow and MT groups had similar values and were not significantly different from

each other (Fig 77). Animals on HF+S displayed significantly greater AUC than chow and MT groups ($p < 0.05$).

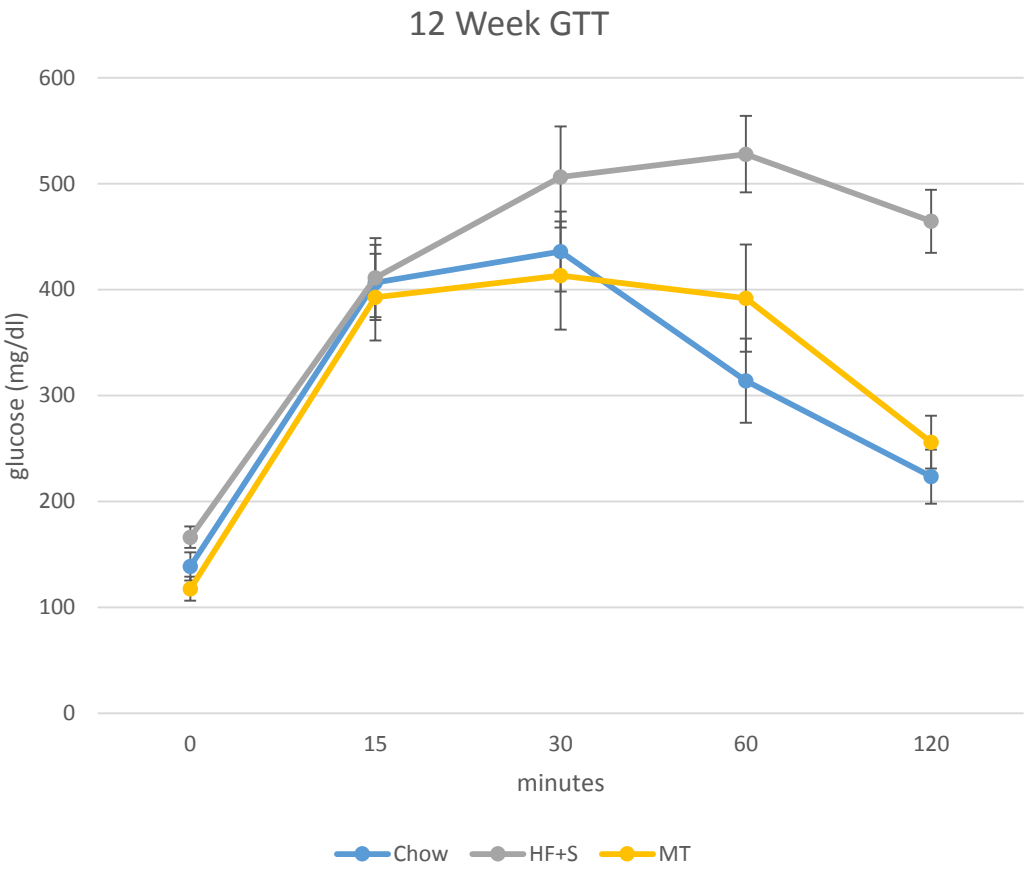

***Figure 76**: Glucose tolerance test for animals on chow, HF+S, and MT diets*

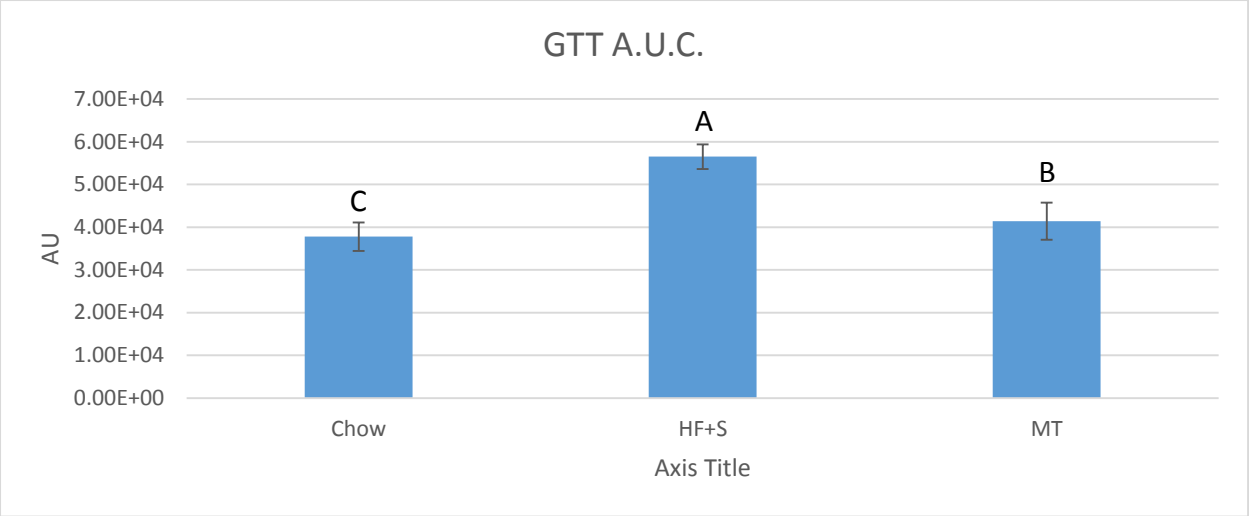

***Figure 77**: Quantification of area under curve from glucose tolerance test for animals on chow, HF+S, and MT diets*

Animals on chow and MT diets both demonstrated the ability to properly clear glucose from the blood and did not show any indications of insulin resistance. HF+S animals, on the other hand, were incredibly hyperglycemic as their glucose concentration continued to rise 60 minutes after glucose injection and was consistently greater than 500 mg/dl. The glucose concentration of HF+S animals was more than double that of chow-fed animals 120 minutes after administration of glucose. This illustrates the ability of meal timing to improve the ability to clear glucose from the blood. Despite the high fat content of the food and the inclusion of sugar to the drinking water, MT animals were as metabolically healthy as control animals on chow diet while non-meal timed animals on the same HF+S diet displayed metabolic dysfunction.

Two days after the glucose tolerance test an insulin tolerance test was performed to determine the different dietary groups' sensitivity to insulin (Fig 78). As expected, the percentage of initial glucose concentration dropped in all three groups within 30 minutes after

insulin injection. However, after 60 minutes, and up to 120 minutes after injection, the percentage of initial glucose concentration in both the chow and MT groups were 122% and 123%, respectively, while the HF+S group was only 106%. Due to the large variability between animals and the transformation of the data to reflect the percentage of initial glucose concentration rather than serum glucose concentrations there were no significant differences between the diets at any of the time points.

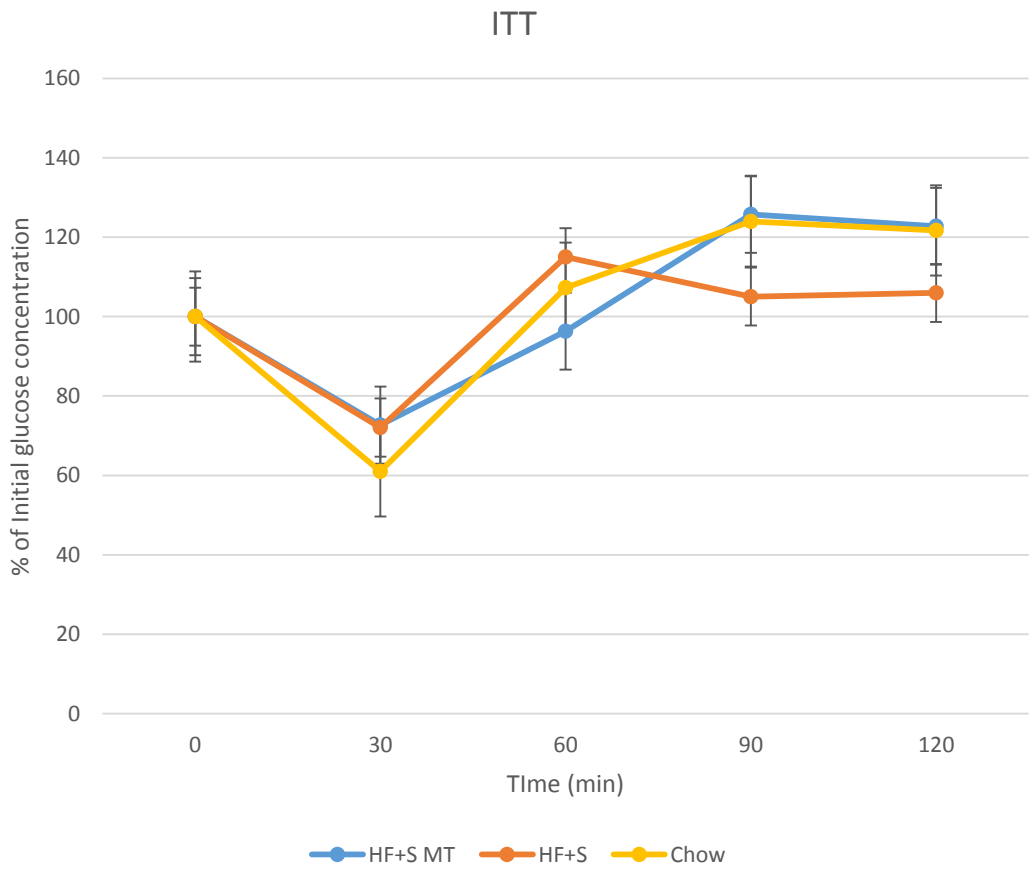

***Figure 78**: Insulin tolerance test from animals on chow, HF+S, and MT diets*

The initial drop in glucose concentration is expected and demonstrates the ability of insulin to clear glucose from the blood. This decrease is expected to continue until the

percentage of initial glucose concentration plateaus and begins to gradually increase. Blood glucose concentration is not expected to exceed 100% of the initial concentration within the 120 minute timeframe. The emphatic increase in glucose concentration that occurred after 30 minutes and persisted to the 120 minute mark in the chow and MT groups indicate an inability to properly clear glucose from the blood and are hallmark signs of insulin insensitivity and type 2 diabetes. Animals on HF+S diet illustrated a similar impairment in insulin action, but to a lesser extent, revealing better insulin sensitivity and less insulin resistance. Other metabolic and physiological parameters, such as the glucose tolerance test, present compelling data to the contrary, leading to some doubts in the insulin tolerance test results. To ensure the effects of one test don't influence another and the assessments are representative of the animals' typical state, glucose tolerance and insulin tolerance tests are commonly performed a week apart from each other. Given the glucose tolerance tests were performed only 48 hours prior to the insulin tolerance tests due to time constraints, it is believed that the massive influx of glucose from the glucose tolerance tests made the animals temporarily insulin resistant and had profound short-term metabolic consequences. Therefore, the results of the insulin tolerance test that suggested all dietary groups, including the control chow group, exhibited insulin resistance, are deemed inconsequential and not representative of the animals' metabolic state.

Overall, physiological assessments indicate that MT animals have preferable health markers compared to the HF+S group and more closely resemble chow-fed animals. Body mass and normalized inguinal fat pad and liver weights were all significantly less in MT animals

compared to HF+S animals. Glucose tolerance tests revealed equal abilities to clear glucose from the blood in chow and MT groups while HF+S animals exhibited extreme hyperglycemia and insulin resistance. Serum cholesterol levels were also similar in MT and chow groups. Meal timed animals were healthier and showed significantly less susceptibility to steatosis and NAFLD than their non-meal timed counterparts.

IV. Conclusion

Data from the metabolic cages and our physiological assessments revealed significant differences in animals on HF+S and MT diets. Specifically, daytime resting, total, and average energy expenditures were significantly reduced in MT animals while nighttime Y breaks, ped speed, and water uptake events, in addition to average RQ during both the day and night were significantly elevated in animals on MT diet compared to HF+S at 12 weeks. Behavioral effects, such as an increased tendency to engage in short lounges compared to long lounges following interaction with the food hopper and a decreased probability of interacting with the food hopper immediately after drinking water were also observed in MT animals. Crucial physiological indicators such as decreased normalized inguinal fat pad and liver weights and decreased body mass in addition to glucose clearance were also identified in animals on MT diet. Although not every parameter from the metabolic cages displayed profound differences between the HF+S and MT groups, physiologically, MT animals appear healthier. Hallmark symptoms associated with the development and progression of NAFLD such as obesity and increased adipose accumulation and, increased hepatic lipid accumulation and weight were all identified in animals fed HF+S diet and subsequently reversed after meal timing. This lower body mass, decreased liver and inguinal lipid deposition, and increased glucose clearance ability observed in MT animals clearly indicates improved metabolism and suggests better health outcomes. Therefore, meal timing can ameliorate of the negative metabolic effects associated with a HF+S diet.

V References

1. Jou J, Choi SS, Diehl AM. Mechanisms of disease progression in nonalcoholic fatty liver disease. Seminars in Liver Disease. 2008;28(4):370–9.

2. Clark JM, Brancati FL, Diehl AM. Nonalcoholic fatty liver disease. Gastroenterology 2002;122(6):1649–1657

3. Ludwig J, Viggiano TR, McGill DB, Oh BJ. Nonalcoholic steatohepatitis: Mayo Clinic experiences with a hitherto unnamed disease. Mayo Clin Proc 1980;55(7):434–438

4. Day CP, James OF. Steatohepatitis: a tale of two hits? Gastroenterology 1998;114(4):842–845

5. Duvnjak M, Lerotic I, Barsic N, et al. Pathogenesis and management issues for non-alcoholic fatty liver disease. World J Gastroenterol 2007;13(34):4539–4550

6. Diraison F, Moulin P, Beylot M. Contribution of hepatic de novo lipogenesis and reesterification of plasma non esterified fatty acids to plasma triglyceride synthesis during nonalcoholic fatty liver disease. Diabetes Metab 2003;29(5):478–485

7. Charlton M, Sreekumar R, Rasmussen D, et al. Apolipoprotein synthesis in nonalcoholic steatohepatitis. Hepatology 2002;35(4):898–904

8. Miele L, Grieco A, Armuzzi A, et al. Hepatic mitochondrial beta-oxidation in patients with nonalcoholic steatohepatitis assessed by 13C-octanoate breath test. Am J Gastroenterol 2003;98(10):2335–2336

9. Cases S, Smith SJ, Zheng YW, et al. Identification of a gene encoding an acyl CoA:diacylglycerol acyltransferase, a key enzyme in triacylglycerol synthesis. Proc Natl Acad Sci U S A 1998;95(22):13018–13023

10. Smith SJ, Cases S, Jensen DR, et al. Obesity resistance and multiple mechanisms of triglyceride synthesis in mice lacking DGAT. Nat Genet 2000;25(1):87–90

11. Chen HC, Smith SJ, Ladha Z, et al. Increased insulin and leptin sensitivity in mice lacking acyl CoA:diacylglycerol acyltransferase 1. J Clin Invest 2002;109(8):1049–1055

12. Yu XX, Murray SF, Pandey SK, et al. Antisense oligonucleotide reduction of DGAT2 expression improves hepatic steatosis and hyperlipidemia in obese mice. Hepatology 2005;42(2):362–371

13. Yamaguchi K, Yang L, McCall S, et al. Inhibiting triglyceride synthesis improves hepatic steatosis but exacerbates liver damage and fibrosis in obese mice with nonalcoholic steatohepatitis. Hepatology 2007;45(6):1366–1374

14. Unger RH, Orci L. Lipoapoptosis: its mechanism and its diseases. Biochim Biophys Acta 2002;1585(2–3):202–212

15. Feldstein AE, Werneburg NW, Canbay A, et al. Free fatty acids promote hepatic lipotoxicity by stimulating TNF-alpha expression via a lysosomal pathway. Hepatology 2004;40(1): 185–194

16. Kaser S, Moschen A, Cayon A, et al. Adiponectin and its receptors in non-alcoholic steatohepatitis. Gut 2005;54(1): 117–121

17. Arner P. The adipocyte in insulin resistance: key molecules and the impact of the thiazolidinediones. Trends Endocrinol Metab 2003;14(3):137–145

18. Xu A, Wang Y, Keshaw H, et al. The fat-derived hormone adiponectin alleviates alcoholic and nonalcoholic fatty liver diseases in mice. J Clin Invest 2003;112(1):91–100

19. Masaki T, Chiba S, Tatsukawa H, et al. Adiponectin protects LPS-induced liver injury through modulation of TNF-alpha in KK-Ay obese mice. Hepatology 2004;40(1):177–184

20. Kugelmas M, Hill DB, Vivian B, Marsano L, McClain CJ. Cytokines and NASH: a pilot study of the effects of lifestyle modification and vitamin E. Hepatology 2003;38(2):413–419

21. Hui JM, Hodge A, Farrell GC, et al. Beyond insulin resistance in NASH: TNF-alpha or adiponectin? Hepatology 2004;40(1):46–54

22. Li Z, Berk M, McIntyre TM, Gores GJ, Feldstein AE. The lysosomal-mitochondrial axis in free fatty acid-induced hepatic lipotoxicity. Hepatology 2008;47:1495–1503

23. Schattenberg JM, Wang Y, Singh R, Rigoli RM, Czaja MJ. Hepatocyte CYP2E1 overexpression and steatohepatitis lead to impaired hepatic insulin signaling. J Biol Chem 2005; 280(11):9887–9894

24. Roskams T, Yang SQ, Koteish A, et al. Oxidative stress and oval cell accumulation in mice and humans with alcoholic and nonalcoholic fatty liver disease. Am J Pathol 2003;163(4): 1301–1311

25. Ng M, Fleming T, Robinson M, Thomson B, Graetz N, Margono C, et al. Global, regional, and national prevalence of overweight and obesity in children and adults during 1980–2013: a systematic analysis for the Global Burden of Disease Study 2013.

26. "Obesity Definition." Obesity Prevention Source. Harvard School of Public Health, 20 Oct. 2012. Web. 29 June 2015.

27. Hruby A, Hu F. The epidemiology of obesity: a big picture. Pharmaco Economics. 2014;33:243

28. Hu FB. Obesity and mortality: watch your waist, not just your weight. Arch Intern Med. 2007;167(9):875.

29. Alberti KGMM, Eckel RH, Grundy SM, Zimmet PZ, Cleeman JI, Donato KA, et al. Harmonizing the Metabolic Syndrome: a Joint Interim Statement of the International Diabetes Federation Task Force on Epidemiology and Prevention; National Heart, Lung, and Blood Institute; American Heart Association; World Heart Federation; International Atherosclerosis Society; and International Association for the Study of Obesity. Circulation. 2009;120(16):1640–5.

30. Kaiyala K.J., Schwartz M.W. Toward a more complete (and less controversial) understanding of energy expenditure and its role in obesity pathogenesis. Diabetes. 2011;60:17–23.

31. White CR, Seymour RS. Allometric scaling of mammalian metabolism. J Exp Biol 2005;208:1611–1619.

32. Breslow MJ, Min-Lee K, Brown DR, Chacko VP, Palmer D, Berkowitz DE. Effect of leptin deficiency on metabolic rate in ob/ob mice. Am J Physiol 1999;276:E443–E449.

33. Butler AA, Kozak LP. A recurring problem with the analysis of energy expenditure in genetic models expressing lean and obese phenotypes. Diabetes 2010;59:323–329.

34. Kaiyala KJ, Morton GJ, Leroux BG, Ogimoto K, Wisse B, Schwartz MW. Identification of body fat mass as a major determinant of metabolic rate in mice. Diabetes 2010;59:1657–1666.

35. Arch JR, Hislop D, Wang SJ, Speakman JR. Some mathematical and technical issues in the measurement and interpretation of open-circuit indirect calorimetry in small animals. Int J Obes (Lond) 2006;30:1322–1331

36. Morton GJ, Cummings DE, Baskin DG, Barsh GS, Schwartz MW. Central nervous system control of food intake and body weight. Nature 2006;443:289–295

37. Tschop M.H. A guide to analysis of mouse energy metabolism. Nature Methods. 2012;9:57–63.

38. Li, B., et al. Skeletal muscle respiratory uncoupling prevents diet-induced obesity and insulin resistance in mice. Nat Med 6, 1115-1120 (2000).

39. Levine, J.A. Measurement of energy expenditure. Public Health Nutr. 8, 1123–1132 (2005).

40. Reaven GM. Banting lecture role of insulin resistance in human disease. Diabetes 1988; 37:1595–1607.

41. Sims EA, Danforth E Jr. Expenditure and storage of energy in man. J Clin Invest 1987; 79:1019–1025.

42. McLaughlin T, Lamendola C, Liu A, Abbasi F. Preferential fat deposition in subcutaneous versus visceral depots is associated with insulin sensitivity. J Clin Endocrinol Metab 2011; 96:E1756–E1760

43. Hardy OT, Czech MP, Corvera S. What causes the insulin resistance underlying obesity? Current opinion in endocrinology, diabetes, and obesity. 2012;19(2):81-87.

44. Kovalik JP, Slentz D, Stevens RD, et al. Metabolic remodeling of human skeletal myocytes by cocultured adipocytes depends on the lipolytic state of the system. Diabetes 2011; 60:1882–1893.

45. Koves TR, Ussher JR, Noland RC, et al. Mitochondrial overload and incomplete fatty acid oxidation contribute to skeletal muscle insulin resistance. Cell metab 2008; 7:45–56.

46. Petersen KF, Dufour S, Savage DB, et al. The role of skeletal muscle insulin resistance in the pathogenesis of the metabolic syndrome. Proc Natl Acad Sci U S A 2007; 104:12587–12594.

47. Brown MS, Goldstein JL. Selective versus total insulin resistance: a pathogenic paradox. Cell Metab 2008; 7:95–96.

48. Gonzalez E, Flier E, Molle D, et al. Hyperinsulinemia leads to uncoupled insulin regulation of the GLUT4 glucose transporter and the FoxO1 transcription factor. Proc Natl Acad Sci U S A 2011; 108:10162–10167.

49. Rytka JM, Wueest S, Schoenle EJ, Konrad D. The portal theory supported by venous drainage-selective fat transplantation. Diabetes 2011; 60:56–63.

50. Hardy OT, Perugini RA, Nicoloro SM, et al. Body mass index-independent inflammation in omental adipose tissue associated with insulin resistance in morbid obesity. Surg Obes Relat Dis 2011; 7:60–67.

51. Kovsan J, Bluher M, Tarnovscki T, et al. Altered autophagy in human adipose tissues in obesity. J Clin Endocrinol Metab 2011; 96:E268–E277.

52. Bjørndal B, Burri L, Staalesen V, Skorve J, Berge RK. Different adipose depots: their role in the development of metabolic syndrome and mitochondrial response to hypolipidemic agents. J Obes 2011;2011:490650.

53. McGillicuddy FC, Harford KA, Reynolds CM, et al. Lack of interleukin-1 receptor I (IL-1RI) protects mice from high-fat diet-induced adipose tissue inflammation coincident with improved glucose homeostasis. Diabetes 2011; 60:1688–1698.

54. Vandanmagsar B, Youm YH, Ravussin A, et al. The NLRP3 inflammasome instigates obesity-induced inflammation and insulin resistance. Nat Med 2011; 17:179–188.

55. Hellmann J, Tang Y, Kosuri M, et al. Resolvin D1 decreases adipose tissue macrophage accumulation and improves insulin sensitivity in obese-diabetic mice. FASEB J 2011; 25:2399–2407.

56. Goldfine AB, Fonseca V, Jablonski KA, et al. The effects of salsalate on glycemic control in patients with type 2 diabetes: a randomized trial. Ann Intern Med 2010; 152:346–357.

57. Lee YS, Li P, Huh JY, et al. Inflammation is necessary for long-term but not short-term high-fat diet-induced insulin resistance. Diabetes 2011; 60:2474–2483.

58. Holland WL, Bikman BT, Wang LP, et al. Lipid-induced insulin resistance mediated by the proinflammatory receptor TLR4 requires saturated fatty acid-induced ceramide biosynthesis in mice. J Clin Invest 2011; 121: 1858–1870.

59. Badin PM, Louche K, Mairal A, et al. Altered skeletal muscle lipase expression and activity contribute to insulin resistance in humans. Diabetes 2011; 60:1734–1742.

60. Kumashiro N, Erion DM, Zhang D, et al. Cellular mechanism of insulin resistance in nonalcoholic fatty liver disease. Proc Natl Acad Sci U S A 2011; 108:16381–16385.

61. Le KA, Mahurkar S, Alderete TL, et al. Subcutaneous adipose tissue macrophage infiltration is associated with hepatic and visceral fat deposition, hyperinsulinemia, and stimulation of NF-kappaB stress pathway. Diabetes 2011; 60:2802–2809.

62. Kabon B, Nagele A, Reddy D, et al. Obesity decreases perioperative tissue oxygenation. Anesthesiology 2004; 100:274–280.

63. Pasarica M, Rood J, Ravussin E, et al. Reduced oxygenation in human obese adipose tissue is associated with impaired insulin suppression of lipolysis. J Clin Endocrinol Metab 2010; 95:4052–4055.

64. Halberg N, Khan T, Trujillo ME, et al. Hypoxia-inducible factor 1alpha induces fibrosis and insulin resistance in white adipose tissue. Mol Cell Biol 2009; 29:4467–4483.

65. Gealekman O, Guseva N, Hartigan C, et al. Depot-specific differences and insufficient subcutaneous adipose tissue angiogenesis in human obesity. Circulation 2011; 123:186–194.

66. Rodeheffer MS, Birsoy K, Friedman JM. Identification of white adipocyte progenitor cells in vivo. Cell 2008; 135:240–249.

67. Han J, Lee JE, Jin J, et al. The spatiotemporal development of adipose tissue. Development 2011; 138:5027–5037.

68. Varela JE. Bariatric surgery: a cure for diabetes? Curr Opin Clin Nutr Metab Care 2011; 14:396–401.

69. Curry TB, Roberts SK, Basu R, et al. Gastric bypass surgery is associated with near-normal insulin suppression of lipolysis in nondiabetic individuals. Am J Physiol Endocrinol Metab 2011; 300:E746–E751.

70. Curry TB, Roberts SK, Basu R, et al. Gastric bypass surgery is associated with near-normal insulin suppression of lipolysis in nondiabetic individuals. Am J Physiol Endocrinol Metab 2011; 300:E746–E751.

71. Fabbrini E, Tamboli RA, Magkos F, et al. Surgical removal of omental fat does not improve insulin sensitivity and cardiovascular risk factors in obese adults. Gastroenterology 2010; 139:448–455.

72. Murphy JC, McDaniel JL, Mora K et al. Preferential reductions in intermuscular and visceral adipose tissue with exercise-induced weight loss as compared to calorie restriction. J Appl Physiol 2012; 112: 79–85.

73. Oliveira AG, Carvalho BM, Tobar N, et al. Physical exercise reduces circulating lipopolysaccharide and TLR4 activation and improves insulin signaling in tissues of DIO rats. Diabetes 2011; 60:784–796.

74. Ellacott et al. (2010) Ellacott KLJ, Morton GJ, Woods SC, Tso P, Schwartz MW. Assessment of feeding behavior in laboratory mice. Cell Metabolism. 2010;12(1):10–17.

75. Havel, P.J., Uriu-Hare, J.Y., Liu, T., Stanhope, K.L., Stern, J.S., Keen, C.L., and Ahren, B. (1998). Am. J. Physiol. 274, R1482–R1491.

76. Gregory, S.G., Sekhon, M., Schein, J., Zhao, S., Osoegawa, K., Scott, C.E., Evans, R.S., Burridge, P.W., Cox, T.V., Fox, C.A., et al. (2002). Nature 418, 743–750.

77. Asarian, L. (2006). J. Neurosci. 26, 11255–11256.

78. Adam, T.C., and Epel, E.S. (2007). Physiol. Behav. 91, 449–458.

79. Mandillo, S., Tucci, V., Holter, S.M., Meziane, H., Banchaabouchi, M.A., Kallnik, M., Lad, H.V., Nolan, P.M., Ouagazzal, A.M., Coghill, E.L., et al. (2008). Physiol. Genomics 34, 243–255.

80. Butler, A.A., Marks, D.L., Fan, W., Kuhn, C.M., Bartolome, M., and Cone, R.D. (2001). Nat. Neurosci. 4, 605–611.

81. Wang, C.Y., and Liao, J.K. (2012). A mouse model of diet-induced obesity and insulin resistance. Methods Mol. Biol. 821, 421–433.

82. Mellor, K.M., Bell, J.R., Young, M.J., Ritchie, R.H., and Delbridge, L.M. (2011). Myocardial autophagy activation and suppressed survival signaling is associated with insulin resistance in fructose-fed mice. J. Mol. Cell. Cardiol. 50, 1035–1043.

83. Bray, G.A., and Ryan, D.H. (2014). Update on obesity pharmacotherapy. Ann. N Y Acad. Sci. 1311, 1–13.

84. Anderson, J.W., Konz, E.C., Frederich, R.C., and Wood, C.L. (2001). Longterm weight-loss maintenance: a meta-analysis of US studies. Am. J. Clin. Nutr. 74, 579–584.

85. Longo, V.D., and Mattson, M.P. (2014). Fasting: molecular mechanisms and clinical applications. Cell Metab. 19, 181–192.

86. Gamble, K.L., Berry, R., Frank, S.J., and Young, M.E. (2014). Circadian clock control of endocrine factors. Nat. Rev. Endocrinol. 10, 466–475.ota

87. Kohsaka, A., Laposky, A.D., Ramsey, K.M., Estrada, C., Joshu, C., Kobayashi, Y., Turek, F.W., and Bass, J. (2007). High-fat diet disrupts behavioral and molecular circadian rhythms in mice. Cell Metab. 6, 414–421.

88. Adamovich, Y., Rousso-Noori, L., Zwighaft, Z., Neufeld-Cohen, A., Golik, M., Kraut-Cohen, J., Wang, M., Han, X., and Asher, G. (2014). Circadian clocks and feeding time regulate the oscillations and levels of hepatic triglycerides. Cell Metab. 19, 319–330.

89. Hatori, M., Vollmers, C., Zarrinpar, A., DiTacchio, L., Bushong, E.A., Gill, S., Leblanc, M., Chaix, A., Joens, M., Fitzpatrick, J.A., et al. (2012). Timerestricted feeding without reducing caloric intake prevents metabolic diseases in mice fed a high-fat diet. Cell Metab. 15, 848–860.

90. Chaix A, Zarrinpar A, Miu P, Panda S. Time-restricted feeding is a preventative and therapeutic intervention against diverse nutritional challenges. Cell Metab.2014;20:991-1005.

91. Stanhope, K.L. (2012). Role of fructose-containing sugars in the epidemics of obesity and metabolic syndrome. Annu. Rev. Med. 63, 329–343.

92. The limited storage capacity of gonadal adipose tissue directs the development of metabolic disorders in male C57Bl/6J mice

VI Appendices

Appendix 1

The specific time that corresponds with the 180 time points from the 24 hour plots detailed below:

Time	Time Point
7:02	1
7:10	2
7:18	3
7:26	4
7:34	5
7:42	6
7:50	7
7:58	8
8:06	9
8:14	10
8:22	11
8:30	12

8:38 13

8:46 14

8:54 15

9:02 16

9:10 17

9:18 18

9:26 19

9:34 20

9:42 21

9:50 22

9:58 23

10:06 24

10:14 25

10:22 26

10:30 27

10:38 28

10:46 29

10:54 30

11:02 31

11:10 32

11:18 33

11:26 34

11:34 35

11:42 36

11:50 37

11:58 38

12:06 39

12:14 40

12:22 41

12:30 42

12:38 43

12:46 44

12:54 45

13:02 46

13:10 47

13:18 48

13:26 49

13:34 50

13:42 51

13:50 52

13:58 53

14:06 54

14:14 55

14:22 56

14:30 57

14:38 58

14:46 59

14:54 60

15:02 61

15:10 62

15:18 63

15:26 64

15:34 65

15:42 66

15:50 67

15:58 68

16:06 69

16:14 70

16:22 71

16:30 72

16:38 73

16:46 74

16:54 75

17:02 76

17:10 77

17:18 78

17:26 79

17:34 80

17:42 81

17:50 82

17:58 83

18:06 84

18:14 85

18:22 86

18:30 87

18:38 88

18:46 89

18:54 90

19:02 91

19:10 92

19:18 93

19:26 94

19:34 95

19:42 96

19:50 97

19:58 98

20:06 99

20:14 100

20:22 101

20:30 102

20:38 103

20:46 104

20:54 105

21:02 106

21:10 107

21:18 108

21:26 109

21:34 110

21:42 111

21:50 112

21:58 113

22:06 114

22:14 115

22:22 116

22:30 117

22:38 118

22:46 119

22:54 120

23:02 121

23:10 122

23:18 123

23:26 124

23:34 125

23:42 126

23:50 127

23:58 128

0:06 129

0:14 130

0:22 131

0:30 132

0:38 133

0:46 134

0:54 135

1:02 136

1:10 137

1:18 138

1:26 139

1:34 140

1:42 141

1:50 142

1:58 143

2:06 144

2:14 145

2:22 146

2:30 147

2:38 148

2:46 149

2:54 150

3:02 151

3:10 152

3:18 153

3:26 154

3:34 155

3:42 156

3:50 157

3:58 158

4:06 159

4:14 160

4:22 161

4:30 162

4:38 163

4:46 164

4:54 165

5:02 166

5:10 167

5:18 168

5:26 169

5:34 170

5:42 171

5:50 172

5:58 173

6:06 174

6:14 175

6:22 176

6:30 177

6:38 178

6:46 179

6:54 180